NATIONAL TECHNICAL UNIVERSITY OF UKRAINE
“IGOR SIKORSKY KYIV POLYTECHNIC INSTITUTE”

E.O. Paton Institute of Materials Science and Welding

Department of High Temperature Materials and Powder Metallurgy

«On the rights of the manuscript»
УДК 621.793.79

«Admission to the defence»
Head of the department
_____I.I. Bogomol
«___»_____2021

Master's thesis
for a master's degree
in the specialty 132 Materials Science
on the topic: «Structure and microhardness of HEA –TiB_2 composite coating deposited by cold gas dynamic spraying»

Performed by
second-year student of group FN-01mn
Lan Jinlong _____

Research supervisor:
professor of the department of HTM and PM, doctor of technical sciences, professor Yurkova A.I. _____

Консультант з економічної частини доц., к.е.н., Нараєвський С.В. _____
(назва розділу) (посада, вчене звання, науковий ступінь, прізвище, ініціали) (підпис)

Консультант з охорони праці та безпеки в надзвичайних ситуаціях проф., д.е.н., Левченко О. Г. _____
(назва розділу) (посада, вчене звання, науковий ступінь, прізвище, ініціали) (підпис)

Консультант з нормоконтролю доц., к.т.н., Троснікова І. Ю. _____
(назва розділу) (посада, вчене звання, науковий ступінь, прізвище, ініціали) (підпис)

Рецензент:
Професор кафедри фізичного матеріалознавства та термічної обробки, проф., д.т.н., Макогон Ю.М. _____

I certify that in this master's dissertation there are no borrowings from the works of other authors without proper references.
Student _____

Kyiv - 2021

NATIONAL TECHNICAL UNIVERSITY OF UKRAINE "IGOR SIKORSKY KYIV POLYTECHNIC INSTITUTE"

E.O. Paton Institute of Materials Science and Welding

High Temperature Materials and Powder Metallurgy Department

Education level	Second (master's)
Specialty	132 Materials science
Educational program	Nanotechnologies and computer design of matrials

«Admission to the defence»
Head of the department
_____I.I. Bogomol
«_____»___2021

TASK

for the master's dissertation of the student

Lan Jinlong

1. Topic of master's thesis: «Structure and microhardness of HEA –TiB_2 composite coating deposited by cold gas dynamic spraying», Research supervisor: professor, doctor of technical science Yurkova Alexandra Ivanovna, approved by order of the University of «19» November 2021 y. No 261/21-ci.

2. The deadline for submission of the dissertation by a student is Dec. 15, 2021

3. Object of the research is AlNiCoFeCr-TiB_2 composite cold-sprayed coating.

4. Subject of the research is structure and microhardness of HEA –TiB_2 composite coating resulted from cold spraying.

5. List of tasks to be developed:

a) Literary review:

– To introduce the research status of contemporary world literary publications of high-entropy alloy and high-entropy alloy coatings

– To introduce the core effects of high-entropy alloys, the law of phase formation and the main properties of high-entropy alloys;

– To introduce the preparation methods and characteristics of high-entropy alloy and high-entropy alloy coatings

– To introduce the application of high-entropy alloy and high-entropy alloy coating;

b) Experimental:

– To select and validate the chemical composition of high-entropy alloy;

– To prepare AlNiCoFeCr HEA and HEA-TiB_2 by mechanical alloying in a planetary mill;

– To select the chemical composition of the powder mixture in order to obtain high-strength protective HEA-ceramic coatings on a steel substrate;

– To prepare powder mixture and steel substrates for HEA-ceramic coating by cold spraying;

– To study a HEA – ceramic coatings on steel substrates by cold spraying;

– To investigate the structure, phase, chemical composition and microhardness of cold-sprayed HEA-ceramic coating on steel substrate;

c) Discussion of the results:

– analyze the results and draw conclusions.

6. Approximate list of graphic (illustrative) material:

– topic of work, its actuality, purpose and main tasks;

– methods of obtaining high-entropy powder alloy and coatings from it;

– selection and validation of research material;

– research methods (characterization techniques) for structure, phase composition of HEA powder and HEA-TiB_2 composite powder and HEA-TiB_2 coatings ;

– experimental data on the structure and phase composition of HEA powder and HEA-TiB_2 composite powder and HEA-TiB_2 coatings;

– experimental data on the microhardness of the HEA-TiB_2 coatings;

– results and conclusions.

7. Approximate list of publications:

8. Date of issue of the assignment: 15.11.2021 y.

CALENDAR PLAN

No. Items	The name of the execution stages of Master's Thesis	The term of the practice stages	Note
1	A patent information retrieval. Write a literary review.	25.8.2021	
2	Select and validate the chemical composition of high-entropy alloy	10.09.2021	
3	Preparation of AlNiCoFeCr HEA by ball milling in a planetary mill	15.09.2021	
4	Investigation of structure and phase composition of mechanically alloyed HEA with SEM, EDX and XRD	18.09.2021	
5	Preparation of powder blend with HEA powder and 30wt.% TiB_2 powder by ball milling in a planetary mill. Analysis of microstructure and particle size distribution	25.9.2021	
6	Deposition of HEA–TiB_2 coatings by cold spraying (CS)	28.09.2021	
7	Investigation of structure, phase and chemical composition of cold sprayed composite coatings with SEM, EDX and XRD	01.10.2021-14.10.2021	
8	Vickers hardness measurements	18.10.2021	
9	Analysis and generalization of the obtained experimental results	20.10.2021-13.11.2021	
10	Section of labor protection	15.11. 2021 -19.11.2021	
11	Economic section	22.11. 2021 -26.11.2021	
12	Design of the graphic part	05.12. 2021 -10.12. 2021	

Undergraduate _____ Lan Jinlong

Supervisor from the institution _____ Alexandra YURKOVA

ABSTRACT

The master's thesis contains: 149 pages, 24 figures, 24 tables, 88 sources.

COATING, COLD SPRAY, HIGH ENTROPY ALLOY, MECHANICAL ALLOYING, MECHANICAL PROPERTIES, PHASE COMPOSITION, POWDER, SOLID SOLUTION, STRUCTURE

The purpose of the study is to prepare HEA–ceramic composite coatings by cold-spraying and to investigate the structure, phase composition, microhardness. In order to achieve this purpose it is necessary to decide the following: 1) To select and validate the chemical composition of high-entropy alloy and the powder mixture for HEA-ceramic coatings; 2) To prepare AlNiCoFeCr HEA by mechanical alloying in a planetary mill, powder mixture, steel substrates and HEA-ceramic coating by cold spraying; 3) To study HEA powders, HEA–ceramic mixture and HEA–ceramic coatings; 4) To investigate the structure, phase, chemical composition and microhardness of cold-sprayed HEA-ceramic coating on steel substrate.

Research methods and equipment: a planetary ball milling (Retsch PM100) was used for mechanical alloying. Spraying was performed on a DYMET 405 equipment. The structure and phase composition were studied using a SEM(REMMA--106И) , and an Ultima IV X-ray diffractometer f. Rigaku. Microhardness was determined by indentation on a PMT-3 device.

Object of the study is the cold sprayed AlNiCoFeCr HEA–TiB2 composite coatings. Subject of study is the formation of structure, phase and chemical composition as well as microhardness of cold sprayed HEA–TiB2 composite coatings on steel substrate.

Scientific novelty of the results:

This wok for the first time proves that solid-state CS technology is promising for the fabrication of thick HEA-ceramic coating while retaining the starting phases in the coating for using the advantage of interesting properties of HEA and ceramic in the form of coatings.

CONTENT

INTRODUCTION

Cold spraying technology, also known as cold gas dynamic spraying, is a new type of spraying technology that has been rapidly developed in recent years. It uses compressed gas (nitrogen, helium, air, etc.) as an accelerating gas flow to drive solid powder particles (particle size 1-50 μm) collide with the substrate at low temperature (room temperature to 600 ℃) and supersonic speed (300~1200 m/s), causing the particles to undergo strong plastic deformation and deposit to form a coating.

Compared with the traditional thermal spraying process, the cold spraying technology has a small thermal impact on the substrate and powder particles, and can avoid the oxidation, burning, phase change and structure changes of the sprayed powder. Therefore, the cold spraying technology is used in the preparation of nano materials , amorphous materials and other heat-sensitive material coatings.

There are currently more than 30 types of alloys developed. Most of the alloy systems are based on one metal element (atomic percentage content is more than 50%), and different properties are obtained by adding other alloying elements, such as steel materials, aluminum alloys, and titanium alloys, etc.

In the 1990s, Professor Yeh Junwei proposed a new design concept, namely, multi-principal high-entropy alloys: "Multiple elements are the main elements, with five or more main elements, and the atomic percentage of each main element is between 5%. and 35%.

At present, many well-known universities and research institutes at home and abroad have conducted a series of studies on high-entropy alloys. The research on multi-principal element high-entropy alloys has become one of the new research hot

spots in the field of metal materials.

There have been several processing routes to prepare HEAs, of which these includes laser cladding, vacuum arc melting, physical vapor deposition and mechanical alloying (MA) It is important to know aside certain contradiction of a single phase HEAs formed after mechanical alloying (MA). In other to address these issues, in the present study, equi-atomic AlNiCoFeCr ,the AlNiCoFeCr - TiB_2 were chosen for synthesis of HEAs by MA, and then AlNiCoFeCr - TiB_2 coating were prepared by cold spraying . The structure and properties of high-entropy alloys and HEA-TiB_2 coating were studied by employing detailed characterization via X-ray diffraction (XRD) and scanning electron microscopy (SEM) and Vickers microhardness.

1 LITERATURE REVIEW

1.1 High entropy alloys as a novel concept of designing materials

The traditional alloy design concept believes that exists of many components at alloy will lead to the formation of a variety complex microstructures such as intermetallic compounds which making the material difficult to analyzing and processing. At present, there are more than 30 kinds of alloy systems that have been developed and put into practical use. Most of the alloy systems are based on one metal element (atomic percentage content is more than 50%) where different properties can be obtained by adding other alloying elements. However, with the rapid development of science and technology, today's development and progress in many fields are dependent on the properties and functions of various materials while traditional alloy systems is unable to meet the higher and higher performance and function requirements. In comparation with traditional mindset of designing alloys with one main element, Yeh 0 propose a new design concept, namely, "multi-principal high-entropy alloys" which consists from five or more main elements are the elements. Atomic percentage of the main elements in alloys is between 5% and 35%. It should be noted that atomic percentage of each minor element, if it exists, is even smaller than 5%. The definition is expressed as follows:

$$n_{major} \geq 5\ ;\ 5\ at.\% \ \leq c_i \leq \ 35\ at.\% \tag{1.1}$$

$$n_{minor} \geq 0\,;\; c_j \leq 5\, at.\% \tag{1.2}$$

where n_{major} and n_{minor} are the numbers of major and minor elements, respectively; c_i and c_j are the atomic percentages of the major element, i, and the minor element, j, respectively.

From this definition, HEAs not need to be equimolar or near-equimolar and can contain minor elements to balance various materials properties. However, there is another definition based on high mixed entropy value caused by multiple principal components 2.

According to the Boltzmann's thermodynamic statistics principle, the quantitative relationship between the entropy and randomness of the system is given by:

$$\Delta S_{\text{conf}} = k \ln w \tag{1.3}$$

where k is the Boltzmann's constant, and w is the number of distinguishable ways of arranging the atoms in the solution.

In material thermodynamics, the total mixing entropy includes configuration entropy $\Delta S_{\text{mix}}^{\text{conf}}$, magnetic entropy $\Delta S_{\text{mix}}^{\text{mag}}$, vibration entropy $\Delta S_{\text{mix}}^{\text{vib}}$ and electronic randomness entropy $\Delta S_{\text{mix}}^{\text{elec}}$. The relationship among total entropy and its contributions is 3:

$$\Delta S_{\text{mix}} = \Delta S_{\text{mix}}^{\text{conf}} + \Delta S_{\text{mix}}^{\text{mag}} + \Delta S_{\text{mix}}^{\text{vib}} + \Delta S_{\text{mix}}^{\text{elec}} \tag{1.4}$$

The configurational entropy is dominant over the other three contributions. Hence, the configurational entropy often represents the mixing entropy in order to avoid complex calculations to determine the other three contributions 3. For an ideal random *n*-component solid solution, its ideal configurational entropy per mole is approximately 4:

$$\Delta S_{conf} = -R[c_1 \ln c_1 + c_2 \ln c_2 + \cdots + c_n \ln c_n] \tag{1.5}$$

$$\Delta S_{conf} = -R \sum_{i=1}^{n} c_i \ln c_i \tag{1.6}$$

where *R* is the gas constant; c_i is the mole fraction of the ith element; *n* is the number of the components.

According to the extreme theorem, when $c_1 = c_2 = \cdots = c_n$, the entropy of system reaches its maximum value.

Considering an equi-atomic alloy in its liquid state or regular solid-solution state, its configurational entropy per mole could be calculated as 5:

$$\Delta S_{conf} = R \ln n \tag{1.7}$$

It defines that HEAs have configurational entropy in a random state larger than 1.5*R*, no matter they are single phase or multiphases at room temperature. This definition could be expressed as 6:

$$\Delta S_{\mathrm{conf}} > 1.5R \tag{1.8}$$

As 1.5R is a lower limit for HEAs, we further define medium-entropy alloys (MEAs) and low-entropy alloys (LEAs) to differentiate the power of the mixing entropy effect for all alloys in the nature. Herein, 1R is the boundary between MEAs and LEAs since the mixing entropy less than 1R are expected to be noncompetitive with a larger mixing enthalpy 3.

So, the alloys are divided into the following three categories 6:

– LEAs: $\Delta S_{\mathrm{conf}} < 1R$, including traditional alloys based on one or two elements;

– MEAs: $1R \leq \Delta S_{\mathrm{conf}} \leq 1.5R$, including alloys based on two to four elements;

– HEAs: $\Delta S_{\mathrm{conf}} > 1.5R$, including alloys based on five elements at least or some quaternary equimolar alloys.

1.2 Core effects in HEAs

The multiprincipal-element character of HEAs leads to some important effects that are much less pronounced in conventional alloys. These can be considered as four ‘core effects’ of HEAs. This section briefly introduces and discusses the core effects.

1.2.1 High-entropy effect

The high-entropy effect was first proposed by Yeh 7. According to the Gibbs phase

rule, the number of phases (P) in a given alloy at constant pressure in equilibrium condition is:

$$P = C + 1 - F \tag{1.9}$$

where C is the number of components and F is the maximum number of thermodynamic degrees of freedom in the system.

From the Gibbs energy expression $\Delta G_{mix} = \Delta H_{mix} - T\Delta S_{mix}$, it can be seen that the mixing entropy and mixing enthalpy are in a state of competition with each other. A high mixing entropy value can effectively reduce the free energy, especially in the high temperature stage. The change of free energy plays a leading role. High-entropy alloys have the highest mixing entropy when the elements are randomly soluble in each other, which can reduce the free energy of the system to a large extent.

The high-entropy effect is mainly used to explain the multi-principal-element solid solution. According to the maximum entropy production principle 2, high entropy tends to stabilize the high-entropy phases, solid-solution phases, rather than intermetallic phases. Intermetallics are usually ordered phases with lower configurational entropy. For stoichiometric intermetallic compounds, their configurational entropy is zero.

1.2.2 Sluggish diffusion effect

The sluggish diffusion effect here is compared with that of the conventional alloys rather than the bulk-glass-forming alloys (fig. 1.1 ~~Fig.1.1~~).

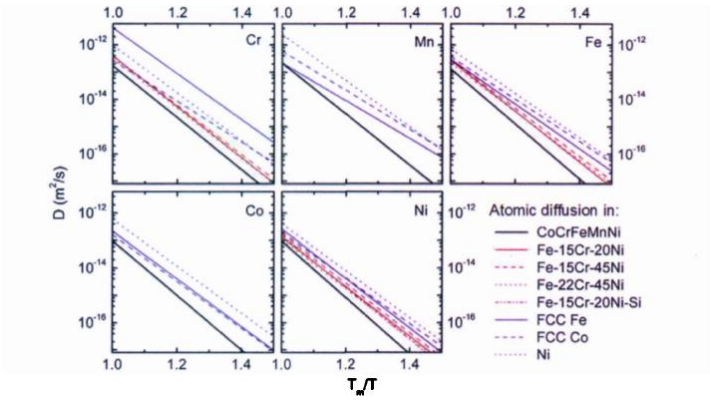

Figure 1.1 – Comparison of the diffusion rate of the five components of FeCoNiCrMn in the high-entropy alloy system and other traditional alloy systems 11

The formation of a new phase requires the coordinated diffusion of different types of atoms in the phase change process controlled by the diffusion mechanism to realize the redistribution of solutes, thereby completing the phase change. The stress field generated by the lattice distortion in the high-entropy alloy hinders the diffusion of atoms, thereby increasing the activation energy of the diffusion of atoms and reducing the effective diffusion rate of atoms in the high-entropy alloy 10, so the new phase nucleation is long. The large rate is slower, or is suppressed to the low temperature area. In 2013, Yeh et al 11 reported accurate experimental results for the first time, confirming this important characteristic. By designing different high-temperature diffusion couples of FeCoNiCrMn system, the self-diffusion rate of different components in the high-entropy alloy matrix and the corresponding lattice diffusion activation energy are calculated. Comparing the traditional FCC crystal structure metal materials containing these components (**Ошибка! Источник ссылки не найден.**), it can be seen that the diffusion rate of all five component elements in the high-entropy alloy matrix is much lower than that of other single-principal alloys. In the high-entropy

alloy, the lattice diffusion resistance becomes larger and the diffusion is slow. By establishing a model of atomic jumping potential well in high-entropy alloys, the slow lattice diffusion effect has also been initially explained.

1.2.3 Severe lattice distortion effect

The severe lattice-distortion effect is usually compared with the one dominant element alloys, where the lattice site is occupied mainly by the dominant constituent. In a high-entropy alloy solid solution phase containing a variety of main components, various atoms are randomly distributed in the crystal lattice, and the difference in atomic radius, chemical bond will cause the position of each lattice of the crystal lattice to shift to different degrees, resulting in the lattice distortion shown in Figure 1.2 (a) to Figure 1.2 (b) is obtained.

For HEAs, each element has the same possibility to occupy the lattice site, if ignoring chemical ordering. Since the size of different elements can be very different in some cases, this can lead to the severe lattice distortion.It can be inferred from this that if the atomic size difference is large enough and the distortion energy is too high to maintain the original stable simple crystal lattice, it will collapse to form a more stable crystal structure, such as an intermetallic compound phase.

Yeh et al 12 systematically studied the decrease of X-ray diffraction intensity in CuNiAlCoCrFeSi alloy system, as shown in Figure 1.2 (c). They studied a series of CuNiAlCoCrFeSi alloys and systematically added the main elements from pure elements to seven elements for quantitative analysis of XRD intensities. As the number

of elements increases, the intensity of diffraction peaks gradually decreases and becomes wider. According to the principle of X-ray diffraction, the lattice distortion of the high-entropy alloy causes uneven surface of the atoms in the same layer, which causes the X-rays to be scattered to the uneven Bragg surface during the diffraction process.

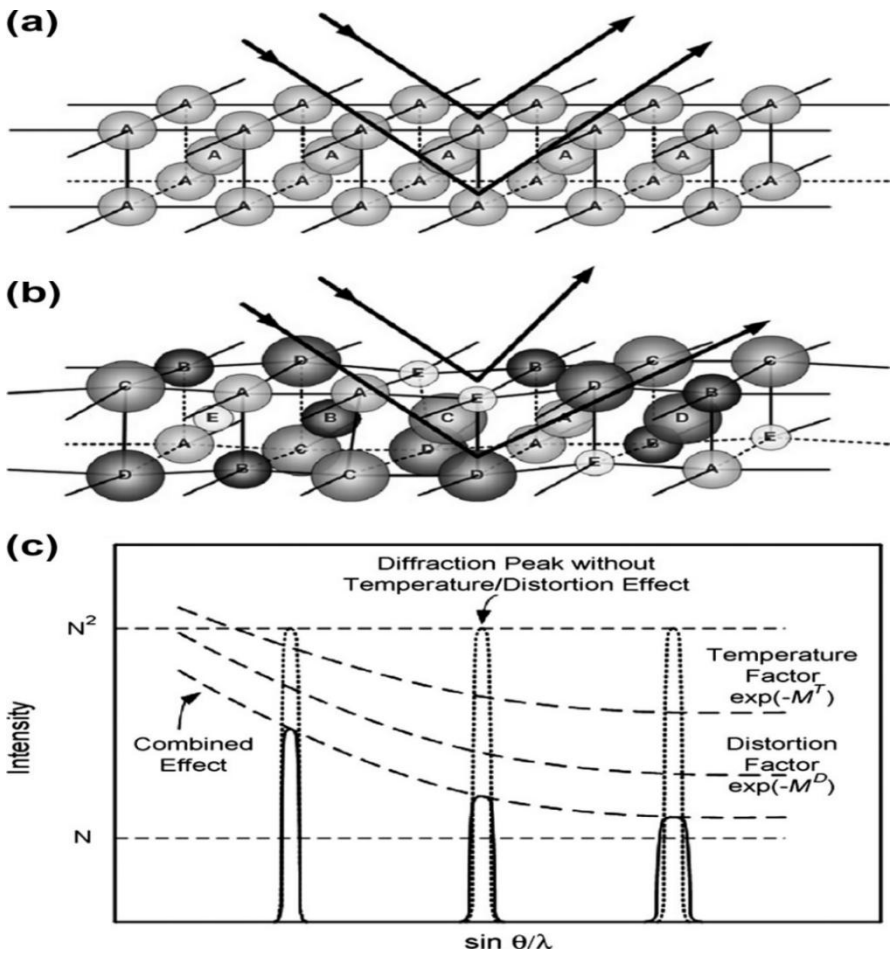

Figure 1.2 – Schematic illustration of intrinsic lattice distortion effects on Bragg diffraction: (a) perfect lattice with the same atoms; (b) distorted lattice with solid solutions of different-sized atoms, which are expected to randomly distribute in the crystal lattice according to a statistical average probability of occupancy; (c) temperature and distortion effects on the XRD intensity 12

1.2.4 Cocktail effect

The cocktail effect for metallic alloys was first mentioned by Ranganathan 13. For metallic alloys, the effect indicates that the unexpected properties can be obtained after mixing many elements, which could not be obtained from any one independent element.

High-entropy alloys can be regarded as composite materials on the atomic scale. Therefore, in addition to the indirect effects of various elements on the microstructure, the basic characteristics of the components and their interactions make the high-entropy alloy exhibit a compound effect, that is, the "cocktail effect." The cocktail effect implies that the alloy properties can be greatly adjusted by the composition change and alloying, as shown in Figure 1.3, which indicates that the hardness of HEAs can be changed by adjusting the Al content in the $CoCrCuNiAl_x$ HEAs.

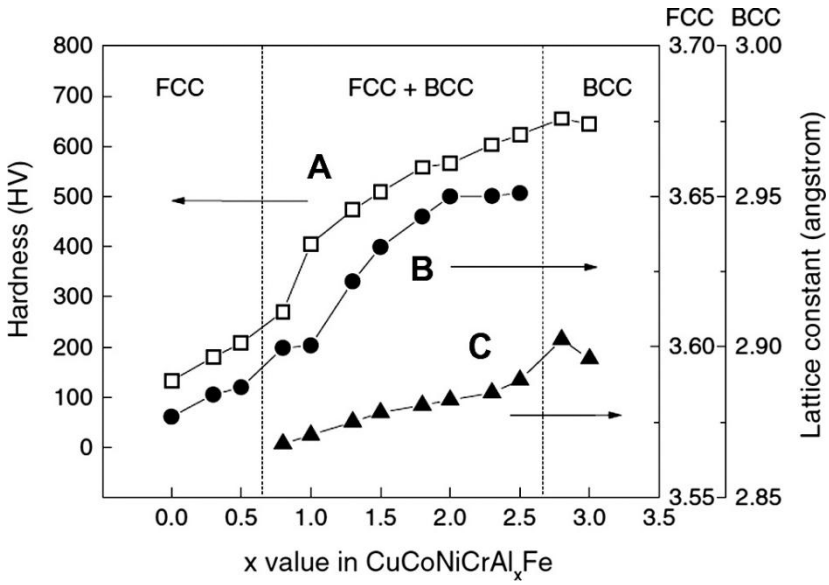

Figure 1.3 – Hardness and lattice constants of a $CuCoNiCrAl_xFe$ alloy system with different x values: (A) hardness of $CuCoNiCrAl_xFe$ alloys, (B) lattice constants of an FCC phase, (C) lattice constants of a BCC phase 0

The cocktail effect implies that the alloy properties can be greatly adjusted by the composition change and alloying, as shown in Figure 1.3, which indicates that the hardness of HEAs can be changed by adjusting the Al content in the $CoCrCuNiAl_x$ HEAs. Al is a soft and low-melting-point element. Addition of Al can actually harden HEAs. As the increase of the Al content, the phases change from FCC to BCC + FCC and then to BCC structures. As a result, the lattice constants for both the BCC and FCC structures increase, and the hardness of the alloys increases.

1.3 Phase and crystal structure

Although there are more than four or five elements in HEAs , high-entropy alloys can often form relatively simple phases after solidification. In addition to simple multi-component solid solutions FCC (face-centered cubic cell), BCC (body-centered cubic cell), HCP (hexagonal closed-packed cell), nanocrystalline precipitates, intermetallic compounds and amorphous phases will also be formed in some alloys.

1.3.1 Simple solid solution structure

The study found that some systems of high-entropy alloys formed structures dominated by simple FCC or BCC phases after solidification.Cantor et al 14 first reported the microstructure of the FeCoNiCrMn component of the multi-principal alloy. It is found that it is composed of simple dendrites, and this alloy has become one of the most typical high-entropy alloy components,which contains Fe (BCC), Co (HCP), Cr (BCC), Mn (BCC), and Ni (FCC) in an equimolar ratio, with only an FCC solid-solution phase

when solidified dendritically in the as-cast sample.

The HCP phase is referred to as a typical simple solid-solution structure of HEAs. The HCP solid solution phase was found in the alloy of TiCrZrNb by Tsau 15. However, they found that the HCP phase did not exist independently, the HCP phase was in the interdendritic region, and the matrix was BCC phase.

1.3.2 Mesophase and other complex phases in HEAs

The high mixing entropy effect will cause the multi-component high-entropy alloy to tend to form a structure dominated by solid solution, but studies have shown that in some alloy systems containing extremely negative mixing enthalpy element pairs, a complex multi-phase coexistence structure will be formed, which indicates high mixing entropy cannot completely overcome the contribution of high mixing enthalpy to free energy. The mesophase or complex multi-phase coexistence forms in HEAs due to the existences of some chemically-compatible elements. Li et al 16 studied the alloy of FeNiCrCuM. They found that FeNiCrCuCo and FeNiCrCuMo alloys consist of a single FCC solid solution. They found that FeNiCrCuCo and FeNiCrCuMo alloys consist of a single FCC solid solution. When the Cu or Co in the alloy is replaced by Al, the structure will change to BCC or BCC + FCC. Cu or Al has an FCC structure promotes or worsens the formation of FCC solid solution. In addition, when Zr is added to the alloy, due to its strong tendency to form compounds with other components, compounds with complex structures will appear.

1.3.3 Nanocrystalline and amorphous phases in HEAs

Conventional alloys can only precipitate nanocrystals under special heat-treatment conditions.The sluggish diffusion effect and lattice distortion effect of high-entropy alloys make it easy to form nanophase and amorphous phase. The $Cu_{0.5}NiAlCoCrFeSi$ as-cast high-entropy alloy developed by Chen et al 17. They found that the dendritic phase is mainly composed of an amorphous phase with a small amount of body-centered cubic (BCC) structure, while the interdendritic phase has an amorphous structure containing a small amount of nano-scale precipitates. Zhao et al. 18 prepared an amorphous alloy that can be uniformly deformed at room temperature without shearing. At the same time, its critical size is greater than 3mm, the amorphous transition temperature of the alloy is close to room temperature, the density is low, the specific strength is high, and the elastic modulus is low.

1.4 Phase formation rules and phase prediction for HEAs/solid solution formation rules and phase prediction

1.4.1 Thermodynamic and geometry effect

According to the Hume-Rothery rules for high degree of solubility in binary alloy systems, two factors are mentioned, which would affect the formation of the solid solution in alloys 19.The first factor is the size effects of component atoms. For alloys whose component atomic-size differences are over 15 %, it’s most improbable to form a substitution solid solution. For binary alloys, their atomic radius difference should be less than 15%. The second factor is the chemical compatibility between components, the

electro-negativity difference, their difference in electro-negativity should be less than 0.4. The larger the electro-negativity difference, the more likely the alloys form compounds rather than solid solutions.

However, high-entropy alloys have many components and cannot distinguish between solvents and solutes, so it is difficult to analyze them with traditional methods.

Zhang et al. extended the "Hume-Rothery criterion" to the field of high-entropy alloys, and proposed three parameters that affect the solid solution phase formation of high-entropy alloys: the difference in atomic radius (δ), the enthalpy of mixing (the energy at which atoms combine with each other, ΔH_{mix}), and mixed entropy (ΔS_{mix}), the calculation method is as follows 19:

$$\Delta H_{mix} = \sum_{i=1, i\neq j}^{n} \Omega_{ij} c_i c_j \tag{1.10}$$

$$\Delta S_{mix} = k \ln \omega = -R \sum_{i=1}^{n} (c_i \ln c_i) \tag{1.11}$$

$$\delta = \sqrt{\sum_{i=1}^{n} c_i (r - \bar{r})^2} \tag{1.12}$$

$$\bar{r} = \sum_{i=1}^{n} c_i r_i \tag{1.13}$$

where Ω_{ij}(=4 ΔH^{mix}_{AB}) is the regular melt-interaction parameter between i^{th} and j^{th}

elements, and ΔH^{mix}_{AB} is the mixing enthalpy of binary liquid alloys,R is the gas constant; c_i is the atomic percentage of the ith element. r_i is the atomic radius of the ith element.

They summarized the published atomic radius difference, mixing enthalpy and mixing entropy of HEAs, and other five elements or more multi-component alloys, the relationship between the atomic radius difference and the mixing enthalpy, and the atomic radius difference, mixing enthalpy and mixing entropy are drawn. The three-dimensional relationship diagrams are shown in Figure 1.4 and Figure 1.5. The Figure 1.4 is relationship between Delta and ΔH_{mix} for MHAs and typical multicomponent bulk metallic glasses.

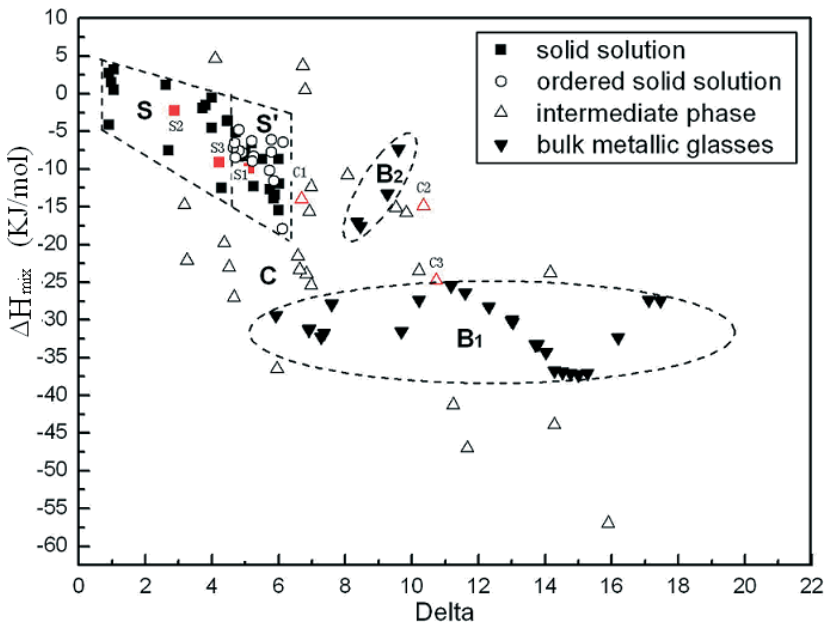

Figure 1.4 – Relationship between Delta and ΔH_{mix} for MHAs and typical multicomponent bulk metallic glasses 19

According to the Figure 1.5, we can know that the range of solid solution phase

formation is: the difference in atomic radius is less than 6.5%; the mixing enthalpy is between –15 KJ/mol to 5 KJ/mol; the mixing entropy is between 12 KJ/mol to 17.5 KJ/mol between. Among them, the S region forms a disordered solid solution, and the S' region corresponds to an ordered solid solution, which indicates that an ordered solid solution is easily formed when the atomic radius difference is large.

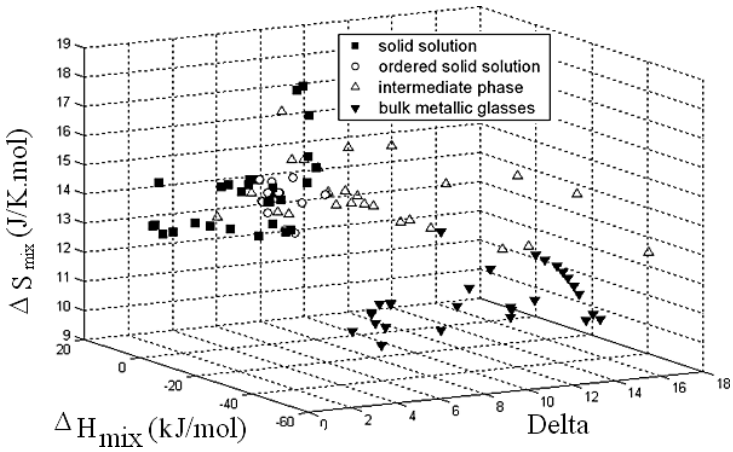

Figure 1.5 – The Effect of ΔS_{mix} on the phase formation of the MHAs and typical multicomponent bulk metallic glasses 19

In order to simplify the prediction standard of high-entropy alloy solid solution structure, Yang and Zhang proposed the Ω parameter, which is defined as 27:

$$\Omega = \frac{T_m \Delta S_{mix}}{\Delta H_{mix}} \tag{1.14}$$

where T_m is the theoretical melting point of the alloy, ΔS_{mix} is the mixing entropy, and ΔH_{mix} is the mixing enthalpy.

$$T_m = \sum_{i=1}^{n} c_i (T_m)_i \tag{1.15}$$

where $(T_m)_i$ is the melting point of the i-th element, and c_i is the atomic percentage of the ith element.

Yang and Zhang drew the Ω-δ diagram 27, as shown in Figure 1.6. The area formed by the solution is Ω ≥ 1.1 and δ ≤ 6.6%, which is the S region in the figure. The formation area of bulk amorphous δ is relatively large, Ω ≤ 1.1.

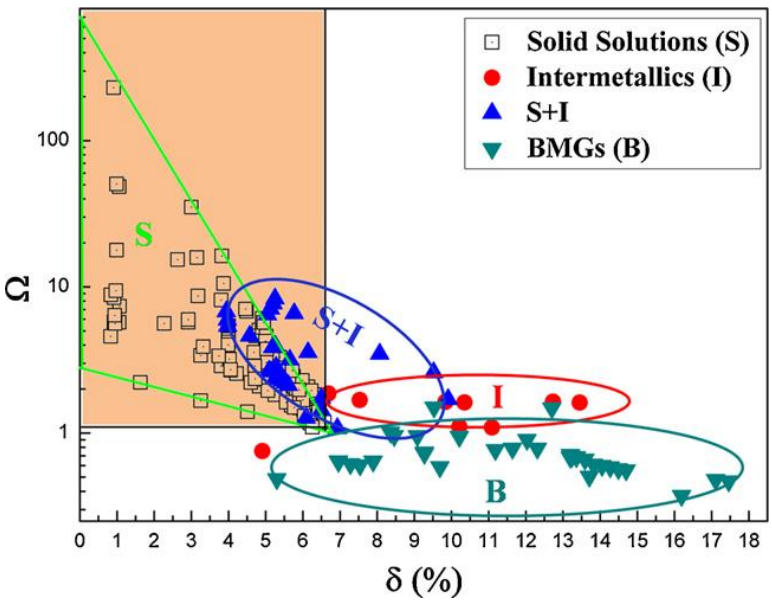

Figure 1.6 – The relationship between parameters δ an Ω for multi-component alloys 27

In the HEAs design, this parameter can effectively predict whether the alloys will form a solid solution structure. However, it is still impossible to predict whether the solid solution structure of the high-entropy alloy is FCC or BCC structure, and whether the solid solution is ordered or disordered. For this reason, for the phase formation law

of high-entropy alloys, other solid solution formation criteria have also appeared. For example, there are valence electron concentration parameters, atomic size difference parameters, and entropy angle Φ parameters, which will be described in detail below.

1.4.2 Valence electron concentration

Guo et al. 21 proposed the relationship between the valence electron concentration (VEC) and the stability of solid solution by summarizing the existing data. They organized and analyzed published data, they believed that when VEC ≥ 8.0, the FCC solid solution phase is relatively stable; when VEC < 6.87, the BCC solid solution phase is relatively stable; when 6.87 < VEC < 8.0, there is a FCC+BCC dual-phase structure.

$$\mathrm{VEC} = \sum_{i=1}^{n} c_i (\mathrm{VEC})_i \tag{1.16}$$

where c_i is the atomic percentage of the i-th element; $(\mathrm{VEC})_i$ is the valence electron concentration of the i-th element

It is worth noting that the valence electron concentration (VEC) plays an important role in the formation of alloy phases.

The Figure 1.7 shows that the relationship diagram of the valence electron concentration of different high-entropy alloy systems.

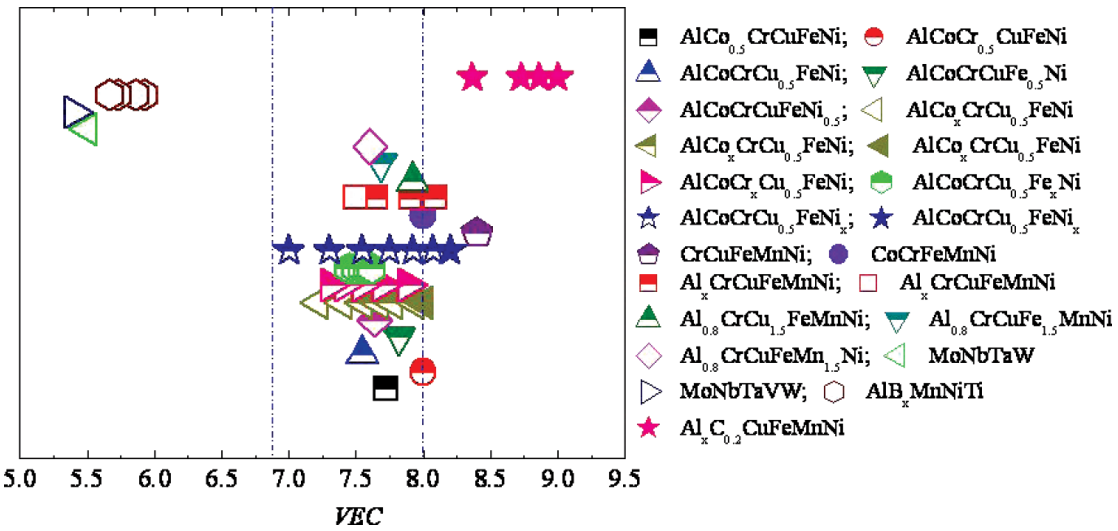

Figure 1.7 – The relationship diagram of the valence electron concentration of different high-entropy alloy systems 21

According to the figure 1.7, it can be concluded that it is mainly manifested in the effect on solid solubility for solid solution alloys. One is the so-called atomic valence effect. In solid solution alloys, the higher the atomic valence of the solute, the smaller its maximum solid solubility; the second is the so-called relative valence effect, that is, the higher the valence of the component. The solid solubility in the valence component is greater than the opposite solid solubility. However, when studying the phase formation law of high-entropy alloys, the valence electron concentration cannot be considered alone, and the atomic size factor is also very important.

For the atomic radius difference δ, Wang et al. 22 believed that δ only represents the average effect of the atomic size difference. The stability of the solid solution depends on the maximum atomic radius and the minimum atomic radius. Therefore, considering the degree of atomic stacking mismatch and topological instability, Wang proposed an atomic size difference parameter γ to predict the formation of solid solutions. The definition of γ is as follows 22:

$$\gamma = \frac{\omega_S}{\omega_L} = \left(1 - \sqrt{\frac{(r_S+\bar{r})^2-\bar{r}^2}{(r_S+\bar{r})^2}}\right)/\left(1 - \sqrt{\frac{(r_L+\bar{r})^2-\bar{r}^2}{(r_L+\bar{r})^2}}\right) \quad (1.17)$$

$$\omega_L = 1 - \sqrt{\frac{(r_s+\bar{r})^2-\bar{r}^2}{(r_s+\bar{r})^2}} \quad (1.18)$$

$$\omega_s = 1 - \sqrt{\frac{(r_L+\bar{r})^2-\bar{r}^2}{(r_L+\bar{r})^2}} \quad (1.19)$$

where r_s is the smallest atomic radius, r_L is the largest atomic radius, r is the average atomic radius.

In Figure 1.8. ω_s and ω_L are shown. When $\gamma < 1.175$, the alloy phase exists in the form of solid solution; when $\gamma > 1.175$, the alloy phase exists in the form of multiphase structure or intermetallic compound.

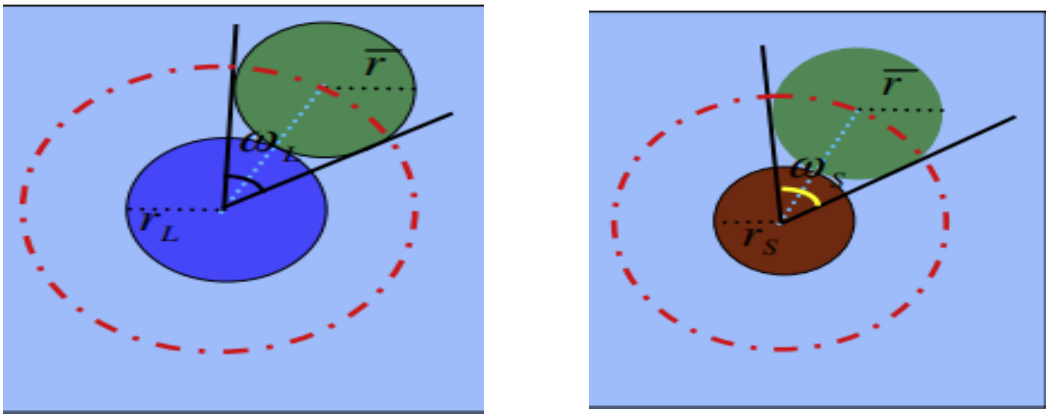

a b

Figure 1.8 – Sketch of the atomic packing around an atom via a solid angle: (a) around a largest atom; (b) around a smallest atom. $\bar{r}$ is the average atomic radius 22

Like the valence electron concentration parameter of Guo [21], the phase

formation law of high-entropy alloys cannot be treated equally or treated in isolation.

1.5 High entropy alloys properties

1.5.1 Mechanical properties

The property of high-entropy alloys depends on its unique structure. In general, the solid solution of BCC structure has high strength and low plasticity; while the solid solution of FCC structure has lower strength and higher plasticity. For different HEAs systems, their properties show great differences.

For room-temperature mechanical properties of HEAs, Zhou designed alloy with composition of AlCoCrFeNiTi*x* by using the strategy of equiatomic ratio and high entropy of mixing 23. The alloy system is mainly composed of BCC solid solution. Through testing, they found that this HEA has excellent compression mechanical properties at room temperature. In particular, the $AlCoCrFeNiTi_{0.5}$ alloy has a yield stress of 2.26 GPa, the fracture strength of 3.14 GPa, and a plastic strain of 23.3%, which is better than most high-strength alloys.

Wang et al. 24 prepared CoCrCuFeNiTi*x* by arc melting of the pure elements and suction casting under an argon atmosphere. The HEA forms a single FCC solid solution of CoCrCuFeNi and $CoCrCuFeNiTi_{0.5}$ alloys. The $CoCrCuFeNiTi_{0.8}$ and CoCrCuFeNiTi alloys are basically composed of a primary FCC solid solution and a eutectic mixture of Fe_2Ti-type FCC phases and Laves phases. With the increase of Ti element addition, the yield strength of the alloy increased from 230 MPa to 1272 MPa. Among them, the compressive strength of $CoCrCuFeNiTi_{0.5}$ alloy was as high as 1650 MPa, and it also

had a wide range of work hardening and a large plastic strain limit of 22 %.

Otto F. 26 produced an equiatomic CoCrFeMnNi high-entropy alloy, which crystallizes in the FCC crystal structure. They found that the HEAs of yield strength, ultimate tensile strength and elongation to fracture all increased with decreasing temperature.

1.5.2 Wear and fatigue properties

Compared to such coatings fabricated from traditional metal-ceramic materials, HEA coatings are characterized by excellent wear resistance and bonding strength, garnering them considerable attention in recent years 27.

Chen et al. 28 investigated the microstructure and mechanical properties of the CoCrCuFeNiNb high-entropy alloy coating. The prepared Nb coating has two phases: the first solid solution phase is FCC; the other is (CoCr) Nb Laves phase. CoCrCuFeNiNb coating shows excellent wear resistance and corrosion resistance. Under the same environmental test conditions, the wear resistance of Nb-containing coatings is about 1.5 times higher than that of non-Nb coatings.

Lin et al. 29 FeCoCrNiAl HEAs coatings were prepared by vacuum heat treatment and laser remelting technology, respectively. Through research, it is found that the spray coating is composed of pure metal and Fe-Cr. The AlNi phase is formed after the vacuum heat treatment process. After laser remelting treatment, BCC structure with less AlNi can be found in the coating. The average hardness value of the sprayed coating is 177 HV, the average hardness value of vacuum heat treatment at different temperatures is 227,266, and the average hardness value of laser remelting is 682 HV.

Experimental data shows that vacuum heat treatment and laser remelting promote the alloying of the coating The process helps to improve the wear resistance of the coating. Among them, the laser remelted coating has the best abrasion resistance.

1.5.3 Corrosion properties

Research has found that the random distribution of elements in the multi-component solid solution and the addition of easily passivating elements (such as Cr, Mo, Ti) make some high-entropy alloys.

Some HEAs present outstanding corrosion resistance even better than the traditional stainless steels.

Shi YunZhu et al. 30 investigated the influence of Al-content and potential-scan-rate on stable / metastable pitting of $Al_xCoCrFeNi$ high-entropy alloys in a 3.5 wt.% NaCl solution. As **Ошибка! Источник ссылки не найден.** showed the comparison of E_p, which represents the resistance to pitting corrosion, and I_{corr}, which is relevant to the corrosion rate of $Al_xCoCrFeNi$ HEAs in the 3.5 wt. % NaCl solution at room temperature with those of some conventional alloys, including stainless steels, Al alloys, Ti alloys, Cu alloys, and Ni alloys. The HEAs data are located at the upper left portion of the figure, which shows that the pitting potential of HEAs are much higher than those of Al alloys, Cu alloys, and some Ti alloys. In addition, the pitting potentials of HEAs are also comparable with those of stainless steel and Ni alloys, which represent the excellent local corrosion resistance of HEAs. The corrosion current densities of HEAs are much lower than those of Cu alloys and some Ti alloys, which indicate the corrosion rate is relatively low.

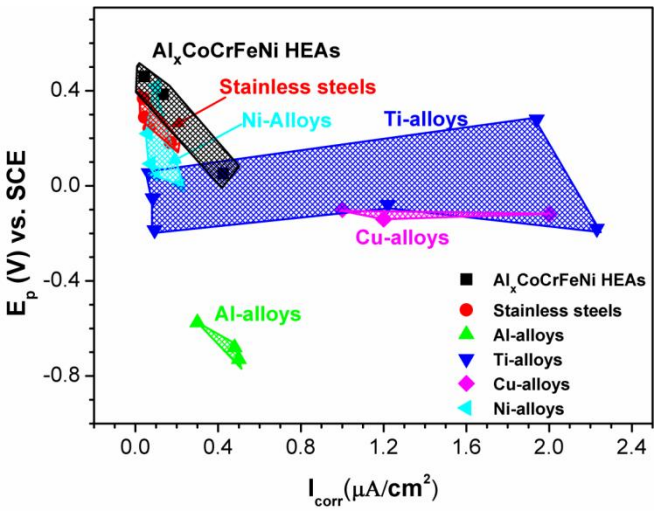

Figure 1.9 – Comparison of E_p and I_{corr} between $Al_xCoCrFeNi$ (x = 0.3, 0.5, and 0.7) HEAs and other conventional alloys in the 3.5 wt. % NaCl solution at room temperature [30]

In general, the local and overall corrosion resistance of $Al_xCoCrFeNi$ HEAs in 3.5 wt. % NaCl solution is equivalent to or better than that of traditional corrosion-resistant alloys.

1.5.4 Oxidation resistance

When a high-entropy alloy is used as a high-temperature material, it not only needs to have good temperature strength, but also requires high temperature resistance.

Qin et al. 31 prepared CoCrCuFeNi–TiO HEAs and researched oxidation resistance of CoCrCuFeNi–TiO HEAs. The results of the oxidation resistance test are shown in Figure 1.10 (a), which shows that the weight of all tested samples increases with the increase of the holding time. In the heat preservation process, the oxidation resistance of the sample is No.2>No.3>No.4>No. 1 sequence. But the rake angle ratio

of the sample after 500 min is No.4>No.3>No.2>No.1, which proves that the larger the amount of Ti_2CO added, the faster the oxidation rate., as shown in**Ошибка! Источник ссылки не найден.** (b) .

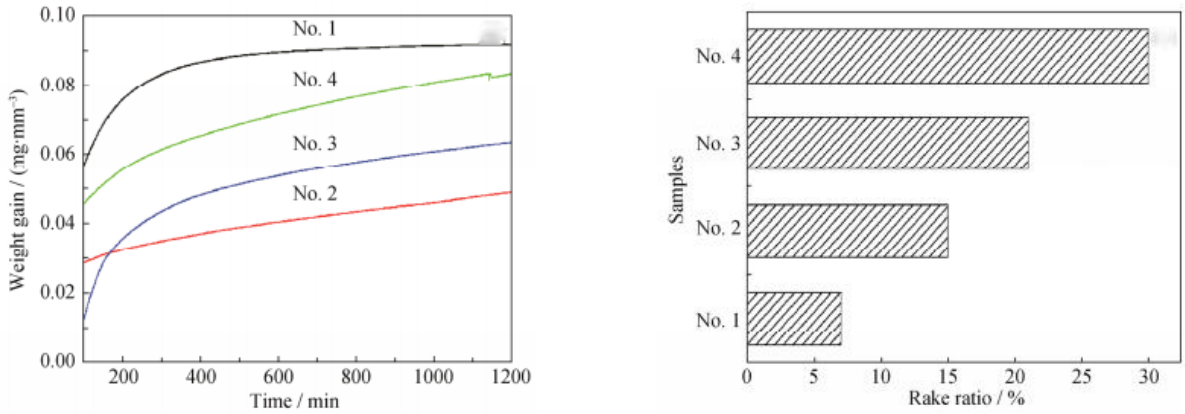

a b

Figure 1.10 – The results of the oxidation resistance tests (a) and the ordering of the rake ratio for the samples (b) 31

This result shows that the oxidation resistance of HEAs increases with the addition of Ti_2CO, and the oxidation rate increases with the formation of TiO.

1.5.5 Other properties

HEAs also have other excellent properties, such as thermoelectric properties, thermal stability, as well as very high resistivity. Thermoelectric materials capable of the direct conversion between heat and electricity have attracted tremendous attention in the past several decades for the engine-waste heat recovery to improve the fuel efficiency. HEAs have a high degree of chaos in its atomic arrangement, resulting in the enhanced

scattering of phonon and effectively reducing its lattice thermal conductivity. The PbSnTeSe HEA was discovered, possessing a quite low lattice thermal conductivity of 0.6 W m^{-1} K^{-1} at room temperature 32. By minor additions of La to substitute Pb, the thermoelectric performance of PbSnTeSe could be further enhanced. At the same time, the HEA has good soft magnetic properties. Zhang et al prepared the $FeCoNi(AlSi)_{0.2}$ HEA by arc-melting method 33, the saturated magnetic strength, coercivity, and electrical resistivity at room temperature reach 1.15 T, 1,400 A m^{-1} and 69.5 mΩ cm^{-1} , which are promising in the high-frequency communication.

1.6 Effect of elements on the structure and properties of HEAs

Because high-entropy alloys are mainly composed of transition metal elements, such as ferromagnetic elements Fe, Co, Ni, ferromagnetic elements Cr and Mn, diamagnetic elements Cu and paramagnetic elements Ti, etc., so high-entropy alloys can achieve excellent electrical, magnetic and other functional characteristics

1.6.1 Effect of Ni on the structure and properties of HEAs

Liu et al 34 investigated the effects of composition and phase constitution on the mechanical properties and magnetic performance of $AlCoCuFeNi_x$ high entropy alloys (HEAs).The results show that Ni element can cause the coexisting phase structure of FCC, BCC and ordered BCC to evolve into a single FCC phase. The change in phase composition increases plasticity but reduces the hardness and strength. $AlCoCuFeNi_{1.5}$ alloy achieves a better balance of mechanical and magnetic properties, it could be used as structure materials and soft magnetic materials.

1.6.2 Effect of Cr and Al on the structure and properties of HEAs

High-entropy alloys containing Al, Cr, Ni and other elements that are easy to oxidize to form a dense oxygen film often have good corrosion resistance. In traditional alloys, adding appropriate amounts of Al, Cr and Si can greatly improve the oxidation resistance of the alloy, because these elements can form a dense and stable oxide layer on the surface at high temperatures. Existing research results show that Al, Cr, Si are beneficial to the improvement of high-entropy alloy high-temperature oxidation performance, while Mn, Ti, Zr, Hf and other elements are not conducive to improving the high-entropy alloy's high-temperature oxidation property.

In the existing high-entropy alloy system, it is found that Cr element can not only promote the formation of eutectic structure of high-entropy alloy and promote the refinement of alloy grains, but also change the solid solution structure of the alloy.Li Xinling 35 explored the effects of Cr and Al on the structure and properties of FeCoCrNiAl high-entropy alloys. the results show that the crystal structures of $Fe_{1.25}CoCr_x$ $Ni_{1.25}Al_{0.25}$ and $Fe_{1.25}CoCrNi_{1.25}Al_x$ alloys are composed of single-phase FCC solid solution. The crystal structure of the alloy does not change with the change of the element content. In mechanical experiments, the yield strength of all as-cast alloys is below 200MPa, and the elongation is above 50 %. After cold rolling and annealing, the strength and hardness of the alloy increase with the increase of element content, but excessive Al element will adversely affect the plasticity of the alloy. In the electrochemical experiment, the appropriate amount of Cr makes the alloy form a denser oxide film during the electrochemical corrosion process, thereby improving the

corrosion resistance of the alloy. The cold rolled and annealed $Fe_{1.25}CoCr_{0.75}Ni_{1.25}Al_{0.25}$ alloy exhibits excellent corrosion resistance. In the magnetic experiment, the reduction of Cr element content helps to improve the soft magnetic properties of the alloy. The cold-rolled and annealed $Fe_{1.25}CoCr_{0.5}Ni_{1.25}Al_{0.25}$ alloy exhibits excellent soft magnetic properties. At the same time, the alloy has an elongation rate of up to 62 % and good workability.

1.6.3 Effect of Co on the structure and properties of HEAs

Co element is ferromagnetic and is a relatively expensive hard and brittle metal. It is usually added to steel in a small amount, but it is not widely used. Under different conditions, the purpose of adding Co is different: sometimes to obtain special magnetism; or to increase hardness; or to increase plasticity; sometimes to increase wear resistance; and it is possible to obtain the above-mentioned comprehensive effect.

Zhang Yong et al 36 found that $Ti_{0.5}CrFeNiAlCo$ high-entropy alloy can form two BCC crystal structures, one with larger lattice parameters and the other with smaller lattice parameters. They added more Co to $Ti_{0.5}CrFeNiAlCo$ alloy to detect changes in crystal structure and properties. Through research, it is found that as the amount of Co added increases, the smaller BCC preferentially transitions to the FCC, and the compressive strength decreases slightly.

1.7 Preparation methods of HEAs materials

The HEAs fabrication technologies were categorized into four main routes. The first route is from the solid state, which involves mechanical alloy (MA), sintering

process, hot pressing process, and spark plasma sintering. The second route is from liquid state, which mainly involves arc melting process, laser melting process, laser cladding process and infiltration process. The third route is thin-film deposition (TFD) techniques, and the last route is additive manufacturing technology (AMT). Discussing below some routes from the four categories.

1.7.1 Mechanical alloying

The preparation method of high-entropy alloy powder is mainly mechanical alloying(MA) method **Ошибка! Источник ссылки не найден.**, which is easier to obtain nanocrystalline or amorphous particles with uniform structure and composition distribution. Mechanical alloying refers to a certain proportion of metal or alloy powder in the ball mill through repeated impacts and collisions between the powder and the grinding ball for a long time.

This method was first used by Benjamin in 1970 to prepare oxide dispersion-strengthened iron-based and nickel-based superalloys 39. Since mechanical alloying is a solid processing technology, it can process raw materials with large melting points, and can also avoid component segregation and eutectic structure caused by liquid phase to solid phase, and ensure that the alloy has a uniform structure and stable property. In the process of preparing high-entropy alloy powder by mechanical alloying, the powder is subjected to various forces such as impact force, shear force and compression force, and diffusion and solid phase reaction occur at the same time. Finally, a nanophase or amorphous phase with uniform structure and composition is obtained. Figure 1.11 is

schematic diagram of mechanical alloying 38.

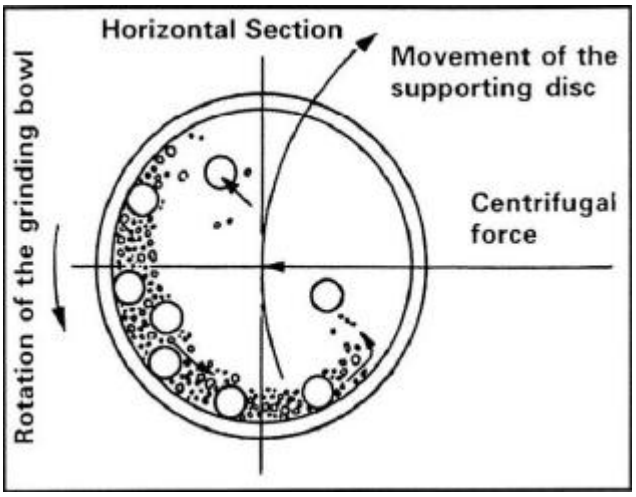

Figure 1.11 – Schematic diagram of the ball moving in the ball mill during mechanical alloying 38

In the process of preparing high-entropy alloy powder by mechanical alloying, the powder is subjected to various forces such as impact force, shear force and compression force, and diffusion and solid phase reaction occur at the same time. Finally, a nanophase or amorphous phase with uniform structure and composition is obtained. Compared with other methods, mechanical alloying to prepare high-entropy alloys can maximize the solid solubility between the main elements and promote the formation of solid solution phases between alloying elements. For some systems with special compositions, mechanical alloys can form a metastable phase or even an amorphous phase 38.

This method has the advantages of simple equipment, low cost, wide range of adjustable components, fine microstructure of the prepared alloy, stable microstructure, good chemical homogeneity, easy formation of unstable phase and supersaturated phase, excellent room temperature processing performance, etc.

Varalakshmi et al 39 reported the nanocrystalline equiatomic HEAs synthesized by

mechanical alloying in the CuNiCoZnAlTi system from the binary CuNi alloy to the senary CuNiCoZnAlTi alloy. The equi-atomic alloys such as nanocrystals have FCC structures up to five-element CuNiCoZn alloys and have BCC structures in six-element CuNiCoZnAlTi alloys. In non-equiatomic alloys, BCC is the main phase in alloys with Cu content lower than 8.33 at.%, while FCC phase is observed in alloys with higher Cu content.

Moravcik I. et al. 40 focused on synthesis and heat treatment of non-equiatomic $AlCoCrFeNiTi_{0.5}$ high entropy alloys, which has a composite structure reinforced by TiC nanoparticles. The initial alloy was prepared by mechanical alloying in a planetary ball mill, compacted by spark plasma sintering and heat-treated at different temperatures. During the mechanical alloying process, a Cr-based supersaturated solid solution with a BCC structure is formed. After spark plasma sintering at 1100 °C, the BCC solid solution decomposed into a nanostructure formed by FCC and ordered BCC solid solution, σ phase and TiC nanoparticles in situ.

Vaidya M. et al. 41 studied the phase transition and thermal stability of nanocrystalline CoCrFeNi and CoCrFeMnNi HEAs prepared through mechanical alloying followed by spark plasma sintering. After mechanical alloying, both alloys showed a single-phase FCC structure, resulting in a small amount of tungsten carbide due to contamination of the grinding media. After Park plasma sintering, with the evolution of Cr_7C_3, the main phase in the two alloys is still FCC.

To further consolidate the powder prepared by mechanical alloying into a bulk sample, the subsequent sintering process is involved. Choosing a suitable sintering process is particularly important for the study of the properties of high-entropy alloys.

In the field of high-entropy alloys, hot isostatic pressing, vacuum hot pressing and spark plasma sintering are all applicable.

~~a)~~ Hot Isostatic Pressing (HIP)

The hot isostatic pressing process takes nitrogen, argon and other inert gases as the pressure transmission medium 42, and places the powder in a closed container. Under the combined action of high temperature and high pressure, the same pressure is applied to the powder in all directions. The powder is pressed and sintered. The processed products are uniformly compressed in all directions, so the processed products have high density, good uniformity and excellent performance. At the same time, the technology has the characteristics of short production cycle, few procedures, low energy consumption, and low material loss. But its equipment is expensive and productivity is low. Hot isostatic pressing sintering will often be used for subsequent processing in the preparation of high-entropy alloys to increase the density of the alloy.

Tang et al 43 studied the microstructure and phase composition of an AlCoCrFeNi high-entropy alloy in as-cast and homogenized conditions. This HEA was synthesized via VAM method followed by consolidation of the as-cast HEA using HIP at 1273 k under 207 MPa for 1 h. The ultimate tensile strength of the as-cast HEA is about 400 MPa and the ductility is 1%, while the ultimate tensile strength of the HIP HEA sample is 393 MPa and the ductility is about 12%. This is because the homogeneous heat treatment of HIP completely changes the microstructure. It can be understood that the improved mechanical properties from HEA can be obtained through the HIP process.

~~b)~~ Hot Pressed Sintering (HPS)

Vacuum hot pressing sintering refers to a sintering method in which dry powder is filled in the model under vacuum, and then pressurized and heated from a uniaxial direction to complete the molding and sintering at the same time. The advantage of vacuum hot pressing sintering is that the purity of the prepared block is relatively high. The disadvantage is that the equipment is complicated, the mold requires high, the energy consumption is high, the process is strict, the efficiency is low, and the cost is high.

Liu X et al 44 prepared $FeCoCrNiMnTi_{0.1}C_{0.1}$ (TiC_{10} alloy) high-entropy alloy by mechanical alloying and vacuum hot-pressing sintering at different temperatures. In the process of the mechanical alloying, the constituent elements were gradually alloyed and formed FCC solid solutions. The microstructure of bulk TiC_{10} alloy is mainly composed of FCC phase as the matrix phase and a small quantity of $M_{23}C_6$, M_7C_3 and $TiMnO_3$ phases. The TiC_{10} alloy has better comprehensive mechanical properties when sintered at 900 °C. The yield strength of the alloy reached 1652 MPa and the hardness of the alloy reached 461 HV.

~~e)~~ Spark Plasma Sintering (SPS)

SPS is a novel sintering technique and is well known as pulsed electric current sintering or pressure-assisted pulse energizing process 45. This technique is mostly used to densify powders in a faster manner due to its effective and remarkable features, namely, energy conservation and fewer procedure steps when compared to the conventional sintering techniques. The principle idea of SPS is that the pressure ram which is work as electrode attached to direct current (DC) source as shown in Figure 1.12. The DC is infltrated (750–1500 A) through the powders by the graphite punch

simultaneously the powder particles are being compressed (25–150 MPa).

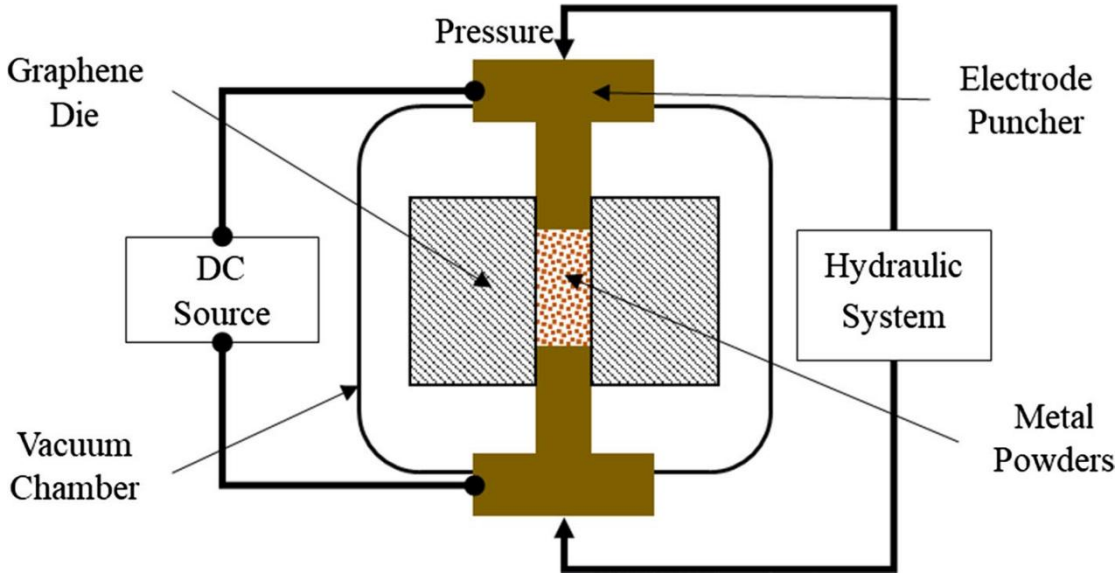

Figure 1.12 – Schematic of the working principle of spark plasma sintering (SPS) process 45

Using SPS, we can make high dense products with nano-structures based on desired sintering parameters. In fact, the principle of SPS is similar to that of HPS, except that SPS applies a controllable pulse current to the mold. Using high pulse current to heat and apply pressure at the same time, the internal particles of the sintered body instantly heat up, and the sintering is completed in a short time, which significantly inhibits the rapid growth of material grains, thereby retaining the internal microcrystalline structure, so that SPS can also be widely used in the preparation of nanocrystalline materials.

1.7.2 Vacuum arc melting

The vacuum arc melting method is currently the most used method for the preparation of high-entropy alloys. Vacuum arc re-melting (VAR) is a process to obtain materials with high degree of homogeneity. It differs from the traditional metallurigal techniques and is able to control the micro-structure more accurately. Usually, the alloy to be VAR is formed into a cylindrical consumable electrode and placed in a crucible in a metallurgical vacuum. Place a small amount of alloy to be remelted at the bottom of the crucible. And put the top electrode close to the material that keeps remelting. The arc between these two parts is generated by passing a few kA of DC current between the two parts. The metal continues to melt, and the top electrode is gradually moved downward by the mechanical pressure head, thereby stably maintaining the arc between the electrodes. The arc between the crucible and the electrode is controlled by designing the crucible to have a larger diameter than the electrode. The crucible is cooled by a water jacket, and the solidification of the material is tightly controlled. The quality of the resulting alloy depends on the cooling rate, the gap between the electrodes and the current.

Yeh et al 0 prepared AlCrCoNiCu bulk high-entropy alloy by the method of "vacuum arc melting + copper mold casting". The powder metallurgy method has the characteristics of low-temperature sintering, avoiding segregation, and high material utilization rate that are not available in the traditional melting and casting method.

Yim et al. 46 have synthesized CoCrFeMnNi HEA reinforced with TiC composite by water atomization, MA and SPS methods. Systematically study of the microstructure evolution and mechanical properties of TiC reinforced HEA composites They believed the role of TiC nano-particles in the strain hardening improvement with

respect to the dislocation-particle interaction and consequently increased dislocation density.

1.7.3 Laser cladding

Laser cladding uses a focused laser beam as a heat source. By focusing on a very small area, it can keep the heat-affected area of the substrate very shallow. Under rapid heating, the substrate is minimally affected by heat and does not deform. The laser cladding structure is a rapid solidification structure. This method not only ensures the excellent performance of the original coating material, but also minimizes the thermal impact on the substrate. Laser cladding can obtain a cladding layer with high hardness, high wear resistance and high corrosion resistance

Qiu Xingwu et al 47 prepared $Al_2CrFeCoxCuNiTi$ high-entropy alloy coating on Q235 steel substrate by laser cladding method, and studied its structure and properties. The study found that the $Al_2CrFeCoxCuNiTi$ high-entropy alloy coating structure is mainly composed of equiaxed crystals with fine spherical particles distributed on the equiaxed crystals. The high-entropy alloy coating is mainly composed of FCC+BCC1+BCC2+Laves phases; with the increase of Co content, the FCC structure increases and the BCC structure decreases; with the increase of Co content, the relative wear resistance of $Al_2CrFeCoxCuNiTi$ high-entropy alloy coating decreases, and the highest value is 3.77.

1.7.4 Physical vapor deposition

Physical vapor deposition processes are atomistic deposition processes in which material is vaporized from a solid or liquid source in the form of atoms or molecules and transported in the form of a vapor through a vacuum or low pressure gaseous (or plasma) environment to the substrate, where it condenses 48. Typically, PVD processes are used to deposit films with thicknesses in the range of a few nanometers to thousands of nanometers; however, they can also be used to form multilayer coatings, graded composition deposits, very thick deposits, and freestanding structures.

Pulsed Laser Deposition (PLD) is also one of the PVD technique. PLD considers fast thin film technique (10–15 min) with high quality compared to other methods. Also, it is a low-temperature process due to which it can be applied to sensitive materials.

Cropper M.D. 49 has been prepared thin films of the high entropy alloy AlCrFeCoNiCu by pulsed laser deposition. The 35nm film was deposited on the glass in ultra-high vacuum at room temperature. The results show that the film deposited at room temperature exhibits a mixture of FCC and BCC reflections. The size of the FCC grains is similar to the film thickness, but the BCC grains are larger. The reflection intensity of the two crystal structures decreases with the increase of the deposition temperature. The decrease of BCC starts at a lower temperature than FCC, which is related to the decrease of Al and Cu content.

1.7.5 Thermal sprayed methods

Thermal spraying refers to a series of processes in which fine and dispersed

metallic or non-metallic coating materials are deposited on the surface of a prepared substrate in a molten or semi-melted state to form a certain spray deposition floor 50.

Liang Xiubing et al 51 used thermal spraying method to prepare FeCrNiCoCu(B) on Mg substrate. They analyzed the structure and properties of the coating. The results show that the two kinds of coatings exhibit compact layered microstructure and the phase lattice type are both FCC, the microhardness of the FeCrNiCoCu coatings reaches 414 $HV_{0.1}$ the bond strength is 36.9 MPa, the microhardness of the FeCrNiCoCuB is 342 $HV_{0.1}$,the bond strength is 33.6 MPa.

1.7.5.1 High-Velocity-Oxygen-Fuel spray (HVOF)

The high-velocity-oxygen-fuel (HVOF) spray process is characterised by high particle velocity (supersonic particle jet) and a comparatively low process temperature. These process characteristics result in coatings with a high bonding strength, as well as a low porosity and oxide content. Lower average particle temperatures, compared to plasma spray, reduce the degree of particle melting and oxidation. Despite the lower average particle temperatures, high coating densities are still achieved through HVOF high particle impact velocities, which deform particles that may not have been well melted 50.

Löbel M. et al 52 investigated the suitability of inert gas-atomised HEA powder for high-velocity-oxygen-fuel (HVOF) thermal spray. The powder and coating showed a multiphase microstructure, while the chemically ordered bcc phase appears as the main phase. The thermal spraying process causes slight changes in the lattice parameters of the main phase and the additional phase. Compared with hard chromium-plated samples,

the wear resistance is improved. In addition, in the scratch test, no brittle behavior occurred under abrasive load. The study of the wear traces shows that there is only slight cracking and peeling under the maximum load.

1.7.5.2 Plasma spray

Plasma spraying uses plasma arc as the heat source to heat the alloy to a molten or semi-molten state and spray it to the surface of the material at high speed. Plasma spraying technology has the following characteristics:

− ultra-high temperature characteristics, which is convenient for spraying high melting point materials;

− the speed of spraying particles is high, the coating is dense, and the bonding strength is high;

− the spraying material is not easy to be oxidized because the inert gas is used as the working gas.

1.7.5.3 Cold spray process

Cold spray is a solid-state material deposition process, which was originally developed as a coating technology in the 1980s 53. In this process, high-temperature compressed gases (typically nitrogen, air, or helium) are used as the propulsive gas to accelerate powder feed-stock to a high velocity (typically higher than 300 m/s), and to induce deposition when the powders impact onto a substrate. The principle is shown in Figure 1.13. In contrast to conventional high-temperature deposition processes, the

formation of a cold spray deposit relies largely on the particle kinetic energy prior to impact rather than the thermal energy. The feed-stock used for cold spray remains solid state during the entire deposition process. Deposition is achieved through local metallurgical bonding and mechanical interlocking which are caused by localized plastic deformation at the inter-particle and particle-substrate interfaces. This allows for the avoidance of defects commonly encountered in high-temperature deposition processes, such as oxidation, residual thermal stress and phase transformation [58]. To improve the deposition effect of cold spraying, the accelerated gas is generally preheated, with a temperature generally less than 600 °C.

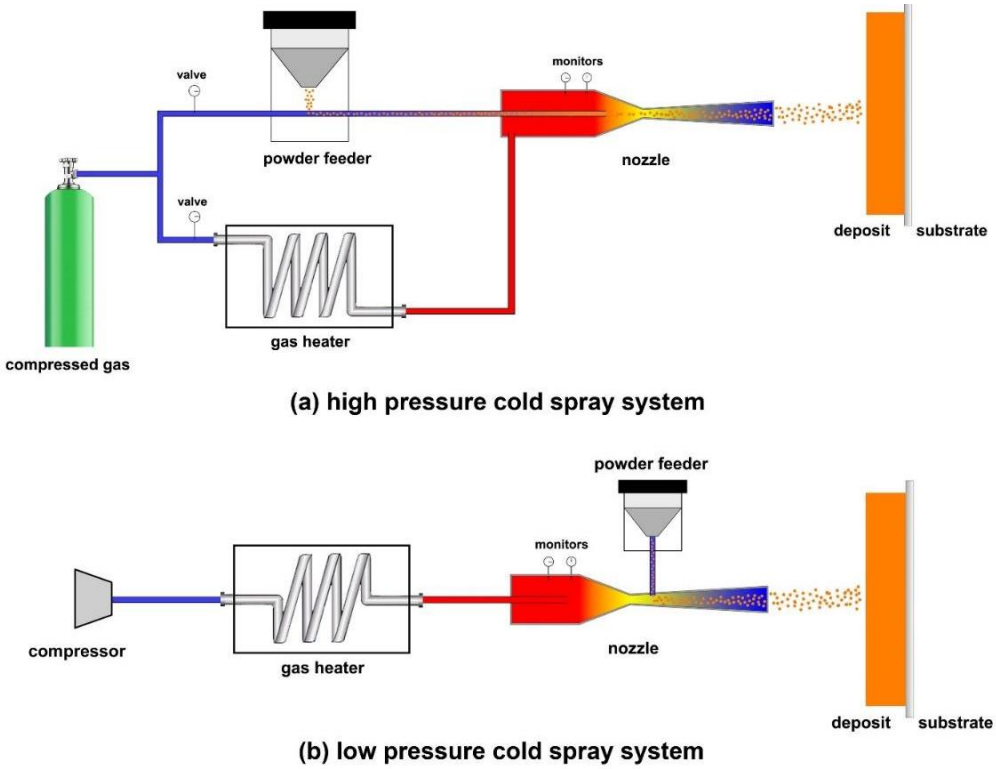

Figure 1.13 – Schematic of high pressure and low pressure cold spray systems 49

Cold spraying is a new surface technology completely different from hot

spraying.Compared with the traditional thermal spraying technology, cold spraying has the following characteristics 54:

a) the deposition temperature is low, with little thermal effect on the coating and substrate.Cold spraying is deposited by strong plastic deformation at low temperature. The deposited particles will not be subjected to obvious thermal action, which can well retain the tissue structure and materialized properties of the original powder, and basically has no oxidation, composition burning, grain growth, composition analysis and other problems;

b) cold spraying on the powder requirements are not high, as long as the particle size can meet the requirements, spraying can generally be implemented.Therefore, the mechanical combination method is usually used freely combined, and the compound powder is prepared, and then cold spraying is applied to obtain a multiple heterogeneous compound coating with uniform composition;

c) the deposition layer has a low porosity and a high binding strength with the substrate. Cold spraying forms the coating based on the high-speed impact of the powder and the substrate and produces severe plastic deformation. During deposition, high velocity impact of subsequent particles tam the first deposited coating. At the same time, the coating did not experience the contraction process of cooling from the melting state, so the obtained coating porosity is low, and the resulting density can be up to 98%, which can be used to prepare some high thermal conductivity, high electrical conductivity, corrosion protection and other coatings. In addition, the compaction of the spray particles enhances the binding strength between the coating and the substrate to over 100 MPa;

d) powder utilization rate is high, safe and environmental friendly. Cold spraying is deposited at low temperature, undeposited powder does not change in low temperature properties, can be recycled to achieve 100% of the spraying powder using .At the same time, the cold spraying operation is simple, safe without radiation, no pollution of the environment, is a green, environmental protection, energy-saving spraying technology.

Zhu Sheng et al 55 prepared AlCrFeCoNi high-entropy alloy coating on Mg substrate by cold spraying method and analyzed its structure and properties. They found that the HEA coatings improve significantly the corrosion resistance of the magnesium alloy surface.

Yin S. 56 prepared FeCoNiCrMn HEA coating by solid-state cold spraying (CS). The experimental results confirm that cold spraying can be used to produce a thick HEA coating with low porosity. As a low-temperature deposition process, cold spraying completely retained the HEA phase structure in the coating without any phase transformation.

Xu Y. et al 57 fabricated about 3 mm thick five-element equimolar high-entropy alloy FeCoCrNiMn by solid-state cold spraying (CS). The FeCoCrNiMn alloy coating exhibits higher parabolic rate constants and more favorable internal oxidation than the bulk HEAs that have similar compositions in the literature.

1.8 Potential applications of high entropy alloys and high entropy coatings

HEAs were widely used in industrial fields due to HEAs have the characteristics of high strength, high hardness, high wear resistance or high temperature softening

resistance:

a) high-entropy alloys can be used to make molds with higher material requirements. Currently, the production of plastic molds and ordinary die steel for extrusion dies is gradually being replaced by high-entropy alloys;

b) HEAs were used welding materials, turbine blades, heat exchangers and heat-resistant materials for high-temperature furnaces, due to its high high-temperature resistance and high compressive strength;

c) the excellent corrosion resistance of HEAs allows it to work in environments prone to corrosion, such as the construction and production of chemical plants and marine vessels;

d) HEAs not only has high hardness and high wear resistance, but also has a low elastic modulus, which makes it very suitable for making golf head hitting surface, hydraulic and pneumatic rods, steel pipes and hard rollers;

e) soft magnetism and high resistivity are also one of the characteristics of high-entropy alloys. Therefore, high-entropy alloys also have great application potential in high-frequency communication devices, which can replace other materials to make high-frequency transformers and motor cores;

f) in addition, high-entropy alloys also have broad development prospects in many other fields, such as biomedical materials, electrical heating materials, hydrogen storage materials, IC diffusion barriers and other industrial fields.

High-entropy alloy coatings exhibit more excellent performance than traditional coating materials and have deep research value. At present, the most extensive research on high-entropy alloy coatings is metal coatings, and some scholars also perform

nitriding, carburizing or adding functional elements to form composite coatings on the basis of which to optimize performance. Researchers have conducted a series of explorations on the application of high-entropy alloy coatings. The main applications of the product are hard protective coatings on the surfaces of tools, molds, etc., and diffusion barrier coatings in microelectronic components 58.

Transition metal nitrides (such as TiN, TiAlN) have the characteristics of high hardness, wear resistance and good oxidation resistance. Some progress has been made in the application research of high-entropy alloys and their nitride coatings on the surface hard coatings of tools, molds, etc.

Shen W.J. et al 59 prepared $(Al_{0.34}Cr_{0.22}Nb_{0.11}Si_{0.11}Ti_{0.22})_{50}N_{50}$ high-entropy nitride coatings by reactive magnetron sputtering. It has been proved to have high hardness and superior oxidation resistance. They founded that hardness of the coating is 36 GPa, which only decreases slightly to 33 GPa after 900 °C annealing either in air or in vacuum for 2 h. No significant change in phase and microstructure were detected after annealing at 1000 °C.

High-entropy nitrides have been attempted as robust diffusion barrier materials to inhibit the severe interdiffusion of Cu and Si; however, the improvement in their diffusion resistance relative to the abilities of few-component nitrides has actually not been verified. Thus, nitride barriers with different numbers of components (metallic elements), from unitary TiN to senary high-entropy (TiTaCrZrAlRu)N (with the same face-centered cubic structure and a thickness of 5 nm), were prepared by Chang S Y 60. The failure of these nitride barrier layers to prevent the mutual diffusion of Cu and Si was examined, and the activation energy of Cu diffusion through the nitride was

determined. With the addition of more components, it was found that the failure temperature of nitrides increased significantly from 550 °C to 900 °C, and the activation energy of Cu diffusion was effectively increased from 107 kJ/mol to 161 kJ/mol. Severe lattice distortion and random cohesion are considered to be the main factors to improve the anti-diffusion ability of multi-component high-entropy nitrides.

At present, the application of high-entropy alloy coatings not only focuses on the above two aspects, but also shows important application prospects in the field of biomedicine.

Biomedical application devices based on high-entropy alloys are mainly focused on load bearing joints, e.g., in knee and hip arthroplasty, and so the proper categorization falls into implant devices, with contact to tissue/bone with a type C duration (more than 30 days) 61.

1.9 Conclusions and statement of the research task

High-entropy alloys are a new type of metal materials that have emerged in the past ten years. High-entropy alloys have unique properties such as high strength, high toughness, high hardness, excellent low temperature toughness, excellent corrosion resistance and radiation resistance due to its effects such as high entropy effect, sluggish diffusion effect, severe lattice-distortion effect and cocktail effect, and high-entropy alloys have a wide range of applications. At the same time, surface treatment technology is an important method to improve and repair the matrix material, which can improve the strength, hardness, wear resistance and corrosion resistance of the material. Preparing a layer of alloy coating on the surface of common industrial materials is one of the most

effective measures for surface treatment. High-entropy alloy coatings are gradually showing superior performance over traditional coatings, and have outstanding performance in terms of hardness, wear resistance, corrosion resistance, and high temperature stability. Regarding the preparation of HEA coatings, various manufacturing methods have been developed. Most of these methods are based on laser cladding, thermal spraying, vapor deposition methods, and a few are related to powder metallurgy 62. At present, there are few studies on the preparation of high-entropy alloys by cold spraying technology. However, there is a series of advantages for preparing HEA coating by cold spraying. The cold sprayed coating has low oxygen content, low porosity, and extremely dense coating due to the spraying temperature is relatively low. At the same time, oxidation reaction, burning loss, and phase change are not prone to occur during the cold spraying process. In order to improve the overall performance of high-entropy alloys, adding appropriate reinforcing phases is also an important way to further improve alloy strength, oxidation resistance, and corrosion resistance.

So, the purpose of this study is to prepare HEA–ceramic composite coatings by cold-spraying and to investigate the structure, phase composition, microhardness. In order to achieve this purpose it is necessary to decide the following:

a) to select and validate the chemical composition of high-entropy alloy;

b) to prepare AlNiCoFeCr HEA by mechanical alloying in a planetary mill;

c) to select the chemical composition of the powder mixture in order to obtain high-strength protective HEA-ceramic coatings on a steel substrate;

d) to prepare powder mixture and steel substrates for HEA-ceramic coating by

cold spraying;

e) to study a HEA–ceramic coatings on steel substrates by cold spraying;

f) to investigate the structure, phase, chemical composition and microhardness of cold-sprayed HEA-ceramic coating on steel substrate;

g) to analyze the results and draw conclusions.

2 EXPERIMENTAL MATERIALS AND PROCEDURES

2.1 The selection of alloy components for multi-component HEA

The high-entropy alloying elements studied in this paper are mainly composed of Al, Co, Cr, Fe, Ni. The atomic radius difference between adjacent elements is small, and there are many similarities in property. Cr, α-Fe and β- Ti has a body-centered cubic structure, and Al, Ni, and γ-Fe have a face-centered cubic structure. Infinite solid solutions can be formed between these elements, which are conducive to the stable combination of elements. The addition of Cr element can make the alloy have higher hardness and good corrosion resistance. Al has larger atomic radii than the first four elements, and has good compatibility with them. The Table 2.1 shows that the basic physical properties of the original elements.

Table 2.1 – The basic physical properties of the original elements

Elements	Atomic number	Atomic radius (Å)	VEC	Melting point (°C)	Crystal structure	Electro-negativity
1	2	3	4	5	6	7
Al	13	1.43	3	660.3	FCC	1.61
Ni	28	1.25	10	1455	FCC	1.91
Co	27	1.25	9	1495	HCP/FCC	1.88
Fe	26	1.24	8	1539	BCC/FCC	1.83

Continuation of table 2.1

1	2	3	4	5	6	7
Cr	24	1.25	6	2130	BCC	1.66

The enthalpy vaviration between different elements ΔH is shown the Table 2.2.

Table 2.2 – The enthalpy vaviration between different elements ΔH(KJ/mol)

Elements	Al	Ni	Co	Fe	Cr
Al	-	-22	-19	-11	-10
Ni	-22	-	0	-2	-7
Co	-19	0	-	-1	-4
Fe	-11	-2	-1	-	-1
Cr	-10	-7	-4	-1	-

In order to select and substantiate the chemical composition of the powder mixture and to predict the phase composition of the AlNiCoFeCr HE alloy / coating, using the Eq. 1.10-1.12 and Eq. 1.16 in the literature 1921 the mixing entropy (ΔS_{mix}), the mixing enthalpy (ΔH_{mix}), the atomic size difference (δ), the valence electron concentration (VEC) were calculated by data in Table 2.1 and

Al	13	1.43	3	660.3	FCC	1.61
Ni	28	1.25	10	1455	FCC	1.91
Co	27	1.25	9	1495	HCP/FCC	1.88

Fe	26	1.24	8	1539	BCC/FCC	1.83

Continuation of table 2.1

1	2	3	4	5	6	7
Cr	24	1.25	6	2130	BCC	1.66

The enthalpy vaviration between different elements ΔH is shown the Table 2.2.

Table 2.2.

The results of calculations of solid solution criteria parameter values in accordance with the mixing entropy (ΔS_{mix}), the mixing enthalpy (ΔH_{mix}), the atomic size difference (δ), the valence electron concentration (VEC) for multi-principle elemental AlNiCoFeCr HEA are generalized in **Ошибка! Неверная ссылка закладки.**.

Table 2.3 – Solid solution criteria parameter values for multi-principle elemental AlNiCoFeCr HEA

S_{mix}(J/mol·K)	H_{mix}(kJ/mol)	δ (%)	VEC(e/at)	Phase composition
13.38	–8.55	5.78	7.2	BCC+FCC

According to the subsection 1.4 phase formation rules and phase prediction for HEAs , the valence electron concentration (VEC) of AlNiCoFeCr HEA is 7.2 . It is known that if this parameter is in the range of values of 6.87 < VEC <8, it can be concluded that the AlNiCoFeCr HEA contains two phases: face-centered cubic structure (FCC) and body-centered cubic (BCC) structure 21.

2.2 The selection of the reinforcing phase

At present, the volume fraction of the reinforcing phase in composite materials is generally 5-20%. The volume fraction of the high-entropy alloy matrix composite reinforcement in the paper was selected as 20 %.

The optional reinforcements usually include carbides, borides, oxides, and can also be intermetallic compounds.

Their common characteristics are high melting point, high specific strength, high specific rigidity and good chemical stability.

In this work, TiB_2 was selected as reinforcement in the composite materials, and its properties were shown in

Table 2.4.

Table 2.4 – Main physical properties of TiB_2 crystal

Density (g/cm^3)	Melting point (℃)	Thermal expansion coefficient (10^{-6}/℃)	Elastic Modulus (GPa)	Tensile Strength (GPa)
4.52	2600	6.39	550	0.28

2.3 Preparation of AlNiCoFeCr high-entropy alloy powder

According to the atomic percentage of AlNiCoFeCr high-entropy alloy, to calculate the mass of each element powder required for each high-entropy alloy. Using an electronic balance (with an accuracy of 0.01 g) to weigh the element powder of the corresponding mass and place it in the same container.

AlNiCoFeCr high-entropy alloy powder was prepared by mechanical alloying .A high-energy planetary mill Retsch PM100 equipment was used to prepare AlNiCoFeCr high-entropy alloy powder. The powders of the elements Al, Ni, Co, Fe, and Cr were mechanically alloyed in a planetary ball mill for 5 hours. Hardened steel balls with a ball-to-powder ratio of 10:1 were used as milling medium. Carbide grinding drums and balls with a diameter of 10 mm were used in the experiment. In order to avoid oxidation, cold welding and excessive agglomeration of AlNiCoFeCr high-entropy alloy powder, the purified gasoline was used as a process control agent. In addition, during the production of HEA alloys in the planetary mill, powder samples were taken at certain intervals to control the structure and phase composition.

2.4 Feed-stock AlNiCoFeCr HEA – TiB_2 powder mixture preparation for cold spraying

The powders of the elements Al, Ni, Co, Fe, and Cr were mechanically alloyed in a planetary ball mill for 5 hours, then add 30 wt. % TiB_2 (ceramics) powder, the alcohol was used as a process control agent. The mass ratio of the initial powders was 70HEA: 30TiB_2.

Drying AlNiCoFeCr HEA powder after the mixture of AlNiCoFeCr (HEA) + 30 wt. % TiB_2 (ceramics) powder.

2.5 Cold spray process for coating deposition

Deposition of powder AlNiCoFeCr - TiB_2 was performed by CS process on a steel substrate using an air with a gun temperature and pressure of 300 °C and 0.85 MPa, respectively.

The stand-off distance between the nozzle and the steel substrate was 30 mm. A commercial cold spray system (DYMET 405) was used in spraying experiments with compressed air.

The cold spray system and the compressor are shown in Figure 2.1 (a) and Figure 2.1 (b), respectively.

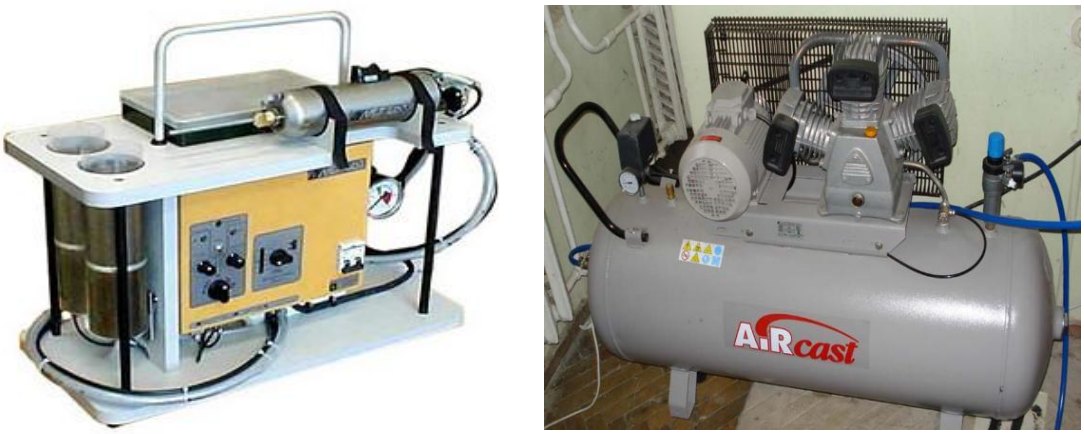

a b

a – Cold spray system; b – compressor

Figure 2.1 – Cold spray system (DYMET 405) and compressor

Just prior to spraying the coatings, the substrate surface was prepared by SiC-blasting, rinsing, and then wiping with solvent to eliminate surface wetness.

2.6 XRD analysis of the structure and phase composition

In this experiment, Ultima IV X-ray diffractometer (Rigaku Co. Japan) was used to analyze the phase composition of the sample and Cold Sprayed coatings . Before the test, first polish one side of the sample smoothly with different types of sandpaper, and then ultrasonically clean the sample with acetone and absolute ethanol.

During the test, in monochromatic Cu-Kα radiation, the operating voltage and current were 30 kV and 20 mA, respectively. The monochromator is a single crystal of graphite in the path of the diffracted beam. The diffraction pattern was obtained by scanning step by step at 2θ (20° – 120°). The scanning angle was 0.04°, and the angular

velocity of the goniometer was 2° / min. The X-ray diffraction data was processed using Powder Cell 2.4 software to perform full profile analysis of X-ray spectra. The lattice parameters of the solid solution were calculated by linear extrapolation according to the position of the center of gravity of the diffraction pattern. The crystallite size (coherent-scattering region) in the milled powders as well as after consolidation by CS process has been calculated from the XRD peak broadening using peak profile analysis after eliminating the instrumental and strain contributions.

2.7 Microstructural characterization

A scanning electron microscope (SEM) was used to examine the microstructure of the feedstock material powder and cold spray coating.

Analysis of chemical element composition was carried out by energy dispersive spectrometer (EDS).

2.8 Vickers microhardness measurements

The Vickers microhardness tester PMT-3 was used to measure Vickers microhardness measurements on the cross-section of the coating in accordance with standard procedures. Due to the unevenness of the material structure, in order to ensure the accuracy of the test data, 5 points on each sample are selected for testing to obtain the average value as the final result.

Experimental parameters: the applied load pressure is 50 g, and the load holding

time is 10 s. The calculation of hardness is shown in formula (2.1):

$$\mathrm{HV} = \frac{2\mathrm{P}\sin(\frac{\propto}{2})}{\mathrm{d}^2}, \tag{2.1}$$

where P is the applied pressure load which unit is g; α is the angle between the opposite sides of the diamond indenter, which is 136º; d is the average value of the diagonal of the indentation which unit is μm.

The standard deviation of the random error of the hardness measurement results is determined by the formula:

$$\pm\sigma = \sqrt{\frac{\sum_n \left(HV_c - HV_n\right)^2}{n-1}}, \tag{2.2}$$

where ±σ is the standard deviation of the random error of the hardness measurement results;

HV_c – is the arithmetic mean value of the hardness numbers obtained in the "n" measurements;

HV_n – hardness number obtained in a concrete measurement;

n – is the number of measurements.

2.9 Experimental program and experimental procedure

In order to ensure that the experimental work is carried out in a planned and orderly manner, the following experimental procedures have been developed.

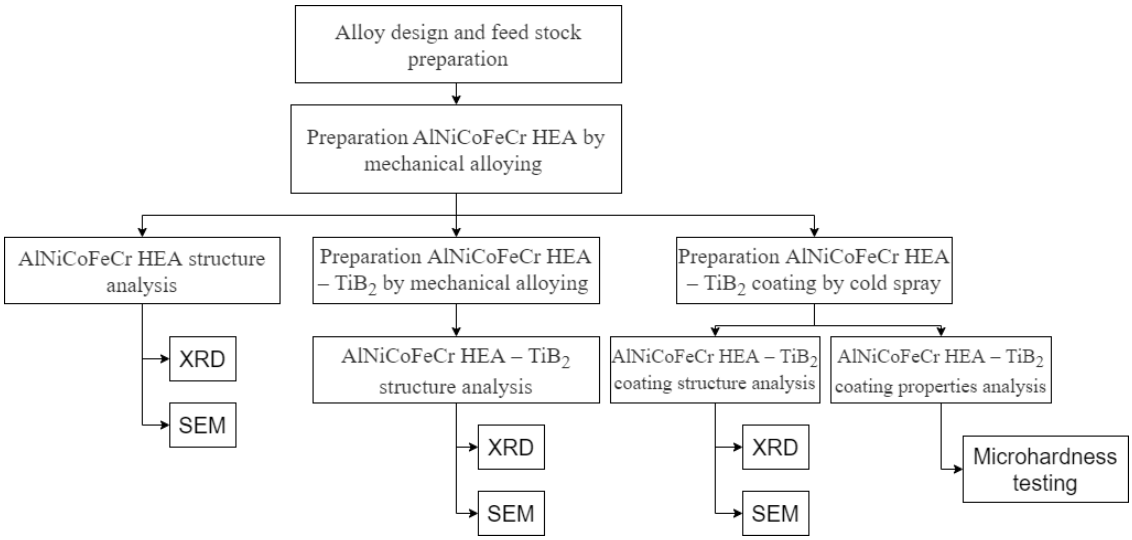

Figure 2.2 – Experimental procedure

Ошибка! Источник ссылки не найден. is the technical procedure for this experiment. It is mainly divided into six parts:

- the AlNiCoFeCr high-entropy alloy powder was prepared by ball milling;
- the structure of AlNiCoFeCr HEA was analyzed;
- the AlNiCoFeCr HEA – TiB_2 mixture was prepared by ball milling;
- the structure of AlNiCoFeCr HEA – TiB_2 mixture was analyzed;
- the AlNiCoFeCr HEA – TiB_2 coating was prepared by cold spray technology;
- the structure and properties of AlNiCoFeCr HEA – TiB_2 coating was analyzed.

3 RESULTS AND DISCUSSION

3.1 Structure and phase composition of AlNiCoFeCr HEA powder resulted from mechanical alloying

The powder of the elements Al、Ni、Co、Fe and Cr were ball milled together through the planetary mill in the gasoline. Powder samples were taken out at different stages of ball milling and enter into characterization. The Figure 3.1 shows the X-ray diffraction spectra of the equiatomic mixture of powders of the AlNiCoFeCr HEA at different stages of mechanical alloying .

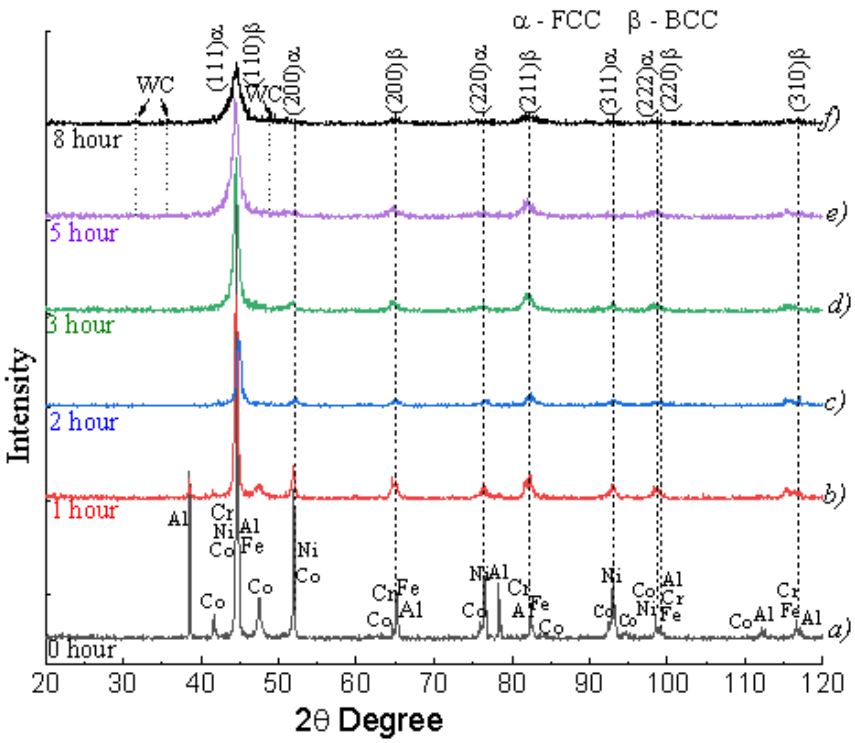

a – mixture of starting powders, 0 hour; b – 1 hour; c – 2 hours; d – 3 hours; e – 5 hours; f – 8 hours

Figure 3.1 – X-ray diffraction spectra of the equiatomic mixture of powders of the Al-Ni-Co-Fe-Cr system at different stages of mechanical alloying

It can be seen from Figure 3.1 that at the initial stage of ball milling (0 h), the diffraction peaks corresponding to the alloy constituent elements (Fe, Ni, Co, Cr, and Al) can be clearly found on the XRD pattern of the initial powder mixture. The X-ray diffraction spectra show that the alloy elements of Co and Al have strong blurring and low intensity after 1 hour of grinding the mixture of initial powders (Figure 3.1, b), and after 2h of ball milling, the diffraction peak intensity of each element decreases sharply. Their diffraction maxima are very complex after 2 hours of MA (Figure 3.1, c), the diffraction peaks corresponding to the Al element basically disappeared, and the intensity of the diffraction peaks of the Ni, Fe and Cr elements continued to decrease. There is a system of lines corresponding to disordered BCC and FCC solid solutions of substitution based on Fe-Cr in the diffraction spectrum, which have a BCC lattice and unlimited mutual solubility and Ni-Co. This indicates the beginning of the alloying process, which occurs during the grinding of grains / crystallites of elementary components to nanoscale 62, 63.

When equiatomic AlNiCoFeCr powder mixture processed to 3 hours by MA (Figure 3.1, d), the maximum diffraction intensity of Fe-Cr and Ni-Co is significant decrease, and the diffraction peaks width is increased, which indicates a significant decrease in the crystallite size and an increase in the magnitude of microstresses due to severe plastic deformation in the process of mechanical alloying, as well as the crystal lattice distortion through the mutual dissolution of atoms of components with different atomic radii 63.

When equiatomic AlNiCoFeCr powder mixture processed to 5 hours and 8 hours by MA (Figure 3.1, e, f), almost all the maximum diffraction of the FCC solid solution (α-phase) disappear and clearly seen diffraction maximum was remained at diffraction

angles in the diffraction X-ray spectrum. The diffraction pattern exhibits 5 peaks at different angles, corresponding to β - phase – (110) β, (200) β; (211) β; (220) β; (310)β, respectively. There are a set of lines of β-phase noticeable intensity can be seen in XRD spectra e and f. As for the FCC phase, there are barely noticeable very blurred lines of this phase. Therefore, this indicates the formation of a nanostructure in the BCC and FCC solid solutions, rather than amorphization. WC contamination was observed after 5 hours of milling and increased thereafter. During 8 hours of MA, the formation of an amorphous phase (partial amorphization of the solid solution) is observed, the diffraction intensity is decreased, but the diffraction peak width is increased, which indicates that severe plastic deformation or the long-range order of atoms in the alloy will be destroyed in the mechanical alloying process.

Yeh et al. 64 prepared $Al_xFeNiCoCr$ (x=0~1.8) high-entropy alloys with different aluminum content by vacuum arc melting, and studied the change trend of the phase composition: when the Al content is 0~0.3, the alloy is a single-phase FCC solid solution; when the aluminum content is 0.5-0.7, the alloy has a dual-phase structure of FCC+BCC; when the Al content is 0.9-1.2, the alloy has a single-phase BCC structure below 873 K, and above 873 K is a FCC+BCC structure; when the content of Al is 1.5~1.8, it has a single-phase BCC structure.

A detailed study of the phase composition and microstructure of the as-cast AlFeNiCoCr high-entropy alloy showed that the BCC phase of HEA was composed of disordered BCC (A2) Fe-Cr rich phase and ordered BCC (B2) Al-Ni rich phase with almost equal lattice parameters. Moreover, there are traces of Ni-rich and Fe-rich phases and composition fluctuations on the atomic scale 65, 66.

Fu Zhiqiang et al. 67 used ball milling to obtain $FeNiCrCo_{0.3}Al_{0.7}$ high-entropy alloy powder for 45 hours, and then solidified the alloy powder at 1000 °C with a spark plasma sintering . The results showed that after 30 hours of ball milling, the high-entropy alloy powder was completely alloyed to form a solid solution with a single-phase BCC structure. During the sintering process, part of the metastable BCC phase was transformed into FCC phase, and the alloy block obtained by sintering has a dual-phase (FCC+BCC) structure. $FeNiCrCo_{0.3}Al_{0.7}$ alloy showed excellent mechanical properties, with its compressive yield strength reaching 2.03 GPa, compressive fracture strength of 2.64 GPa, fracture strain of 8.12 %, and hardness of 624 HV.

The AlNiCoFeCr HEA finally formed of BCC and FCC solid solution phases during the process of mechanical alloying. Our results indicate that AlNiCoFeCr HEA was finally formed from the BCC and FCC solid solution phases during mechanical alloying.

As calculated before, the valence electron concentration (VEC) of AlNiCoFeCr HEA is 7.2. It is known that if this parameter is in the range of values of 6.87 <VEC <8, then there is the formation of solid solutions with BCC and FCC crystal structures 21, which we observe in the spectra of X-ray diffraction (see Figure 3.1).

It can be seen from table 2.2 that the mixing enthalpy of Fe, Co, Cr, and Ni is negative and close to 0, indicating that these elements are prone to solid solution during the alloying process. However, Al and Ni have a relatively negative mixing enthalpy, which is easy to combine into intermetallic compounds. Taking into account the atomic radius of each element and the mixing enthalpy of the atom, in the AlNiCoFeCr high-entropy alloy, the Al element has a greater influence on the formation of the BCC

phase or FCC phase in the alloy. In summary, it is inferred that the alloying order of the elements in the AlNiCoFeCr high-entropy alloy is Al→Co→Ni→Fe→Cr, which is consistent with the results of Chen et al 68 . The alloying rate of the elements and the melting point of the metal is negatively correlated in the high-entropy alloy, that is, the lower the melting point, the faster the alloying. Because the low melting point element has a higher intrinsic diffusion coefficient, it will dissolve into the new crystal structure faster. In addition, when the melting point of the elements are close each other, such as Co and Ni, their alloying rate is determined by their plasticity, that is, the element Co with poor plasticity is more easily broken during the ball milling process than the element Ni with better plasticity, which is conducive to alloying .

Morphology and microstructure of the equiatomic AlNiCoFeCr HEA powder are shown in Figure 3.3 (a-h).

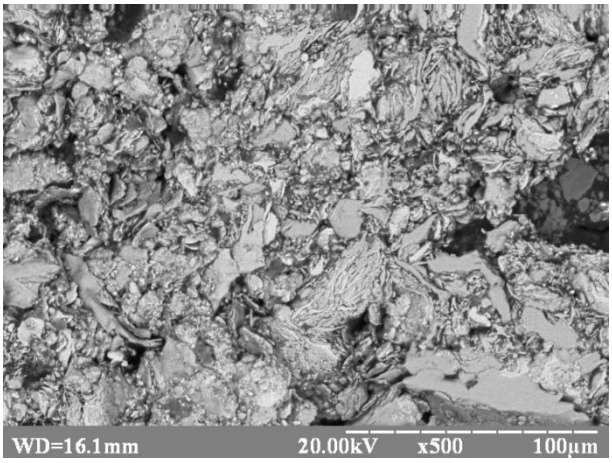

a

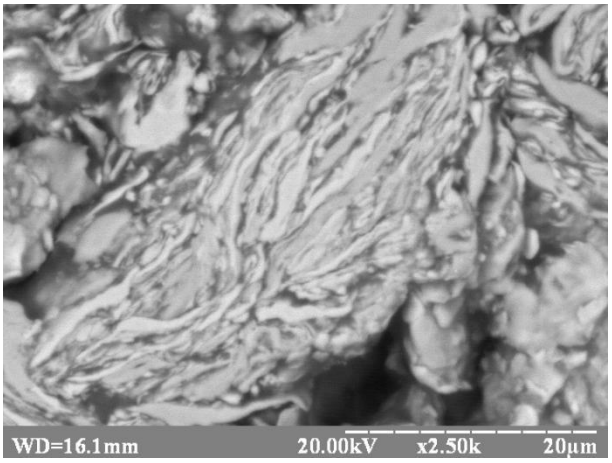

b

a, b – 1 hour; c, d – 2 hours; e, f – 3 hours; g, h – 5 hours

Figure 3.2, sheet 1 – SEM images of equiatomic AlNiCoFeCr HEA alloy powder at different stages of mechanical alloying

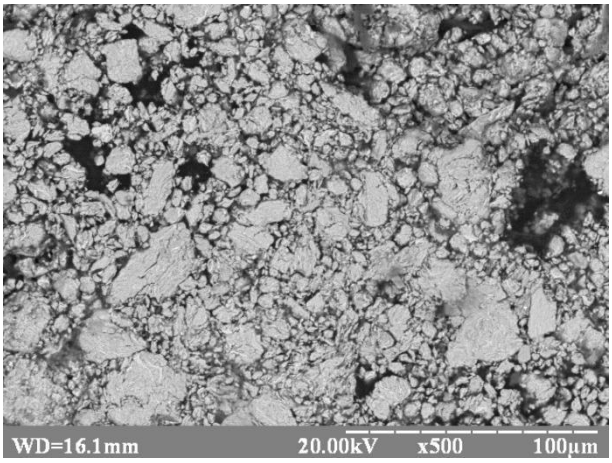

c

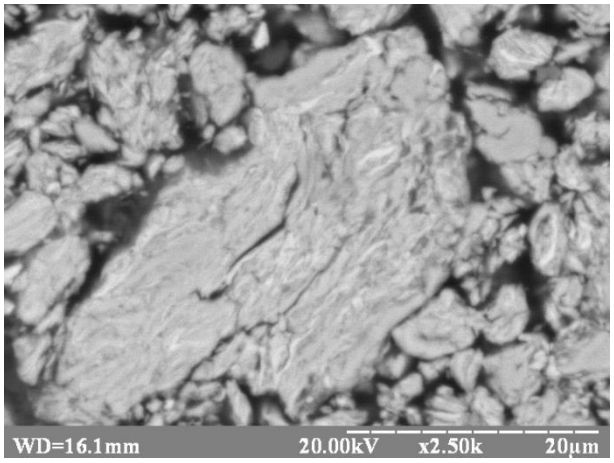

d

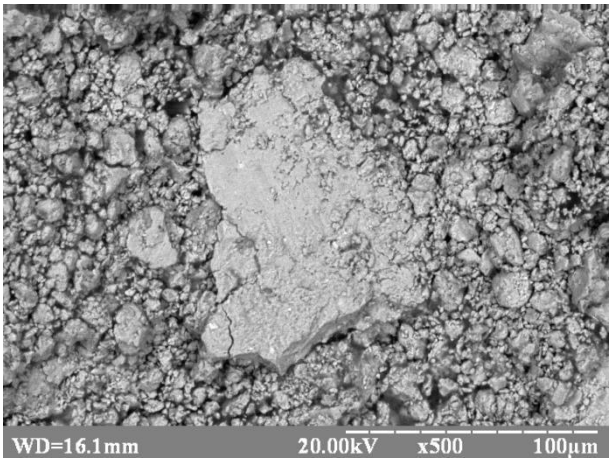

e

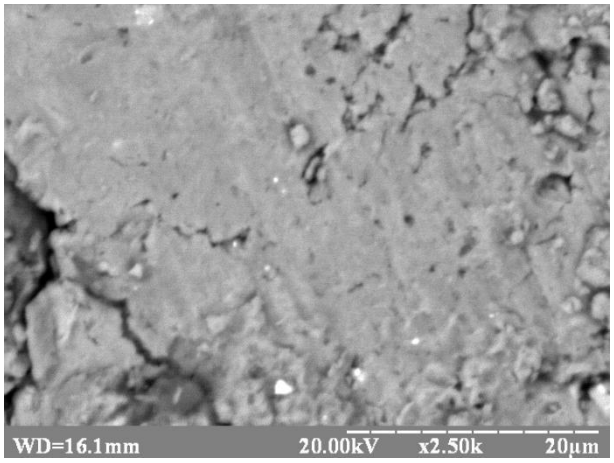

f

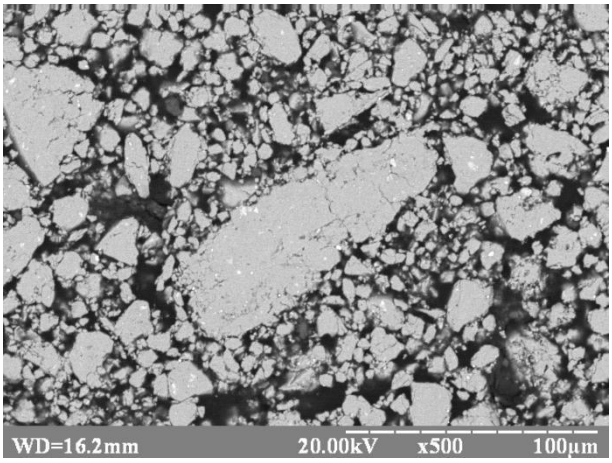

g

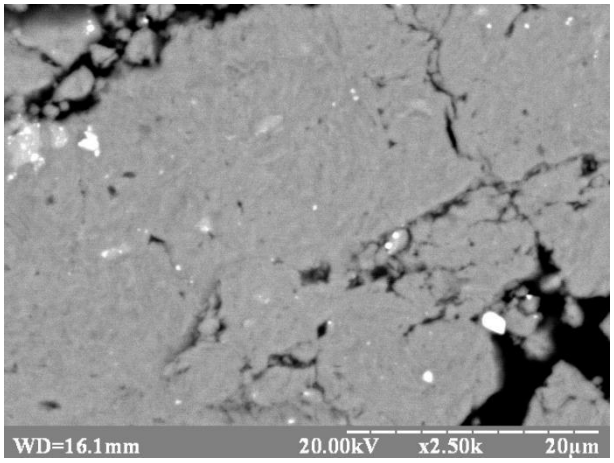

h

a, b - 1 hour; c, d - 2 hour; e, f -3 hour; g, h - 5 hours

Figure 3.3, sheet 2 – SEM images of equiatomic AlNiCoFeCr HEA alloy powder at different stages of mechanical alloying

When the initial powders of the equiatomic AlNiCoFeCr HEA was mixed and reacted in a planetary ball mill for 1 hour, the alloy solid solution is not formed, and the alloy powder has only significant plastic deformation, corresponding to the reduction of diffraction intensity (Figure 3.1 b). SEM images of equiatomic AlNiCoFeCr HEA alloy powder of the microstructure (Figure 3.3 a, 3.2 b) are fully consistent with the X-ray diffraction spectra (Figure 3.1, b).

When the powders of the equiatomic AlNiCoFeCr HEA was mixed and reacted in a planetary ball mill for 2 hours, the AlNiCoFeCr powder mixture (Figure 3.3, c, d) still have a layered structure, however, the lamella thickness becomes much smaller, and the structure is more homogeneous. In the X-ray diffraction spectrum (Figure 3.1, c), the reduction of the maximum diffraction intensity and the increase of their blur phenomenon are obvious, which indicates that the size of the grains/crystallites is reduced, which in turn leads to the diffusion process enhancement between the components. At this stage, it was observed that solid solutions with FCC and BCC crystal structures based on Ni (α-phase) and Cr and Fe (β-phase) began to form.

When the initial powders of the equiatomic AlNiCoFeCr HEA was mixed and reacted in a planetary ball mill for 3 hours, the microstructure of the AlNiCoFeCr HEA powder becomes homogeneous (Figure 3.3 e, 3.2 f); when the powders of the equiatomic AlNiCoFeCr HEA was mixed and reacted in a planetary ball mill for 5 hours, the microstructure of the AlNiCoFeCr HEA powder becomes more homogeneous (Figure 3.3 g, 3.2 h). In addition, in the microstructure clearly detected particles of WC carbide, which is also observed in the X-ray diffraction spectrum (Figure 3.1 e, 3.1 f), it shows that the alloy is contaminated by the cemented carbide WC from the vial and milling

balls during the long time ball milling process. The microstructure analysis results of structure and phase composition formation stages of the equiatomic AlNiCoFeCr HEA alloy are completely consistent with the X-ray diffraction data.

Analysis of chemical element composition of equiatomic AlNiCoFeCr HEA alloy powder at different stages of mechanical alloying was carried out by energy dispersive spectrometer (EDS). The

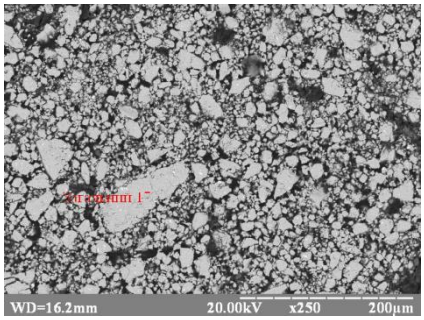

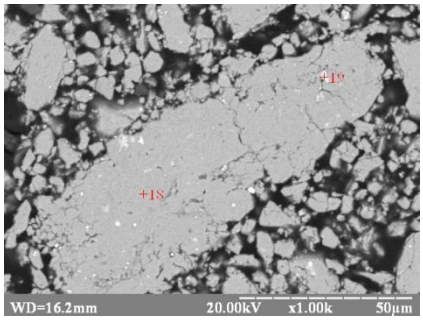

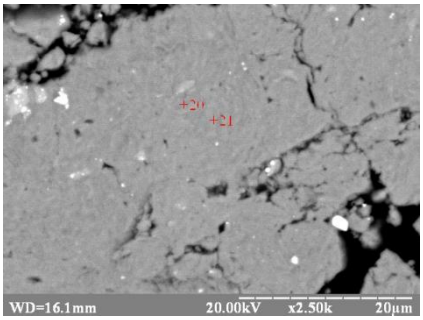

i j k

a-c – 1 hour.; d-e – 2 hours.; f-h – 3 hours.; i-k – 5 hours

Figure 3.5 is SEM images of equiatomic AlNiCoFeCr HEA powder at different stages of mechanical alloying, and designation the analysis area.

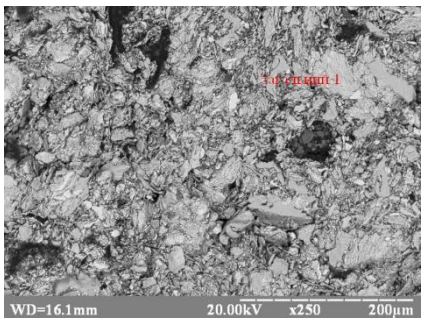

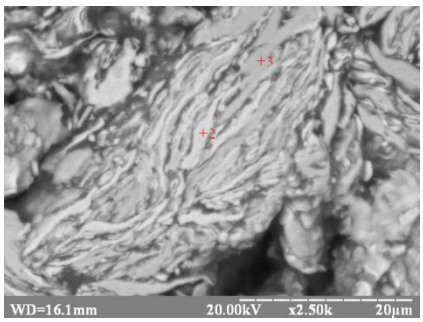

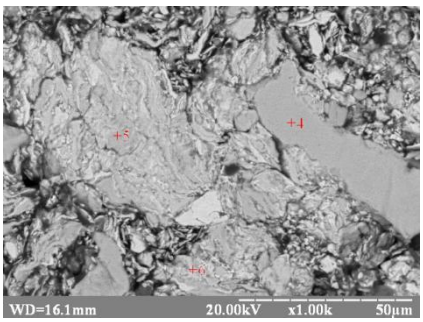

a b c

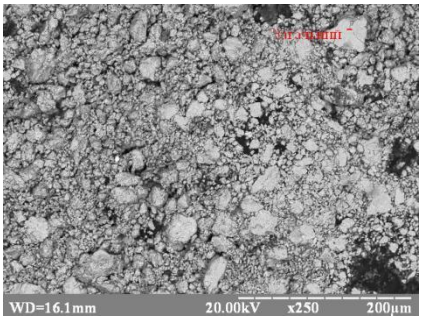

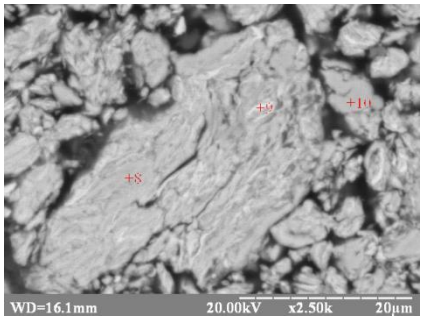

d e

a - c – 1 hour; d - e – 2 hours; f - h – 3 hours; i - k – 5 hours

Figure 3.4, sheet 1 – SEM images of equiatomic AlNiCoFeCr HEA alloy powder at different stages of mechanical alloying, and designation the analysis area

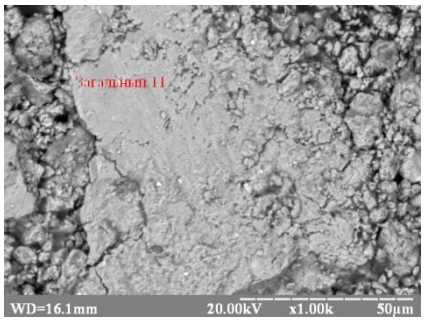

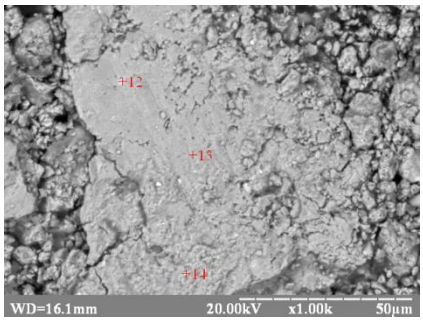

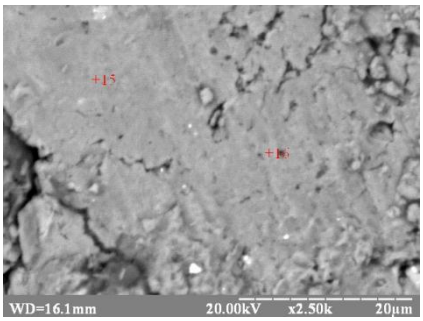

f g h

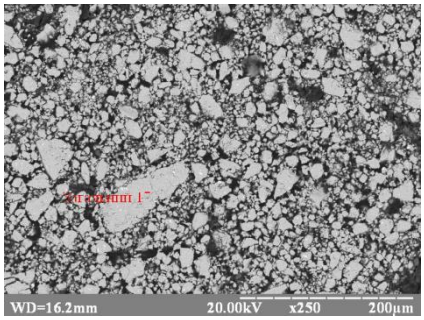

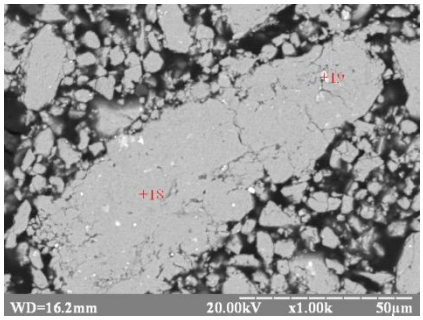

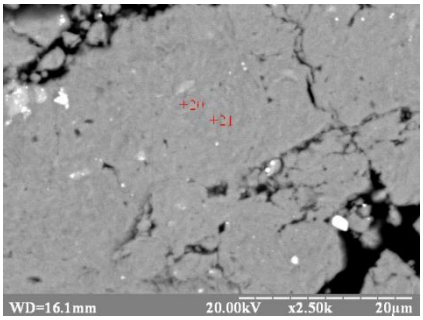

i j k

a-c – 1 hour.; d-e – 2 hours.; f-h – 3 hours.; i-k – 5 hours

Figure 3.5, sheet 2 – SEM images of equiatomic AlNiCoFeCr HEA alloy powder at different stages of mechanical alloying, and designation the analysis area

It can be seen from figure 3.3 that the microstructure morphology of HEA is

composed of large irregularly shaped areas and small elliptical areas. The table 3.1 is the EDS analysis result of the designated areas 1-21 in the SEM images of the equiatomic AlNiCoFeCr high-entropy alloy. It can be seen from table 3.1 that regions 3, 4, 5, 8, and 10 have Cr content higher than the nominal composition, which means that Cr is segregated. The reason for the formation of this Cr-rich phase is that the element Cr has the highest melting point among the various components of HEA (Fe, Ni, Co, Cr), its self-diffusion coefficient is the lowest, and the alloying rate is the slowest. A small part of the Cr element is not fully diffused and solid-dissolved into the new phase during the process of mechanical alloying.

Table 3.1 – Chemical composition of the AlNiCoFeCr HEA at different stages of mechanical alloying

Time (MA) /hour	Designation	Elements, at. %								σ
		Al	Ni	Co	Fe	Cr	O	impu-rities*	W	
	Nominal	20,00	20,00	20,00	20,00	20,00	–	–	–	
1	1(General)	18,30	12,34	4,16	5,18	17,95	19,10	0,65	–	6,75
	2	2,62	83,21	4,71	3,91	1,72	3,83	–		35,78
	3	4,12	1,45	2,03	3,90	87,8	–	0,71		38,00
	4	–	–	–	0,25	98,88	–	0,86		69,74
	5	6,25	12,36	11,69	4,12	65,59	–	–		25,73
	6	4,95	6,27	7,72	70,69	2,77	6,66	0,94	–	29,24

2	7(General)	22,31	13,39	14,80	22,82	9,43	17,25	–		5,84
	8	6,76	3,37	8,28	3,92	76,93	–	0,73		31,97
	9	8,27	68,34	6,21	4,38	5,37	6,55	0,88		27,89
	10	1,03	1,66	1,01	1,22	94,05	–	1,04		41,51
3	11(General)	14,67	14,27	16,79	13,33	28,15	12,80	–	–	6,12
	12	16,15	3,82	6,17	12,59	12,13	18,35	29,42	22,01	5,04
	13	16,85	11,88	16,54	27,76	16,18	9,76	1,02	–	5,90
	14	5,28	7,64	7,02	7,48	7,32	27,32	–	37,94	0,96

Continuation of table 3.1

Time (MA) /hour	Designation	Elements, at. %								σ
		Al	Ni	Co	Fe	Cr	O	impu-rities*	W	
	Nominal	20,00	20,00	20,00	20,00	20,00	–	–	–	
3	15	17,31	16,37	20,68	24,03	15,66	55,95	–	–	33,50
	16	15,92	24,31	21,21	24,12	9,26	5,18	–	–	6,40
5	17 (general)	17,98	15,99	18,14	20,02	15,06	12,81	–	–	1,95
	18	18,85	15,63	17,56	22,30	19,82	4,61	1,24	–	2,49
	19	15,96	2,45	3,79	15,4	15,83	–	31,24	2,63	6,93
	20	18,77	20,99	17,04	16,52	25,61	–	1,07	–	3,69
	21	17,43	17,97	17,79	17,9	23,31	4,63	0,96	–	2,49

* Impurities obtained both from the original powders and in the process of MA: Si, S, Mo,Nb.

According to the EDS results, it can be seen that there are fluctuations in composition in some designated areas, and segregation of different elements occurs. In fact, compared with other principal elements, the atomic radius of Al is much larger, and the lattice distortion caused by solid solution is larger, which is not conducive to its diffusion between atoms. In the AlNiCoFeCr high-entropy alloy, Al and Ni have the most negative atom pair mixing enthalpy (–22 $kJ \cdot mol^{-1}$), which means that Ni atoms tend to occupy the positions of Al atoms, and the two are easy to combine. At the same time, there is also a relatively negative mixing enthalpy between Co and Al elements, the mixing enthalpy is –19 $kJ \cdot mol^{-1}$, and the mixing enthalpy between Co and Ni elements with similar atomic sizes is 0 $kJ \cdot mol^{-1}$, which makes it easy for Co and Ni to form a solid solution. The atomic size difference between Fe, Cr and Co elements is very small, the mixing enthalpy of Fe-Cr is –1 $kJ \cdot mol^{-1}$, the mixing enthalpy of Fe-Co is –1 $kJ \cdot mol^{-1}$, the mixing enthalpy of Co-Cr is –4 $kJ \cdot mol^{-1}$ and the enthalpy of mixing between them is very close to 0 $kJ \cdot mol^{-1}$, which is conducive to the formation of solid solution, thus, the solid solution phase rich Fe-Ni-Co to form in AlNiCoFeCr high-entropy alloy. Therefore, in the two phases formed by the AlNiCoFeCr high-entropy alloy, one phase usually is the Al-Cr-rich BCC structure, and the other phase is the Fe-Ni-Co-rich FCC structure.

From the standard deviation value in table 3.1, it can be seen that the standard deviation of the mechanical alloying for 3 hours is reduced from 6.75% to 6.12% compared with that of the mechanical alloying for 1 hour. The local standard deviation decreased from 35.73 % – 38 % to 3.5 % – 6.4 %.

3.2 Characterization of feedstock AlNiCoFeCr HEA–TiB_2 powder for cold spraying coating

The mechanical alloyed HEA powder and the TiB_2 powder were ball milled together through the planetary mill in the alcohol. The content of the HEA powders was 70 wt. % and the TiB_2 content was 30 wt. %.

The Figure 3.6 shows the X-ray diffraction spectra of AlNiCoFeCr HEA – TiB_2 powder mixture at different stages of mechanical milling.

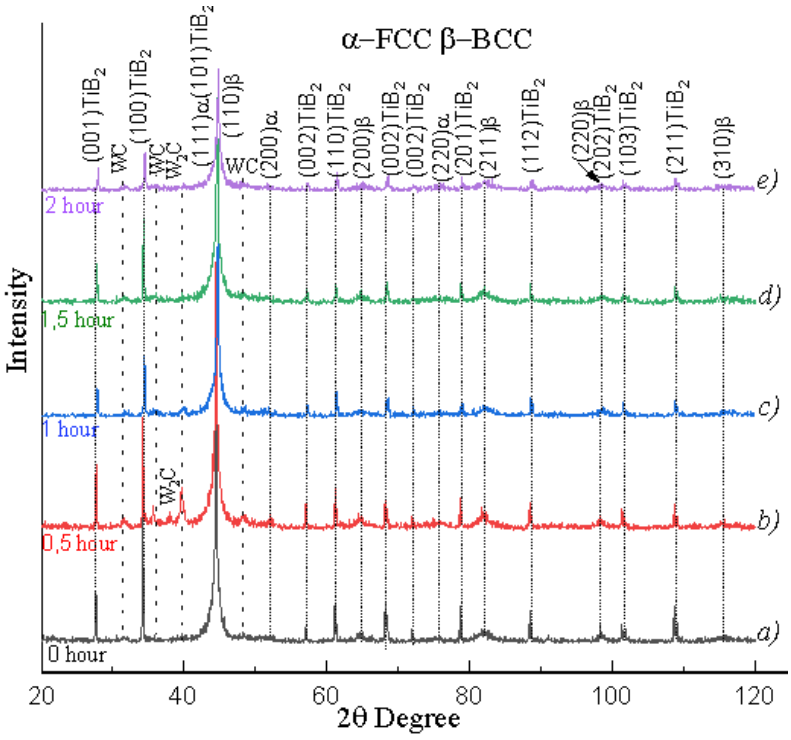

a – the initial mixture of powders, 0 hour; b – 0.5 hour; c – 1 hour; d – 1.5 hours; e – 2 hours

Figure 3.6 – X-ray diffraction spectra of a mixture of AlNiCoFeCr – 30 wt.% TiB_2 powders with different mixing time

It can be seen from figure 3.4 that at the initial stage of ball milling (0 h), the diffraction peaks are main 3 phases in the HEA – TiB_2 composite materials: (i) the FCC solid solution (α-phase), (ii) the BCC solid solution (β-phase), (iii) TiB_2. After 0.5 hour of ball milling, the diffraction peak intensity of TiB_2 decreased, which may be due to the smaller particle size of TiB_2 powder after ball milling and the increase of lattice strain, resulting in decreased diffraction intensity of each crystal plane. At the same time, a small amount of WC and W_2C were detected, which indicates that the alloy was contaminated by cemented carbide balls during the ball milling process. After 1 hour of ball milling, the intensity of diffraction peaks decreased. After the alloy powders continues to be ball milling for 1.5 hours, the diffraction peaks can be seen to broaden, which indicates that the grains are further refined. At the same time, the grain refinement process is accompanied by strong lattice strain, which is mainly due to the process of mixing, the phase composition does not change, the formation of the alloy has already occurred in the process of MA and the initial elements have already been dissolved, the increase in the volume fraction of the grain boundary caused by the grain refinement. As well, it also leads to strong deformation caused by cold welding and crushing during the ball milling process due to the grain refinement. After the alloy powder is ball milled for 2 hours, the intensity of the diffraction lines of BCC and FCC solid solutions as well as titanium diboride lines intensity decreases and they become even more broadened.

Morphology and microstructure of the AlNiCoFeCr HEA + 30 wt. % TiB_2 powder mixture are shown in Figure 3.8 (a-h).

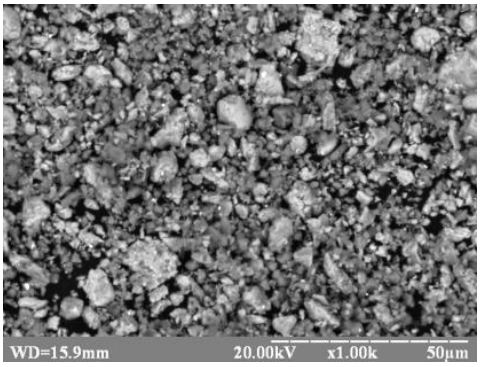

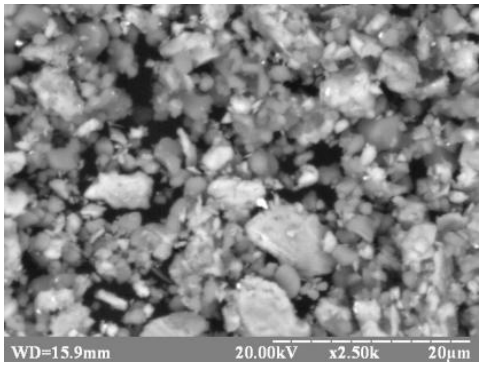

a b

a, b – 0,5 hour.; c,d – 1 hour.; e, f –1,5 hours.; g, h – 2 hours

Figure 3.7, sheet 1– SEM images of a mixture of powders AlNiCoFeCr HEA + 30 wt. % TiB_2 after different mixing times in a planetary mill

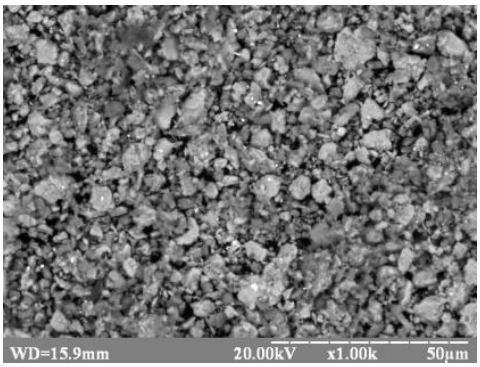

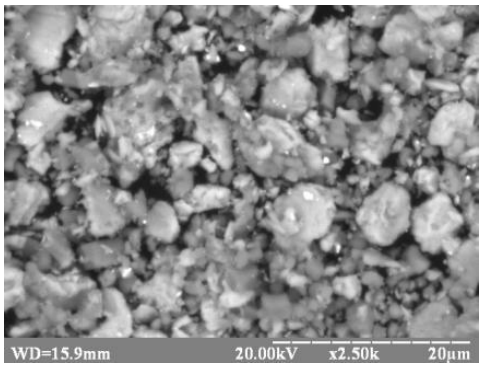

c d

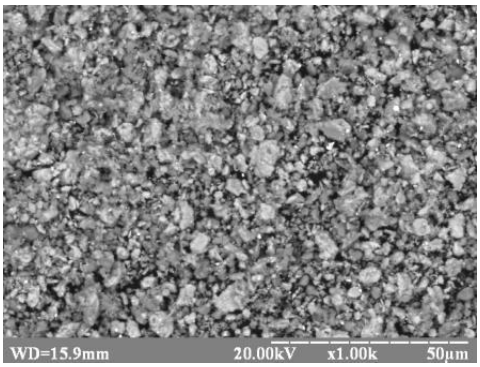

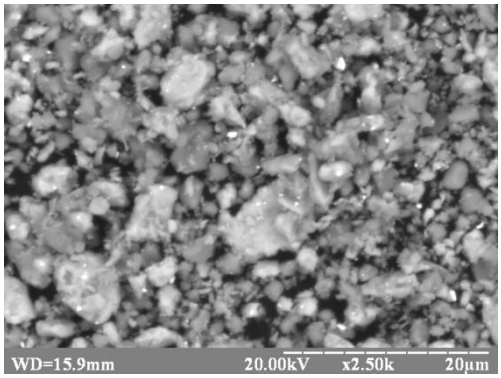

e f

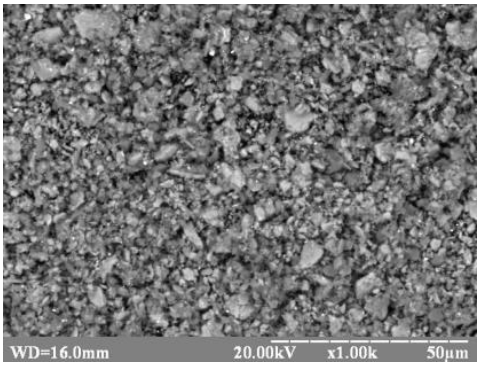

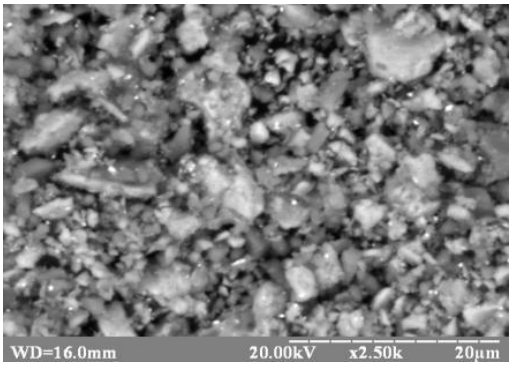

g h

a, b – 0,5 hour; c,d – 1 hour; e, f –1,5 hours; g, h – 2 hours

Figure 3.8, sheet 2 – SEM images of a mixture of powders AlNiCoFeCr HEA + 30 wt. % TiB_2 after different mixing times in a planetary mill

As above figures of a mixture of AlNiCoFeCr HEA + 30 wt. % TiB_2 powders different mixing times shown, it can be concluded that HEA-TiB_2 composite powder particles have an irregular, nearly look likes lamellar shape after 30 minutes the process of mechanical alloying, the microstructure morphology of the high-entropy alloy composite material is composed of large irregularly shaped areas and small elliptical areas, nano-level protrusions are evenly dispersed between the large areas and small and the shape of the particles does not change with the increase of the mixing time. As process of mechanical alloying time increases, the grains gradually become finer.After 0.5 h of ball milling, the powder particles have different shapes and sizes below 40 μ m; continuing the ball milling, it was found that both the powder was broken into smaller particles, and some were reunited and welded together to form larger particles, with uneven size distribution and different shapes. The a – 0,5 hour; b – 1 hour; c –1,5 hour; d – 2 hours

Figure 3.10 is SEM image of AlNiCoFeCr HEA + 30 wt. % TiB_2 powders mixture after different milling times in a planetary mill, and designation the areas of analysis.

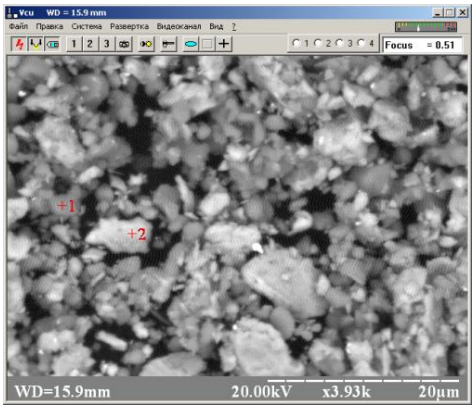

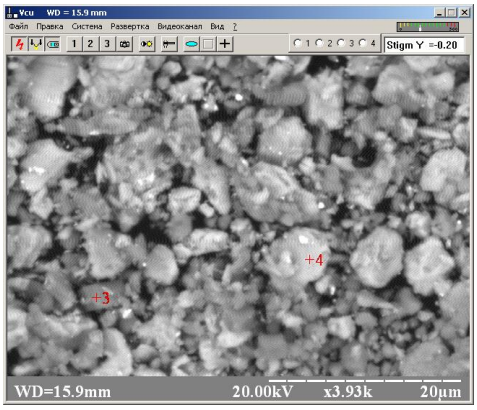

a b

a – 0,5 hour; b – 1 hour; c –1,5 hour; d – 2 hours

Figure 3.9, sheet 1 – SEM images (designating the areas of analysis) of a mixture of powders AlNiCoFeCr HEA + 30 wt. % TiB_2 after different mixing times in a planetary mill

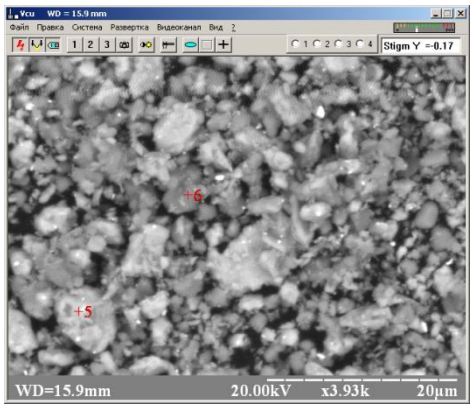

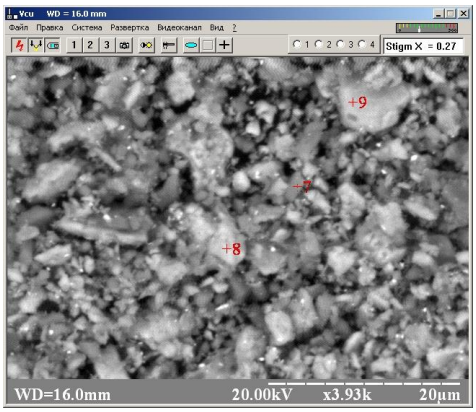

c d

a – 0,5 hour; b – 1 hour; c –1,5 hour; d – 2 hours

Figure 3.10, sheet 2 – SEM images (designating the areas of analysis) of a mixture of powders AlNiCoFeCr HEA + 30 wt. % TiB_2 after different mixing times in a planetary mill

At the same time, the analysis of EDS results shows that elemental carbon and elemental tungsten are detected, because the process of mechanical alloying is carried out by grinding the carbonized object.

Table 3.2 is the EDS analysis results of the designated areas 1-9 in the SEM images of the AlNiCoFeCr HEA + 30 wt. % TiB_2 powders.

According to the results of EDS analysis, designated areas 1, 3, 6, 7 have higher Ti content. On particles larger than 6 μm, the Ti content ranges from 1.58 wt. % to 5.68 wt. %, however, on more dispersed particles, the content of Ti is in the range from 34.27 wt. % to 79.36 wt. %.

There are small concentrations of W in the general analysis after 0.5 hours ball milling, and on particles larger than 10 μm, the W content ranges from 1.24 ± 0.02 wt. % after 0.5 hour ball milling to 2.92 ± 0.07 wt.% .

At the same time, the analysis of EDS results shows that elemental carbon and elemental tungsten are detected, because the process of mechanical alloying is carried out by grinding the carbonized object.

Table 3.2 – Chemical composition of a mixture of powders AlNiCoFeCr + 30 wt. % TiB_2 after different mixing times in a planetary mill

Time /hour	Designation	Elements, wt. %									
		Al	Ni	Co	Fe	Cr	Ti	B	C	O	W
0,5	1	0,75	1,59	1,14	2,05	1,82	74,06	13,55	1,26	3,77	-
	2	4,17	14,49	12,46	13,1	11,26	5,68	26,78	9,46	2,59	-

	General	3,42	11,25	11,51	11,51	10,73	23,62	26,73	-	-	1,24
1	3	0,41	1,2	1,2	1,57	1,27	43,06	43,34	6,6	1,35	-
	4	8,52	17,36	16,49	17,75	17,37	1,58	10,79	8,09	2,05	-
	General	6,75	17,6	17,13	17,54	16,36	21,9	-	-	-	2,72
1,5	5	6,87	18,13	19,65	14,93	11,96	2,74	10,66	4,17	2,53	8,36
	6	0,66	1,35	1,18	2,3	1,35	79,34	8,58	1,66	3,57	-
	General	6,95	15,22	15,66	16,34	14,72	27,94	-	-	-	3,15
2	7	1,27	2,74	3,27	3,48	2,88	39,27	34,98	8,32	3,79	-
	8	1,1	2,52	2,73	61,26	2,5	1,98	13,44	12,38	1,98	-
	9	6,22	15,79	15,39	19,78	10,86	1,41	8,02	15,13	1,85	-
	General	6,01	15,24	16,15	16,52	14,47	22,24	-	-	6,45	2,92

Therefore, elemental carbon and elemental tungsten will appear in the mixture. These two impurities come from HEA powder and during the process of ball milling. In addition, oxygen was detected in the powder mixture on the TiB_2 and HEA particles due to the fact that the process of ball milling was carried out without a protective atmosphere and an alcohol medium.

3.3 Characterization of AlNiCoFeCr HEA – TiB_2 cold sprayed composite coatings

The Figure 3.11 (a) shows the X-ray diffraction spectra of AlNiCoFeCr HEA – TiB_2 of feedstock powder mixture, the Figure 3.11 (b) shows the X-ray diffraction

spectra of AlNiCoFeCr HEA – TiB_2 cold sprayed composite coating.

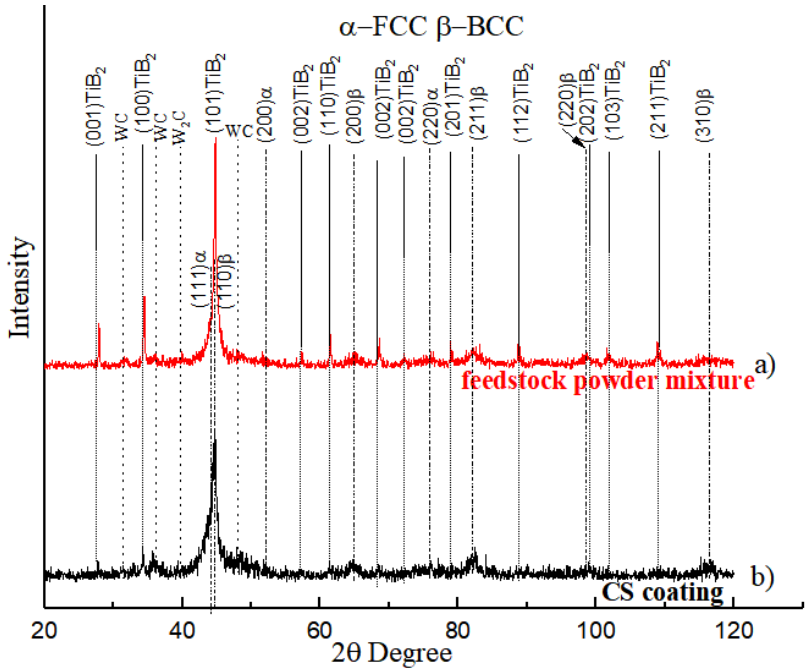

a – the initial AlNiCoFeCr–TiB_2 mixture of powders; b – AlNiCoFeCr–TiB_2 coating

Figure 3.11 – XRD spectra of the initial mixture and HEA –TiB_2 coatings obtained by cold spraying at a pressure and temperature of 0.85 MPa and 300 °C, respectively

According to the XRD spectra (Figure 3.11 a), it can be concluded that the initial AlNiCoFeCr–TiB_2 mixture of powders mainly includes 3 phases: (i) the FCC solid solution, α-phase, (ii) the BCC solid solution, β- phase, (iii) TiB_2, which did not form other complex phases. Comparison of XRD spectra on Figure 3.11 (a) and Figure 3.11 (b) shows that the same phases are present in the X-ray diffraction patterns of the feedstock AlNiCoFeCr – TiB_2 powder mixture and AlNiCoFeCr – TiB_2 coatings obtained by cold gas-dynamic spraying, i.e. the phase composition of the powder after spraying does not change and remains the same as it was before spraying. Due to the low temperature of

the cold spraying process, the coatings do not undergo phase transformations and oxidation, which helps to preserve the phase composition and structural state in the same way as in the initial mixture before spraying. It should be noted that the intensity of diffraction maxima of BCC and FCC solid solutions of AlNiCoFeCr HEA and TiB_2 decreases, and their profiles broaden (Figure 3.11, b), compared with the lines of these phases for the initial AlNiCoFeCr–TiB_2 powders mixture (Figure 3.11, a), which indicates that the microstresses increases in the coating due to the severe plastic deformation, which occurs during the formation of the coating at the supersonic flow rate of the air-powder mixture in the spraying process at low temperature.

Morphology and microstructure of the AlNiCoFeCr HEA cold sprayed coating are shown in Figure 3.13 (a) and 3.8 (b). Microstructural analysis of AlNiCoFeCr coatings (Figure 3.13 (a) and 3.8 (b)) showed that the obtained coating layer is about 20-30 μm at a pressure and temperature of compressed air of about 0.85 MPa and 300 °C, respectively, while the coating itself has a layered structure. It should be noted that the surface of the coating is similar to the surface of the substrate treated with silicon carbide particles before spraying. It is necessary to pay attention to the surface between the coating and the substrate (Figure 3.13 a and 3.8 b), the greater continuity of which indicates easier formation of adhesion between the soft phase (steel substrate) and the harder phase (high-entropy alloy), it is easier to form a strong adhesion between phases of different hardness.

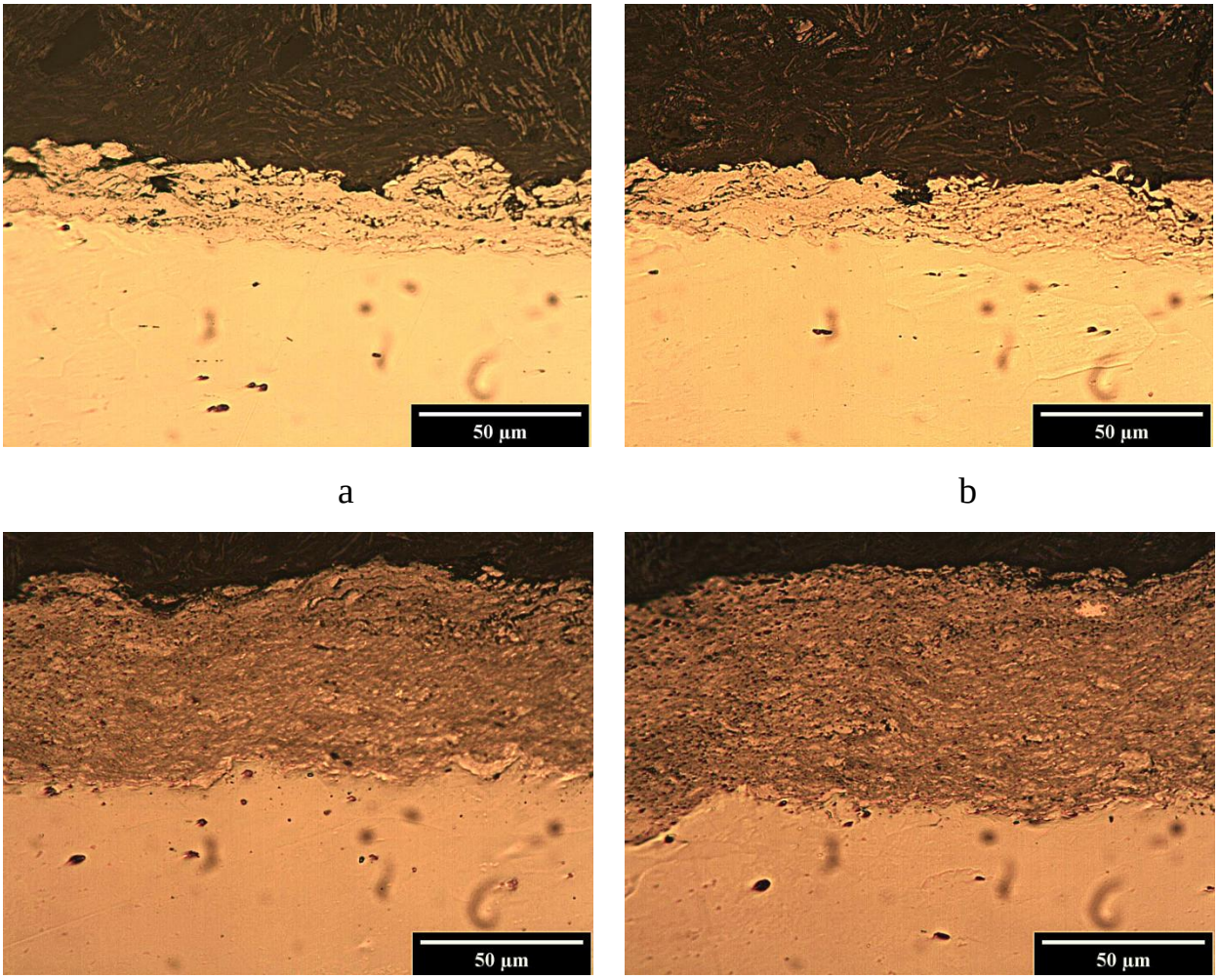

a b

c d

a, b – AlNiCoFeCr high-entropy coatings; c-f – AlNiCoFeCr-TiB_2 composite coating

Figure 3.12, sheet 1 – Microstructure (optical micrographs) of AlNiCoFeCr and AlNiCoFeCr - TiB_2 coatings obtained by cold gas-dynamic spraying at a pressure and temperature of compressed air flow of about 0.85 MPa and 300 °C, respectively

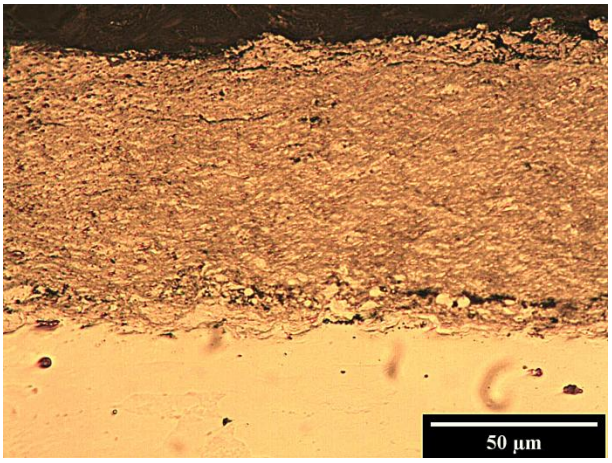

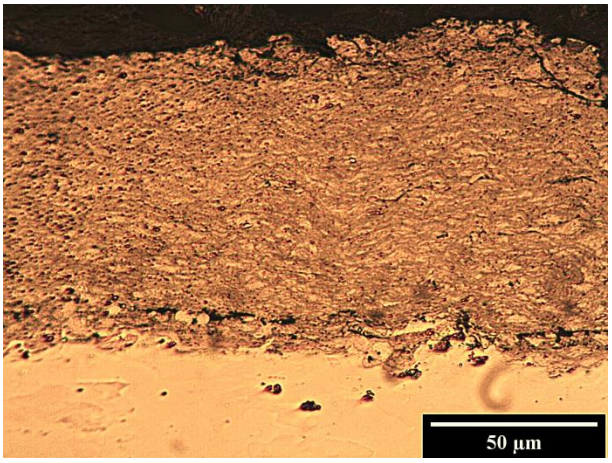

e f

a, b – AlNiCoFeCr high-entropy coatings; c, f – AlNiCoFeCr-TiB_2 composite coating

Figure 3.13, sheet 2 – Microstructure (optical micrographs) of AlNiCoFeCr and AlNiCoFeCr - TiB_2 coatings obtained by cold gas-dynamic spraying at a pressure and temperature of compressed air flow of about 0.85 MPa and 300 °C, respectively

Morphology and microstructure of the AlNiCoFeCr HEA–TiB_2 cold sprayed composite coatings are shown in Figure 3.13 (c - f). It can be concluded that the thickness of the obtained composite coatings is from 80 µm to 100 µm. The coating itself has a fairly homogeneous structure and consists of darker and lighter phases. The coating has virtually no delamination, and its surface is much smoother than that of the AlNiCoFeCr high-entropy coating (see Figure 3.13, a, b), which indicates at least the achievement of "critical speed" of powder particles and the transition to material spraying. Minor stratifications are observed only near the boundary of the "substrate - coating" section, where there are small clusters of both darker and lighter phases. This indicates that some particles, especially larger particles, arrive at the surface earlier and there is a

slight delamination. However, in the places of these strata, particles of the lighter phase are clearly observed, which act as a kind of "bridge" between the two layers, connecting them and creating a strong contact. Thus, the use of a mixture of powders with significantly different hardness values leads to the fact that one of the phases acts as a binder and contributes to the formation of the coating 69.

3.4 Microhardness of the HEA -TiB_2 cold spraying coatings

Hardness is a comprehensive index, which can reflect the relationship between material strength and plasticity. Figure 3.14 shows the microhardness profile along the cross section of AlNiCoFeCr–TiB_2 coatings. Since the indentation topography shows a complete and clear rhombus, the error in the measurement process is small, and the result is relatively accurate and reliable. The calculation of hardness is shown in formula (2.1).

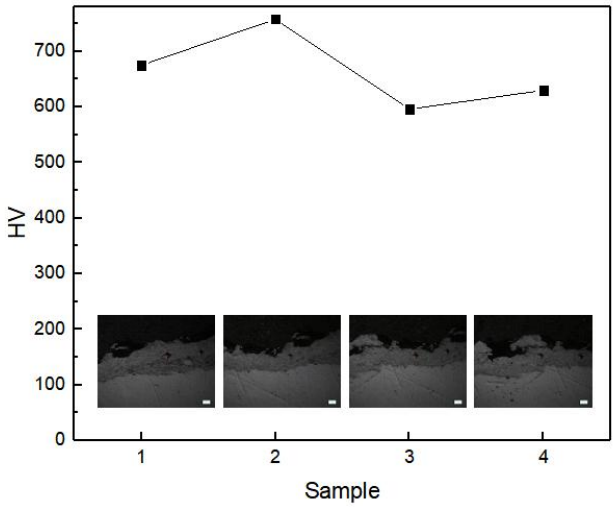

Figure 3.14 – Microhardness profile along the cross section of AlNiCoFeCr - TiB_2 coatings obtained by cold gas-dynamic spraying at a pressure and temperature of compressed air flow of about 0.85 MPa and 300 °C, respectively

The variable in the formula is the average value of the indentation diagonal, and the average value is inversely proportional to the hardness. Therefore, the larger the value of the indented sample diagonal, the worse the alloy's ability to resist deformation. The sample has an average hardness of 665 HV.

In the process of ball milling, high-entropy alloy composites often produce solid solution strengthening, second phase strengthening, precipitation strengthening and other strengthening mechanisms, which make the alloy exhibit higher strength and hardness. Wang et al. 64 prepared $Al_xFeNiCoCr$ series high-entropy alloys by casting method, of which $Al_{0.9}Fe$ NiCoCr has the highest hardness, which is 527 HV.

According to the formula (2.2), the standard deviation of the random error of the hardness measurement is calculated as followed:

$$\pm\sigma = \sqrt{\frac{\sum_n (HV_c - HV_n)^2}{n-1}} = 40.09$$

It can be seen from the Figure 3.14 that compared with the cast $Al_xFeNiCoCr$ high-entropy alloy, the high-entropy alloy composite coating has higher hardness. This may be due to the very small grains of the HEA-TiB_2 composite prepared by the mechanical alloying. According to Hall-Petch effect, it can be seen that small crystal grains are beneficial to increase the strength. At the same time, the dislocation movement is hindered by the high volume fraction of grain boundaries in the fine grains. The deformation of the alloy is mainly through the distortion or sliding of the grain boundaries, which requires higher energy, so it has higher strength and hardness, and relatively poor plasticity.

4 OCCUPATIONAL HEALTH AND SAFETY IN EMERGENCIES

The purpose of this study is to prepare HEA–ceramic composite coatings by cold-spraying and to investigate the structure and phase composition.

Firstly, we prepared AlNiCoFeCr and AlNiCoFeCr-TiB_2 alloy powders by mechanical alloying technology, and then prepared high-entropy alloy composite coatings by cold spraying technology.

Mechanical alloying refers to a certain proportion of metal or alloy powder in the ball mill through repeated impacts and collisions between the powder and the grinding ball for a long time.

Cold spraying technology (also known as cold gas dynamic spraying), also known as cold gas dynamic spraying, is a new type of spraying technology that has been rapidly developed in recent years. It uses compressed gas (nitrogen, helium, air, etc.) as an accelerating gas flow to drive solid powder particles (particle size 1-50 μm) collide with the substrate at low temperature (room temperature to 600 ℃) and supersonic speed (300~1200 m/s), causing the particles to undergo strong plastic deformation and deposit to form a coating.

In the process of using mechanical alloying and cold spray technology, the process will produce metal dust and noise that are unsafe for experimenters. This chapter will analyze the unsafe factors of the experimental process and propose solutions.

4.1 Analysis of harmful and dangerous production factors (HDPF)

According to their origin and nature of action on the human body HDPF divided into physical, chemical, psychophysiological, biological and social 70.

The physical factors include that create a risk of mechanical injury, burns, frostbite; vibroacoustic factors (noise, vibration, ultrasound and infrasound); electric (static electricity, high voltage levels, circuit closure through the human body); ionizing, electromagnetic, ultraviolet (UV) and infrared (IR) radiation; light (insufficient lighting, increased brightness, etc.); dust of fibrogenic action (insoluble in biological fluids, such as SiO_2 particles.

Chemical factors include harmful chemicals in any physical state that can enter the body and dissolve in biological fluids.

Psychophysiological factors include: physical overload (static and dynamic) and neuropsychological (mental and emotional, monotony of work, emotional overload).

In the course of this experiment, biological factors actually do not exist.

Social HDPF is poor organization of work, overtime work, bad relations between team members, social isolation with separation from the family, change of biorhythms, dissatisfaction with work, etc.

As a rule, the processes of gas-dynamic spraying and other materials processing processes are accompanied by a number of harmful and dangerous production consequences.

Harmful production factors include: increased dust and air pollution of the working area; ultraviolet, visible and infrared radiation; electromagnetic fields; ionizing radiation;

noise; ultrasound; vibration; static load on the human body.

When using various thermal technologies of materials processing (for example, gas-dynamic spraying, etc.) harmful substances (dust, aerosols) containing compounds of various metals can get into the breathing zone of workers. manganese, chromium, nickel, copper, titanium, aluminum, iron, tungsten, etc.), as well as toxic gases (carbon monoxide, nitrogen oxides, ozone, hydrogen fluoride, silicon tetrafluoride, etc.) The amount, composition and toxicity of these substances depend on the type of technological process and chemical composition of materials used in this process.The concentration of these substances in the air of the working area can exceed the MAC (Maximum Allowable Concentration) by tens of times.

There is a danger of ionizing radiation of workers during the operation of electron-beam installations, gamma and X-ray irradiation of metal products, the use of toned tungsten electrodes.

Sources of increased noise are plasma trons, pneumatic actuators, generators, vacuum pumps, etc., and ultrasound - ultrasonic generators, working equipment.

When using manual labor with the use of special devices and tools, there is a static load on the hands, which can cause diseases of the neuro muscular system of the shoulder girdle.

Dangerous production factors include: exposure to electric current, sparks and splashes, emissions of molten metal and slag; the possibility of explosion of cylinders and systems under pressure; moving mechanisms and products.

The cause of electric shock can be contact with exposed live parts, which are under voltage: to de-energized live parts, where voltage occurs accidentally; to non-conducting

parts that were energized due to insulation defects; impression of electric arc and step voltage.

The use of open electric arcs, gas flames, plasma jets, sparks, splashes and emissions of molten metal and slag not only create the possibility of burns, but also increase the risk of fire. The latter can occur during the use of flammable gases and oxygen, the operation of vessels operating at pressures greater than atmospheric.

When performing work at height and in the absence of appropriate protective equipment, workers may fall. Machines, moving mechanisms, products, due to the lack of protective devices can injure workers.

Characteristics of hazardous and harmful production factors in the use of gas-dynamic spraying are given in **Ошибка! Источник ссылки не найден.**.

Table 4.1 - Dangerous and harmful production factors gas-dynamic spraying process

Types of processes	Harmful production factors										Dangerous production factors			
	Hazardous substances	Radiation in the optical range			Electromagnetic	Magnetic fields	Ionizing	Noise	Ultrasound	Static load on	Electric current	Sparks, splashes	Mechanisms and moving products	Systems that are under pressure
		Ultraviolet	visible	Infrared										
Gas-dynamic spraying	xx	x x	x	x	–	–	–	x x	x x	x	x	x	x	xx

Notes: xx – intense factor; x – moderate factor; (-) – insignificant factor or its absence

4.2 Engineering solutions to ensure occupational safety

4.2.1 Requirements for technological processes

When choosing the technology of the process of processing metals and materials, preference should be given to the process that will provide better working conditions. It is necessary to use those types and brands of materials which at application of these processes will provide the minimum release in air of harmful substances. It is not allowed to use materials that have not passed the hygienic assessment in the prescribed manner.

When creating technological processes of materials processing it is necessary to provide the maximum possible mechanization and automation of processes and its separate elements.

Production equipment used in technological processes must meet the general requirements of the state regulatory act on labor protection ДНАОП 0.00-1.21-98 74.

The processes of applying metal coatings should be performed in accordance with the legal act on labor protection НПАОП 28.0-1.37-14 75.

The obligatory stage of design of technological processes is the development of appropriate means and measures of collective protection against the influence of harmful and dangerous production factors characteristic of this process. One of such measures is the use of local exhaust ventilation devices with purification systems for removed air from aerosols and gases in accordance with the requirements of ДБН В.2.5-67:2013 76. Mechanized production equipment must have built-in air intake devices to capture aerosols and gases. It should be borne in mind that the use of technological processes that are accompanied by the release of harmful substances into the air, with inactive local exhaust ventilation is not allowed.

Gas-dynamic spraying, as well as other thermal processes of processing metals, materials and products of medium and small sizes in stationary conditions should be performed in specially equipped cabins. The cab must have an open top and be made of non-combustible materials. There must be a gap between the wall and the floor of the cab, the height of which is determined by the type of technology. The cabin area must be sufficient to accommodate production equipment, a table, a local exhaust ventilation device, the work piece and the tool.

Operation of cylinders, containers with compressed and liquefied gas, ramps, should be carried out in accordance with the norms of ДНАОП 0.00-1.07-94 77. "Rules for the design and safe operation of pressure vessels."

Cylinders with compressed gases should be placed at a distance of not less than 5 m from the welding torch and 1 m - from the heaters. If there are screens on the heaters that protect the cylinders from heating, the distance from the cylinder to the screen must be at least 0.1 m.

When spraying large parts to reduce noise and ultrasound should be used soundproof covers, not firmly attached to the equipment.

If under the conditions of the technological process, it is not possible to use sound-insulating casings on the installations, the operators must be located in sound-insulated cabins with windows for observation and remote control of the process.

If the local exhaust and general exchange ventilation cannot ensure proper air purity, for example, when cutting in closed and semi-closed spaces, it is necessary to carry out forced supply of clean air to the breathing zone of the worker.

To eliminate the possibility of electric shock, together with general electrical safety equipment, it is necessary to check the operation of push-button devices for remote on

and off the unit to prevent accidental start-up of equipment and blocking devices that provide automatic power failure closes the current-carrying parts of the oscillator and turns off the power when removing the casing.

4.2.2 Requirements for production facilities

Workplaces for gas-dynamic spraying must be protected by stationary or portable opaque fences made of non-combustible materials, the height of which must be at least 2.5 m and ensure the reliability of protection.

The distance between the equipment, from the equipment to the walls and columns of the room, other structures, the width of the aisles and passages must comply with current building codes, standards of technological design of shops and ДБН В.2.2-28:2010 78.

The width of the aisles around the perimeter of the desktop, stand, product on which they work, must be at least 1 m.

Floors for industrial premises for electric arc metallization, gas-flame, plasma, detonation-gas and gas-dynamic spraying must be made of materials that do not burn and have low thermal conductivity. The floor must have a smooth non-slip surface and meet sanitary and hygienic requirements.

Production facilities must be equipped with general exchange supply and exhaust ventilation in accordance with ДБН В.2.5-67:2013 76.

Air exchange of industrial premises should be expected to dilute harmful substances not captured by local exhaust devices to the level of the MPC. The amount of air supplied by supply systems should be calculated in accordance with ДБН

В.2.5-67:2013 76.

The air removed from the production premises into the atmosphere must be filtered (purified) from harmful substances to concentrations not exceeding the permissible emission levels.

Supply air must be supplied to the work area or in the direction of the work area. The temperature of the air supplied by the ventilation systems must not be lower than +20 °C according to ДСН 3.3.6.042-99 71.

The parameters of the microclimate of industrial premises must meet the requirements 71. If the intensity of thermal radiation of workers exceeds the value of ДСН 3.3.6.042-99 71 , special means of protection should be provided: shielding of the source, air suffocation, personal protective equipment.

Noise, ultrasound and infrasound levels must meet the requirements 72, and general and local vibration 73.

Gas-dynamic spraying, must comply with ДБН В.2.5-28-2006 79. When performing these works inside closed and hard-to-reach spaces (vessels, housings, compartments), lighting should be carried out by external directional light sources or local lighting with a voltage of not more than 12 V, and the illumination of the working area should be at least 30 lux.

4.2.3 Requirements for the organization of jobs

The organization, arrangement and equipment of workplaces for gas-dynamic spraying must comply with ДСТУ ГОСТ 12.2.061:2009 80. These jobs can be stationary, non-stationary, permanent and non-permanent (temporary).

Permanent workplaces that are powered by electricity from multi-station sources must be equipped with shields with a signal lamp, which shows the worker the presence or absence of voltage in the electrical circuit of production equipment.

Work using gas-dynamic spraying in a closed or confined space should be carried out under the supervision of two observers with a qualification group for occupational safety not lower than II, who should be outside. The worker performing these works must have a safety belt with a rope, the end of which is in the hands of observers.

Workplaces located above 1.3 m above ground level or solid cover must be equipped with fences at least 1.1 m high

4.2.4 Requirements for ventilation

When conducting electric arc, plasma, gas-flame and other thermal processes of materials processing, it is advisable to use local ventilation. In other cases, general exchange ventilation may be used. It should also be used in combination with local ventilation, designed to remove from the production room harmful substances not localized by local exhaust devices (suction).

The design of local extractors is chosen depending on the type of technological process, equipment and facilities. It must ensure the necessary cleanliness of air in the workplace with minimal consumption of air that is removed, prevent the spread of harmful substances in the volume of the room, do not interfere with technological operations.

To protect workers from the effects of hazardous and harmful production factors under the existing technology and working conditions, it is necessary to use personal

protective equipment. The main means of personal protection about during the experiment are: special shoes, special clothing, goggles, respirators. When working with acids and alkalis should use protective dermatological agents for hands: film-forming paste, cream and gloves. To protect the face and eyes from splashes of molten salts and heat radiation, it is necessary to use a metal mesh with cells of 0.8x0.8 mm, in which at eye level is inserted organic glass size 80x80 mm and a thickness of 3 mm, curved along the oval face.

Precinct managers should periodically instruct staff on the proper use and care of personal protective equipment. The administration is obliged to ensure the storage, washing, drying, disinfection, degassing, decontamination and repair of special clothing, special footwear and other personal protective equipment issued to employees.

Workers performing work on electric arc metallization, gas-flame spraying, plasma spraying, detonation-gas spraying and gas-dynamic spraying must be provided with personal protective equipment in accordance with industry standards, depending on the nature of hazardous and harmful production factors and the relevant requirements of ДСТУ 7239:2011 82.

The manufacture and appointment of personal respiratory protective equipment must be carried out in accordance with the requirements of DSTU EN 133: 2005 83.

To protect your hands, use gloves in accordance with ДСТУ EN 420-2017 84.

To reduce the risk of electric shock, workers must be provided with dielectric rubber mats, as well as in conditions of increased danger (limited spaces) with rubber shoes and gloves type E_n and E_v in accordance with regulatory and technical documentation.

Protective helmets in accordance with ДСТУ EN 397:2001 85 should be used to

protect the head during welding of large products in conditions of increased danger and electroslag welding.

4.3 Calculation of engineering solution

The design of local extractors is chosen depending on the type of technological process, equipment and facilities. It must ensure the necessary cleanliness of air in the workplace with minimal consumption of air that is removed, prevent the spread of harmful substances in the volume of the room, do not interfere with technological operations. The suction of the suction to the equipment must be carried out taking into account as close as possible to the source of harmful emissions. Typical schemes and designs of suction pumps, as well as methods of their calculation are summarized in the guidelines for design 81.

The amount of air to be removed or supplied by the ventilation system (required air exchange of production premises L in m^3/h) is determined by different methods depending on specific conditions: , according to empirical formulas or recommended air exchange.

In the presence of data on the intensity of the release of harmful substances into the atmosphere of the room air exchange in general cases is calculated by the formula (4.1) :

$$L = \frac{1000\beta V}{C_{ex} - C_{in}} \tag{4.1}$$

where V is the intensity of the release of harmful substances per unit time g/h; β – coefficient of uneven distribution of harmful substances in the volume of the room; C_{ex},

C_{in} – concentration of harmful substances in the air exhaust and incoming (inflow), mg/m^3.

For general exchange ventilation β it is recommended to take from 1.2 to 2.0: smaller values - for low-toxic substances and with a relatively uniform distribution of sources of their formation; maximum – for more toxic substances with their uneven release.

Concentrations of harmful substances in the exhaust and supply air C_{ex}, Cin are taken as follows. The concentration of harmful substances in the supply air should be minimal and not exceed 30% of the MAC in the air of the working area, and in the exhaust air should not exceed the MAC in the air of the working area 76. Therefore, the value of C_{ex} is usually taken to be equal to the maximum concentration limit. Then the general formula takes a more specific form:

$$L = \frac{1000\beta V}{C_{MAC} - C_{in}} \tag{4.2}$$

If the air is removed from the work area and $C_{in} = 0$

$$L = \frac{1000\beta V}{C_{MAC}} \tag{4.3}$$

If from the upper zone, then:

$$L = \frac{1000\beta V}{K_a C_{MAC}} \tag{4.4}$$

where K_a – air exchange coefficient (has a value of 0.9 … 1.1 when supplying air with horizontal jets; 1.65 … 1.85 – when supplying to the working area; 1.25 … 1.4 at a height of 4 m). Larger values of Ka are used at a multiplicity of air exchange equal to 3, smaller – 10.

According to the website https://zakon.rada.gov.ua/, it is about the statement of hygienic regulations of admissible maintenance of chemical and biological substances in air of a working zone. We found that the maximum allowable concentration of aluminum and alloys in the air is 2 mg/m^3 , substituting into the formula to calculate:

When supplying air with horizontal jets:

$$L = \frac{1000\beta V}{K_a C_{MAC}} = \frac{1000*1.6*0.044}{1*2} = 35.20\ \mathrm{m}^3/\mathrm{h};$$

When supplying to the working area:

$$L = \frac{1000\beta V}{K_a C_{MAC}} = \frac{1000*1.6*0.044}{1.75*2} = 20.11\ \mathrm{m}^3/\mathrm{h}.$$

4.4 Safety requirements in emergency situations

Types of hazards that may occur in the workplace include: fire; explosion (inside equipment, buildings or the environment); rupture or destruction of equipment; emissions of harmful substances; combination of these types of danger 86-87. In order to prevent the emergence and elimination of emergencies (emergencies) at the enterprise should be a plan for localization and elimination of emergencies and accidents in accordance with the provisions 88. During the analysis of the danger of the enterprise (object) it is necessary to identify all possible emergencies and accidents, including unlikely, with catastrophic

consequences that may occur at the enterprise, to consider scenarios for their development and assess the consequences. Identification of opportunities and conditions of accidents should be performed on the basis of analysis of features of individual equipment (devices, machines, etc.) and their group (technological units), as well as taking into account the hazardous properties of substances and materials (explosive and harmful) used in production. It is necessary to take into account the parameters of the state of substances (temperature, pressure, physical state, etc.) and the state of the equipment, which correspond to both the normal technological regime and the modes that are possible during the onset and development of the accident.

According to НАПБ Б.03.002-2007 88 premises in which works on gas-dynamic spraying are performed, according to the requirements of explosion fire danger belong to category D (non-combustible substances and materials in hot , hot, molten states, the processing of which is accompanied by the release of radiant heat, sparks and flames; combustible gases, liquids, solids that are burned or disposed of as fuel).

At the sections of the production room, where gas-dynamic spraying are used, we envisage the installation of fire shields equipped with carbon dioxide fire extinguishers, diggers, crowbars, buckets, axes. Near the boards we assume the presence of boxes with sand, the dryness of which is regularly checked. To extinguish possible fires, we also envisage the use of asbestos blankets.

For automatic detection of fires in the production room, which uses gas-thermal spraying, we provide the presence of sensors that timely notify of a fire and give the command to turn on the automatic fire extinguishing system.

In case of breakdown of electric voltage on the case of the electric arc unit it is necessary to disconnect the switch and to inform about it the master or the chief of a site.

If someone is exposed to voltage, it is necessary to disconnect the electric arc unit from the network, put the victim on a wooden floor, put a quilt under his head, call a doctor at 103 and, if necessary, give the victim artificial respiration.

In case of ignition of the electric arc unit it is necessary to disconnect the switch and to start extinguishing of fire by means of the fire extinguisher.

Every worker and employee who discovers a fire or arson is obliged to:

- immediately notify the factory fire brigade by phone 101;

- start extinguishing the fire with fire extinguishing means available in the shop (on the site) (fire extinguisher, sand, fire hydrant, etc.);

- call officials (shop manager, precinct) to the place of fire.

In case of injury it is necessary to inform the foreman, the chief of a site and to address in a medical center.

5 ENERGY SECTION

The task of the energy section of the project is to calculate the amount of electricity needed to ensure the operation of the shop, as well as fuel, gas and other energy costs.

The amount of electricity consumption is determined on the basis of the choice and calculation of the number of technological equipment, the use of its installed capacity at the planned mode of operation:

$$E = M\Phi_0 \eta_{\text{lf}} K_1 K_2 \tag{5.1}$$

where M is the installed power of the equipment, kW;

Φ_0 - annual fund of equipment operation time, hours;

η_{lf} - equipment load factor;

K_1 - coefficient of simultaneity of work (assumed to be equal: for electric furnaces - 0.6; for electric motors - 0.3; for high-frequency heating generators - 0.8);

K_2 - power utilization factor (assumed to be equal to 0.7).

The Table 2.1 shows that electricity costs for the operation of process equipment.

Table 5.1 – Electricity costs for the operation of process equipment

Equipment name	Amount	Power, kW	Working time fund per year, hours	Coefficient of load	Coefficient of timeliness	Power utilization factor	Annual electricity consumption, kW·h
1	2	3	4	5	6	7	8
Muffle furnace	1	4,0	1920	0,28	0,6	0,7	903,17

Continuation of Table 5.1

1	2	3	4	5	6	7	8
Press machine	1	27	1920	0,53	0,3	0,7	5769,79
Retsch PM100	1	0.75	1920	0,25	0.6	0,7	151.20
Total costs, kWh							6824.16

As shown the Table 5.2, it is the electricity costs for lighting.

Table 5.2 – Electricity costs for lighting

Equipment name	Lighting area, m^2	Surface heat flux density, w/m^2	Number of burning hours per year, hours	Coefficient of combustion simultaneity	Annual electricity consumption, kWh
Composition of raw materials	23,86	10	1920	0,7	320,68
Preparatory department	23,86	11	1920	0,8	403,14
Mixing department	25,11	11	1920	0,8	424,26
Pressing department	35,44	11	1920	0,8	598,79
Composition of finished products	25,21	10	1920	0,7	338,82
Equipment storage area	23,86	11	1920	0,8	403,14
Corridor	60,18	10	1920	0,7	808,82
Total costs, kWh					3297.65

The total cost of electricity consists of the amount electricity costs for the operation of process equipment and electricity costs for lighting:

$$6824.16 + 3297.65 = 10121.81 \text{ kWh}$$

6 ECONOMIC SECTION

6.1 The composition of the costs of research work

The cost of research consists of the following components:

– costs for theoretical research (choice of object and research methods, literature review, patent research, etc.);

– costs of laboratory tests (experiments, processing and generalization of their results);

– costs of experimental production (design and construction of the experimental installation, obtaining and testing of the experimental batch of products or product);

– costs of industrial design.

The work covered only the first two stages of the study, so the cost estimate for their implementation takes into account only the cost of materials, electricity, wages and other costs.

6.2 Calculation of costs for research

6.2.1 Worker's salary

The number of workers is calculated on the basis of data on the complexity of individual works in this work, as shown the

Table 6.1.

Table 6.1 - The complexity of work in this work

Name of works on the research topic	Professor (days)	Technician (days)	Laboratory assistant (days)	Experiment executor (days)
1	2	3	4	5

1. Clarification and specification of tasks on the research topic	3	–	–	–

Continuation of

Table 6.1

1	2	3	4	5
2. Analysis of scientific and technical publications on the topic	–	–	–	60
3. Synthesis of HEA by mechanical alloying in a planetary mill.	1	–	5	5
4. Investigation of structure and phase composition of mechanically alloyed HEA with SEM, EDX and XRD	1	1	3	3
5. Synthesis of HEA-TiB_2 by mechanical alloying in a planetary mill	1	–	5	5
6. Deposition of HEA–TiB_2 coatings by cold spraying (CS)	1	–	2	2
7. Investigation of structure, phase and chemical composition of CS coatings with SEM, EDX and XRD	5	4	16	16

Further calculations of labor costs are carried out according to the algorithm understood from **Ошибка! Источник ссылки не найден.**.

Table 6.2 – Calculation of labor costs

Position of performers of the theme	Planned labor intensity, (days)	Salary, UAH		
		Monthly salary	Average daily salary	Total for workers
1	2	3	4	5

1. Professor	12	20507,09	970,29	11643.48
2.Technician	5	7895	263.17	1315.85

Continuation of table 6.2

1	2	3	4	5
3.Laboratory assistant	31	6245	294.58	9131.98
Total salary in this work (UAH)				22091.31

6.2.2 Single social contribution

The Single Social Contribution (SSC) is a compulsory contribution to national social insurance. From January 1, 2016, the SSC rate is 22%. The basis for the calculation of SSC are the total labor costs in this work.

$$SSC = TC \cdot 0.22 \tag{6.1}$$

where TC – total labor costs in this work.

Currently, the SSC will be:

$SSC = 22091.31 \cdot 0.22 = 4860.09$ UAH.

6.2.3 Material cost for research

This work takes into account the cost of all types of materials required for research, minus the cost of returnable waste.

Al, Co, Cr, Fe, Ni and Ti powders were used as starting materials for the production of high-entropy alloys. The technical conditions for powders are given in Table 6.3.

Table 6.3 - Experimental material price

Name of material	Brand	Standard, technical conditions	Unit	Mass	Market price per unit, UAH	Amount, UAH
1. Al	ПА-1	ГОСТ 6058-73	kg	1	224.70	224.70
2. Ni	ПНЭ-1	ГОСТ 9722-97	kg	1	1098.00	1098.00
3. Co	ПК-1у	ГОСТ 9721-79	kg	1	2854.80	2854.80
4. Fe	ПЖР5	ГОСТ 9849-86	kg	1	549.00	549.00
5. Cr	ПХ1С	ТУ14-1-1474-75	kg	1	375.90	375.90
6. Sand paper	P800	ГОСТ Р 52381-2005	pcs	1	14	14
7. Sand paper	P1000	ГОСТ Р 52381-2005	pcs	1	14	14
8. Sand paper	P1500	ГОСТ Р 52381-2005	pcs	1	14	14
9. Sand paper	P2000	ГОСТ Р 52381-2005	pcs	1	14	14
10. Alcohol			l	1	70	70
Total cost of materials						5228.40

We accept transport and procurement costs at the level of 10 % of the planned cost of total costs for materials:

$T_C = 5228.40 \cdot 0{,}1 = 522.84$ UAH.

In this case, the total cost of purchasing materials and transporting them will be:

$C_M = 5228.40 + 522.84 = 5751.24$ UAH.

6.2.4 Energy for research

The task of the energy section of the project is to calculate the amount of electricity needed to ensure the operation of the shop, as well as fuel, gas and other energy costs.

The total cost of electricity consists of the amount electricity costs for the operation of process equipment and electricity costs for lighting.

6824.16 + 3297.65 =10121.81 kWh.

https://yasno.com.ua/business/b2b-tariffs

Take the 1st voltage class.

$\mathrm{C_E} = 10121.81 \cdot 3.4504 = 34924.29$ UAH.

6.2.5 Costs for special equipment

The experimental work is all done in the laboratory of Department of High Temperature Materials and Powder Metallurgy, and there are no travel expenses.

6.2.6 The cost of third-party services

The experimental work is all done in the laboratory of Department of High Temperature Materials and Powder Metallurgy, the structural organization characterization of the material is also completed in the laboratory, so there is no cost of

third-party services.

6.2.7 Business trip expenses

The experimental work is all done in the laboratory of Department of High Temperature Materials and Powder Metallurgy, and there are no business trip expenses.

6.2.8 Other direct unaccounted costs

This work combines all the costs of research work that are not included in the previous articles. When carrying out work, we accept other direct costs at the level of 10% of the amount of accrued costs for research work.

$$O_C = (TC + SSC + C_M + C_E) \cdot 0{,}1 \tag{6.2}$$

It will currently be:

$O_C = (22091.31 + 4860.09 + 5751.24 + 34924.29) \cdot 0{,}1 = 6762.69$ UAH.

6.2.9 Indirect costs

This work includes the costs associated with the management of the executing organization, the costs of invention and rationalization; depreciation costs of fixed assets; costs of scientific and technical information; costs of ensuring normal working conditions and safety; costs of paying for bank services; taxes, fees and other obligatory payments

and expenses, etc.

Consider the option of calculating indirect costs in proportion to the amount of direct costs at the level of 20%.

$$I_C = (TC + SSC + C_M + C_E + O_C) \cdot 0.2 \quad (6.3)$$

It will currently be:

$I_C = (22091.31 + 4860.09 + 5751.24 + 34924.29 + 6762.69\ ) \cdot 0{,}2 = 14877.92$ UAH.

6.2.10 Development of a planned calculation of the estimated cost of the work

The planned calculation of the cost of research in this work is based on the calculations and regulatory data, as shown the Table 6.4.

Table 6.4 - Planned calculation of the estimated cost of research

Name of cost items	Amount, UAH	Rationale
1	2	3
1. Salary expenses	22091.31	According to the calculations
2. Single social contribution	4860.09	22.0% of total labor costs
3. Material cost for research	5751.24	According to the calculations
4. Energy for research	34924.29	According to the calculations
5. Costs for special equipment	–	In our work, the part includes overhead costs
6. The cost of third-party services	–	Under the agreement with third-party organizations (in our work, the part

		includes overhead costs)
7. Business trip expenses	–	No travel expenses

Continuation of Table 6.4

1	2	3
8. Other direct unaccounted costs	6762.69	10% of the amount of direct estimated costs in this work
9. Indirect costs	14877.92	According to the standards of the organization-executor of the topic (in our work 20% of the amount of direct costs)
10. Total costs in this work	89267.54	Sum of all items

6.3 Scientific and technical efficiency of research

The calculation of the expected economic effect of research work is necessary to determine the feasibility of this work. However, it can be calculated only for of research work, which is directly aimed at creating new materials, improving product quality parameters, as well as creating new designs.

To determine the annual economic effect, we use a scoring system to assess economic efficiency on the following indicators:

- the importance of development (K 1);
- the possibility of using the results of development (K 2);
- theoretical significance and level of novelty (K 3);
- the complexity of the study (K 4).

The total score (S) is calculated by multiplying the coefficients.

$$S = K_1 \cdot K_2 \cdot K_3 \cdot K_4 \quad (6.4)$$

In our work, the scoring of efficiency according to

Table 6.5 is:

$S = 3 \cdot 8 \cdot 3 \cdot 5 = 360.$

Table 6.5 – Score evaluation of the effectiveness of research

Research work performance evaluation indicator	Symbol of the indicator	Characteristics of this work	Scores
1. The importance of development	K_1	work is performed under the agreement on scientific and technical cooperation	3
2.The possibility of using the results of development	K_2	the results of development can be used on the scale of one industry	8
3. Theoretical significance and level of novelty	K_3	during the work received new information that complements the idea of the essence of the studied processes	3
4. The complexity of the study	K_4	the work is performed by one unit, costs from 50,000 to 100,000 hryvnias	5

The conditional effect of research work is calculated by the formula:

$$E_{RW}^{C} = 500 \cdot S - \mathrm{E}_N \cdot C_{RW} \tag{6.5}$$

where 500 is the notional value of one point;

E_N – normative coefficient of economic efficiency (can be in the range of 0.1 - 0.3);

C_{RW} – total costs of research work (RW) (summary of Table 6.4);

In our work, the conditional effect of research work will be:

$E_{RW} = 500 \cdot 360 - 0{,}25 \cdot 89267.54$ =157683.12 UAH.

The economic efficiency of research is determined by the coefficient of conditional economic efficiency E_e.It is the ratio of the conditional effect of research work to the total cost of research work and is calculated by the formula:

$$E_e = \frac{E_{RW}}{C_{RW}} \tag{6.6}$$

In our work, E_e will be:

$$E_e = \frac{157683.12}{89267.54} = 1.77$$

The coefficient of conditional economic efficiency of research work is 1.77 (> 1), which indicates the feasibility of its implementation.

7 DEVELOPMENT STARTUP PROJECT

7.1 Description of the project idea

For the machinery industry, important projects currently developing in the world include: high-speed precision cutting, cutting with little or no cooling lubricant or dry cutting, and cutting under high-hardness conditions. All of these, as well as the emergence of modern new materials, are increasingly demanding cutting tools. Under the new situation, special requirements are also put forward for cutting processing, such as hard processing with processing hardness above 50 HRC, micro-lubrication and dry cutting without lubrication, which make the individual characteristics of cutting processing increasingly appear. In the face of these changes, if it is required to adapt to these requirements in the design and manufacturing process of the tool or the overall performance of the tool material, the technical difficulty is very great. Especially for the tool material, it is not only extremely uneconomical in terms of resource utilization, Moreover, materials are required to meet the increasingly complex comprehensive cutting performance, which is usually difficult to achieve. The energy level of the processed materials continues to increase, such as high-strength and ultra-high-strength materials, high toughness, and difficult-to-cut materials.

The use of coated tools is one of the best solutions to the above problems. Coated tools play a very important role in improving the performance of the tools. Coated cutting tools have greatly improved processing efficiency, processing accuracy, extended tool life, and reduced processing costs. It can be said that the development of modern manufacturing has promoted the development of the tool industry.

High-entropy alloys are generally alloys formed from five or more metals with

equal atomic weight or approximately equal atomic weight. High-entropy alloys are different from traditional alloys and are a new material. High-entropy alloys are proposed on the basis of traditional alloys. As a new type of solid solution alloy, its strength, fracture resistance, tensile strength, corrosion resistance and oxidation resistance are better than traditional alloys.

Hard tool coating refers to the coating of a thin layer of high-hardness and wear-resistant alloy on the surface of the cemented carbide blade as a protective coating for commonly used tool knives for turning, milling, planing, and grinding. The high hardness and high strength of high-entropy alloys can just meet the needs of this material.

Because the surface coating material has high hardness, strength and wear resistance. Therefore, compared with the uncoated blade, the coated tool allows the use of a higher cutting speed, thereby improving the cutting efficiency; or it can improve the tool life at the same cutting speed. As shown the Table 7.1, it is description of the idea of a startup project.

Table 7.1 - Description of the idea of a startup project

Content of the idea	Directions of application	Benefits for the user
High-entropy alloy coating materials have excellent characteristics such as high hardness and high strength, which meet the needs of hard tool coating materials	Carbide alloy drill	Improve cutting efficiency and extend equipment life
	Carbide alloy blade	Improve cutting efficiency and extend equipment life

As shown the Table 7.2, the comparative analysis of indicators is carried out: for the own idea the indicators having a) worse values (W, weak); b) similar values (N, neutral) ; c) the best values (S, strong).

Table 7.2 – Identification of strong, weak and neutral characteristics of the project idea

№	Technical and economic characteristics of the idea	(potential) products / concepts of competitors			
		My project	Competitor1	Competitor2	Competitor3
1.	New technology	N	N	N	N
2.	Less consumables	S	N	W	N
3.	Excellent performance	S	W	N	N
4.	Service life	S	W	W	N

7.2 Technological audit of the project idea

Within the limits of this division it is necessary to carry out audit of technology by means of which it is possible to realize the idea of the project (technology of creation of the goods).

Determining the technological feasibility of the project idea involves the analysis of the following components.

The analysis of the results in the table 7.3 shows that the high-entropy alloy powder is prepared by the mechanized alloy technology, and then the coating material is prepared by the cold spray technology.This method can prepare the designed project product.

As shown the Table 7.3, it is an idea about the technological feasibility of the

project.

Table 7.3 – Technological feasibility of the project idea

№	Project idea	Technologies for its implementation	Technology availability	Availability of technologies
1.	Tool coating	Mechanical alloying (MA)	Available	Available
		Cold spraying (CS)	Available	Available
Selected technology for implementing the project idea: MA and CS				

7.3 Analysis of market opportunities to start a startup project

Since the advent of the first generation of CVD vapor deposited TiC cemented carbide inserts in the late 1960s, coating technology has greatly promoted the development of cemented carbide tools. In the early 1980s, PVD vapor deposition TiN was successfully applied to high-speed steel cutting tools, and it was hailed as a revolution in the performance of high-speed steel cutting tools. Since then, coating technology has achieved rapid development, coating technology has become more and more mature, and the application range of coated tools has become less and more extensive.

Coating the tool is a major change on the way forward in the machining industry. It is to attach a layer of compound to the tool, so that the performance of the tool is greatly improved. Coated tools can improve machining efficiency, machining accuracy, extend life, and reduce costs. Therefore, coated tools have received widespread attention from all over the world.

The development of coated tools is mainly reflected in the development of coating materials. The coating materials must have high hardness, good wear resistance, stable chemical properties, no chemical reaction with the workpiece material, heat resistance and oxidation resistance, and low friction coefficient; and The substrate is firmly attached and other requirements. Obviously, it is difficult for a single coating material to meet the above requirements. Therefore, hard coating materials have moved from a single coating of TiC and TiN to a new stage of developing thick film, composite and multiple coatings. The newly developed TiCN, TiA1N, TiA1N multi-element, ultra-thin, ultra-multi-layer coating and TiC-$A1_20_3$-TiN coating composite, in the composite coating, the thickness of each single component coating will become thinner and thinner, and Gradually tend to be nano-sized. Coupled with a new type of plastic deformation resistant substrate, significant progress has been made in improving the toughness of the coating, the bonding strength of the coating and the substrate, and improving the wear resistance of the coating.

At the same time, high-entropy alloy composite materials also meet a series of requirements for coating materials, such as high hardness, good wear resistance and high temperature resistance, so this product considers using high-entropy alloy composite materials as coating materials to attach to the tool surface to enhance tool performance. The Table 7.4 shows that preliminary description of the potential market of a startup project.

Table 7.4 – Preliminary description of the potential market of a startup project

№	Market indicators (name)	Characteristics
1	2	3
1	Number of main players, units	10

Continuation of table 7.4

1	2	3
2	Total sales, RMB / （100 million ）	7.23
3	Market dynamics (qualitative assessment)	Growing
4	Presence of entry restrictions (specify nature of restrictions)	No restrictions
5	Specific requirements for standardization and certification	1. Good mechanics and cutting performance 2. The coating can be evenly attached to the surface of the tool 3. Strong versatility
6	Average rate of return in the industry (or market),%	5.86%

Compare the industry (or market) average rate of return with the bank's investment interest (3.78 %). The average rate of return in this industry is higher, so the investment in this industry makes sense

According to the statistics, survey and analysis of the Tool Branch of China Machine Tool Industry Association, the total scale of consumption and import and export of the coating tool market in China have been estimated. The total consumption scale of China's coated tool market is on the rise. At the same time, coated tools have great potential in the field of digital control processing machining and will be the most important tool variety in the field digital control processing machining in the future.

With the increase in demand for special materials in the automotive, aerospace,

electronics, and military industries,the application of coated tools has become more advantageous.Characteristics of potential clients of the startup project is shown table 7.5.

Table 7.5 – Characteristics of potential clients of the startup project

№	The need that shapes the market	Target audience (target market segments)	Differences in the behavior of different potential target customer groups	Consumer requirements for the product
1	Carbide alloy drill/Carbide alloy blade	Coated tools can be used in drilling, tapping and cutting	The market demand is large, and the supply may be in short supply Affected by processing technology and global economy, the price is high	1. It is suitable for drilling of more complex materials and can choose a higher cutting speed. 2. The high-performance alloy blades specially selected for alloy drills can effectively reduce the chipping and maintain good wear resistance.

After identifying potential groups of clients, the market environment is analyzed: tables of factors that contribute to the market implementation of the project and factors that hinder it are compiled . The factors in the table are presented in descending order of importance.

The Table 7.6 shows that threat factors.

Table 7.6 - Threat factors

Factor	The content of the threat	The reaction of the company is possible
1	2	3
New competitor	Strong new competitors appearing to enter the market	Strengthen product technology innovation
Substitutes	Substitutes grab the company's sales	Strengthen product technology innovation

The Table 7.6 shows that factors of opportunities.

Table 7.7 – Factors of opportunities

Factor	The content of the opportunities	The reaction of the company is possible
1	2	3
Market demand	Increase in market demand	Cooperate with other companies
new technology	New technology research	Technology transfer to new products to serve a larger customer base

Further analysis of the proposal is carried out: the general features of competition in the market are defined , as shown the Table 7.8.

Table 7.8 – Step analysis of competition in the market

Features of the competitive environment	What is this characteristic	Impact on the company's activities
1	2	3
1. Specify the type of competition - monopoly / oligopoly / monopolistic / pure	monopoly	Technology monopoly (independent research and development and production of products)
2. By level of competition - local / national /	local	Affect company performance
3. On a departmental basis between departments / industries	between industries	Research and development independent production line
4. Competition by types of goods:	freight-generic	Make the product apply to more fields
5. By the nature of competitive advantages - price / non-price	non-price	Improve product quality
6. By intensity - vintage / non-vintage	non-vintage	-

The list of market threats and market opportunities is based on the analysis of threat

factors and opportunities factors of the marketing environment. Market threats and market opportunities are the consequences (projected results) of the influence of factors, in contrast, are not yet realized in the market and have a certain probability of implementation.

The final stage of the market analysis of project implementation opportunities is the compilation of SWOT-analysis (matrix of analysis of Strength and Weak, Threats and Opportunities), as shown the Table 7.9.

Table 7.9 – SWOT analysis of a startup project

S	Technical skill advantage: Tangible assets advantage; Human resources advantage.	W	Lack of competitive tangible assets, intangible assets, and organizational assets
O	Expanding trend of customer base or product segmentation; Strong market demand growth and rapid expansion; There is an opportunity to expand to other geographic regions and expand market share.	T	Strong new competitors appearing to enter the market; Substitutes grab the company's sales; Decline in the growth rate of the main product market; Adverse changes in exchange rates and foreign trade policies

7.4 Development of market strategy of the project

The development of a market strategy as a first step involves determining the strategy of market coverage: a description of target groups of potential consumers.

Based on the results of the analysis of potential consumer groups (segments), the authors of the idea choose the target groups for which they will offer their product and determine the market coverage strategy: it chooses a strategy of concentrated marketing, as shown the Table 7.10.

Table 7.10 – Selection of target groups of potential consumers

№	Description of the profile of the target group of potential customers	Readiness of consumers to accept the product	Estimated demand within the target group(segment)	Intensity of competition in the segment	Easy to enter the segment
1	Coated tools can be used in drilling, tapping and cutting	Have confidence in the product and can accept it	High demand	Market competition is not fierce	Easy
Which target groups are selected:Automotive, aerospace, electronics, military and other industries that have large applications for coated tools					

To work in selected market segments it is necessary to form a basic development strategy.

Company development strategy:

a) corporate mission: a good tool for the manufacturing industry. The company focuses on the field of machine tools, serving manufacturing companies all over the

world, improving production efficiency, improving product quality, and reducing production costs;

b) corporate vision: to become the world's top precision tool company. The company adopts the culture of precision manufacturing, producing precision tools, and serving precision manufacturing. What we call “precision tools” is the general term for family products of precision tools, precision measuring tools, and precision equipment, which is different from low-end tool measuring tools and machine tool equipment products. Precision Knives are different from ordinary metal products. The products are sophisticated, have high technical content, involve a wide range of technologies, and face a wide range of customers. They are necessities and consumables for modern high-end manufacturing. The market space is vast and promising. We should continue to focus on this Direction, and strive to become the world's top precision tool company;

c) development strategy for the recent 5-10 years. To become the world's top precision tool company is our goal and dream for 20 to 30 years. For the past 5-10 years, after careful research and analysis, it is determined that our development strategy is "internationalization, intelligence, lean, large-scale, and build the world's top precision tool company.

Competitive advantage of startups:

a) research and technical advantages. The company has outstanding independent research and development capabilities, and attaches great importance to technical investment, has a core team of professionals and operators with first-class theory and technology. The company has high-end production equipment with independent intellectual property rights, which meets the special process requirements of its own coated tool products, greatly improves the quality of the company’s coated tools, firmly

builds a higher technical barrier, and effectively improves production efficiency. Product cost provides performance and price advantages for the company's domestic and foreign competition.

b) product performance advantage. It is capable of preparing and producing precision tools with high technical content, involving a wide range of technologies, and facing a wide range of customers. It is a necessity and consumable for modern high-end manufacturing;

c) industry priority development advantage. At present, the overall technical level of China's coated tool industry is low, and the proportion of high-end coated superhard tool products is low, and the performance and quality cannot meet the development of high-end equipment sideline industry. The country has launched a series of policies to encourage the development of high-efficiency, high-performance, sophisticated and complex tools. The company focuses on the research and development and production of high-end coated tools, which is conducive to the development trend of the industry and timely develops high-end equipment manufacturing in accordance with the needs of customers in the high-end application market. Industry's high-efficiency, high-performance, high-precision coated tools.

Defining positioning strategy

a) target market positioning. Coated cutting tools have the characteristics of high processing efficiency, long service life and good processing quality. They are mainly used in the finishing of automobile by-products, aerospace, electronic information and other industries, and their applications are constantly expanding. Coated tools are not only suitable for general finishing and semi-finishing, but also for roughing. They are recognized internationally as one of the most effective tools for improving productivity.

b) corporate positioning (establish corporate brand). The products that companies sell are often closely related to their brands. Customers' recognition of your products actually starts from the recognition of the product's brand. Brand positioning must be based on product positioning. It is achieved through product positioning, but once the brand positioning is successful, the brand as an intangible asset will be separated from the product and show its value separately. Through the implementation of brand strategy, the company has established a good brand system and established a good market reputation.

c) product positioning. Product positioning is the positioning of a specific product in the minds of consumers. If consumers have similar needs, they will be associated with products of this brand. The company adopts precision manufacturing to produce precision coated knives and serves the culture of precision manufacturing, which is different from low-end coated knives and measuring tools. Precision coated tools are different from ordinary metal products. The products are precise, have high technical content, involve a wide range of technologies, and face a wide range of customers. They are necessities and consumables for modern high-end manufacturing, and have a broad market space and promise.

7.5 Development of a marketing program for a startup project

The first step is to form a marketing concept of the product that the consumer will receive.

The quality advantages of the coated tools produced by the start-up company are mainly manifested in the following aspects:

- long service life: that is, under the same processing conditions, the tool life

can be increased several times or even dozens of times, especially in harsh processing conditions. Under the circumstances (such as difficult-to-machine material cutting, high-speed cutting, dry cutting and high-precision machining, etc.);

- high processing efficiency: mainly by greatly increasing the cutting speed of the tool to achieve the purpose of improving production efficiency;
- quality stability Good: The tool life of products of the same specification and variety is roughly the same under the same processing conditions;
- high processing accuracy: including high processing surface accuracy and high qualification rate of parts.

The next step is to determine the optimal sales system within which the decision is made:

a) what the customer base is. The customer base of coated tools is very wide-mold factories, hardware factories, machining factories, auto and motorcycle parts factories, machinery factories, precision manufacturing factories, CNC machining factories, as well as aerospace, shipbuilding, Electronics manufacturing. As long as the manufacturers who use CNC machine tools (CNC lathes, CNC milling machines, milling machines, CNC drilling machines, etc.) must use tools. These customers can be contacted through their company's name, website, and other methods. This is very helpful for us to carry out the next step. And record the collected information, sort, analyze, and prepare for the next step;

b) establish contact or relationship with customers. To sell products to customers, sales staff must let customers know who you are, what company you are, what products you sell, and what products you have are advantageous. Therefore, whether it is a phone call or an unfamiliar visit, these basic information must be clearly

understood by the customer. Our purpose is to help customers solve problems, help customers improve production efficiency, improve quality, and provide technical support in coating tool technology, so as to improve customers' competitiveness and achieve our purpose of selling coated tools. To sell our products, we must find the person responsible for using or purchasing our products. Generally speaking, it is to find the person in charge of the purchase or the workshop tool;

c) tap customer needs (arouse their desire to buy). Analyze and digest the collected data. Analyze the customer’s company organizational structure, from the customer’s level functions, and the role they play in procurement, to find out the customers related to procurement, straighten out the relationship, and find sales clues. Compare the price of the same model, the quality of the same price, the better the service, the higher the price and the effect, and the price-performance ratio. Find an excitement point for them to buy our products, so as to arouse their desire to buy. When customers encounter problems and challenges, they need help, and they will ask whether they want to buy a product or provide some kind of service, and they will put forward their requirements. Their potential needs are their top priority. If we can solve the problem on time, according to quality, and according to their requirements, then it will not be a problem to make a business. The core of our sales is to solve the urgent needs of our customers;

d) competitive strategy. Take advantage of price advantages, cost-effective advantages, technical advantages, after-sales service advantages, and relationship advantages. Stick to the advantages and eliminate the disadvantages;

e) follow-up service. Monitor the process of arrival and test tools, fulfill the promise of after-sales service, and ensure customer satisfaction. Establish a collection

mechanism to ensure that accounts can be collected on time and in quantity. Continuously strengthen communication, understanding, and continuously enhance mutual trust, so as to be a permanent customer. In allowing customers to introduce new customers to themselves, the customer base continues to expand.

7.6 Startup company conclusion

National policies support industry development. Super-hard coating tools and material products are important supporting facilities for the development of modern manufacturing, which play an irreplaceable role in improving the efficiency of the manufacturing industry and promoting the upgrading of the manufacturing industry. For the development of the new materials and equipment industry, the Chinese government has issued a series of industry promotion policies. The high-intelligence manufacturing industry represented by aircraft, automobiles, digital cultural equipment and related high-end CNC machine tools and new materials industries have repeatedly emphasized and put forward clear development requirements. It is clearly required to focus on the development of high-efficiency, high-performance, sophisticated and complex tools, the development of new super hard materials and equipment, high-speed cutting tools, etc. The support of industrial policy will be beneficial to the rapid development of enterprises in the industry, so start-up companies have commercial possibilities.

CONCLUSIONS

In this work, AlNiCoFeCr high entropy alloy (HEA) was prepared by mechanical alloying in a planetary mill, and then AlNiCoFeCr HEA–TiB_2 composite blend was prepared by ball milling in a planetary mill, and the last AlNiCoFeCr HEA– TiB_2 coatings by cold spraying on steel substrate. The AlNiCoFeCr HEA, AlNiCoFeCr HEA–TiB_2 powder and AlNiCoFeCr HEA–TiB_2 coatings were studied. These are necessary to extend the life of the components. The samples were characterized in the terms of their microstructure, phase composition and microhardness by various characterization methods. Scanning Electron Microscope (SEM), Ultima IV X-ray diffractometer (XRD), Vickers microhardness machine PMT-3 were used to describe the morphology, microstructure and phase composition of the feedstock powder and the HEA coating. And analysis of chemical element composition of equiatomic AlNiCoFeCr HEA powder and HEA-TiB_2 composite powders was carried out by energy dispersive spectrometer (EDS). The following findings can be summarized:

1. The important literature review shows that HEAs as well as ceramic have aroused great interest in materials science and engineering due to their unique structure and properties whereas the CS technology is a promising way to protect details and has been widely applied as a coating technology in a broad range of industries. But until now this method for preparing composite metal-ceramic coatings with HEA matrices has not been studied.

2. In accordance with the results of X-ray diffraction analysis, the bcc and fcc solid solutions with nanostructure are obtained in the AlNiCoFeCr alloy by 8 h mechanical alloying.

3. AlNiCoFeCr HEA–30 wt.% TiB_2 powder mixture was prepared by 2h ball

milling , which decrease d the crystallite size without affecting the lattice parameters and phase composition of powder mixture.

4. AlNiCoFeCr HEA–TiB_2 composite coatings with mean thickness about 80-100 μm were prepared by cold spraying and completely retained the feedstock powder mixture phase composition without any phase transformation. It has been demonstrated that AlNiCoFeCr HEA–TiB_2 nanocomposite powder formed by ball milling can be used as the feedstock for cold spray deposition on the steel substrates.

5. The CS coating hardness of HEA-TiB_2 composite material is 665 HV, which is greater than AlNiCoFeCr HEA hardness. That is explained by the additional strain hardening of the material at low temperature and extremely high strain rate during CS, along with the effects of dispersive hardening by TiB_2 particles. Cold spraying is a feasible and potentially effective coating technology that can be used to produce HEA and composite coatings while maintaining the coating's intrinsic feedstock powder phases.

6. The coating parameters can be further adjusted to reduce inter-splat porosity and improve adhesion between particles. So, further work should be aimed at improving the quality of the coating by optimizing the parameters of the CS process, namely, the temperature and pressure of compressed air flow, as well as composition of the initial powder mixture.

7. The measures to ensure healthy working conditions and principles of safety in an emergency were developed.

REFERENCES

1. Yeh J W, Chen S K, Lin S J, et al. Nanostructured high-entropy alloys with multiple principal elements: novel alloy design concepts and outcomes [J]. Advanced Engineering Materials, 2004, 6(5): 299-303.
2. Zhang Y, Zuo T T, Tang Z, et al. Microstructures and properties of high-entropy alloys [J]. Progress in materials science, 2014, 61: 1-93.
3. Zhang Y, Gao M C, Yeh J W, et al. High-Entropy alloys: fundamentals and applications [J]. 2016.
4. Miracle D B, Senkov O N. A critical review of high entropy alloys and related concepts[J]. Acta Materialia, 2017, 122: 448-511.
5. Lu Z P, Wang H, Chen M W, et al. Summary from a recent workshop[J]. Intermetallics, 2015, 66: 67-76.
6. Yeh J W. Alloy design strategies and future trends in high-entropy alloys [J]. Jom, 2013, 65(12): 1759-1771.
7. Yeh JW. Recent progress in high-entropy alloys. Presentation at Changsha meeting; 2011.
8. Zhang Y, Yang X, Liaw P K. Alloy design and properties optimization of high-entropy alloys[J]. Jom, 2012, 64(7): 830-838.
9. Zhang Y, Zhou Y J, Lin J P, et al. Solid-solution phase formation rules for multi-component alloys[J]. Advanced engineering materials, 2008, 10(6): 534-538.
10. Beke D L, Erdélyi G. On the diffusion in high-entropy alloys [J]. Materials Letters, 2016, 164: 111-113.
11. Tsai K Y, Tsai M H, Yeh J W. Sluggish diffusion in Co–Cr–Fe–Mn–Ni high-entropy alloys[J]. Acta Materialia, 2013, 61(13): 4887-4897.

12. Yeh J W, Chang S Y, Hong Y D, et al. Anomalous decrease in X-ray diffraction intensities of Cu–Ni–Al–Co–Cr–Fe–Si alloy systems with multi-principal elements[J]. Materials chemistry and physics, 2007, 103(1): 41-46.
13. Ranganathan S. Alloyed pleasures: multimetallic cocktails[J]. Current science, 2003, 85(10): 1404-1406.
14. Cantor B, Chang I T H, Knight P, et al. Microstructural development in equiatomic multicomponent alloys[J]. Materials Science and Engineering: A, 2004, 375: 213-218.
15. Tsau C H, Chang Y H. Microstructures and mechanical properties of TiCrZrNbNx alloy nitride thin films[J]. Entropy, 2013, 15(11): 5012-5021.
16. Li C, Li J C, Zhao M, et al. Effect of alloying elements on microstructure and properties of multiprincipal elements high-entropy alloys[J]. Journal of Alloys and Compounds, 2009, 475(1-2): 752-757.
17. Chen Y Y, Duval T, Hung U D, et al. Microstructure and electrochemical properties of high entropy alloys—a comparison with type-304 stainless steel[J]. Corrosion science, 2005, 47(9): 2257-2279.
18. Zhao K, Xia X X, Bai H Y, et al. Room temperature homogeneous flow in a bulk metallic glass with low glass transition temperature[J]. Applied Physics Letters, 2011, 98(14): 141913.
19. Zhang Y, Zhou Y J, Lin J P, et al. Solid- solution phase formation rules for multi- component alloys[J]. Advanced engineering materials, 2008, 10(6): 534-538.
20. Yang X, Zhang Y. Prediction of high-entropy stabilized solid-solution in multi-component alloys[J]. Materials Chemistry and Physics, 2012, 132(2-3): 233-238.

21. Guo S, Ng C, Lu J, et al. Effect of valence electron concentration on stability of fcc or bcc phase in high entropy alloys[J]. Journal of applied physics, 2011, 109(10): 103505.

22. Wang Z, Huang Y, Yang Y, et al. Atomic-size effect and solid solubility of multicomponent alloys[J]. Scripta Materialia, 2015, 94: 28-31.

23. Zhou Y J, Zhang Y, Wang Y L, et al. Solid solution alloys of Al Co Cr Fe Ni Ti x with excellent room-temperature mechanical properties[J]. Applied physics letters, 2007, 90(18): 181904.

24. Wang X F, Zhang Y, Qiao Y, et al. Novel microstructure and properties of multicomponent CoCrCuFeNiTix alloys[J]. Intermetallics, 2007, 15(3): 357-362.

25. Senkov O N, Wilks G B, Scott J M, et al. Mechanical properties of Nb25Mo25Ta25W25 and V20Nb20Mo20Ta20W20 refractory high entropy alloys[J]. Intermetallics, 2011, 19(5): 698-706.

26. Otto F, Dlouhý A, Somsen C, et al. The influences of temperature and microstructure on the tensile properties of a CoCrFeMnNi high-entropy alloy[J]. Acta Materialia, 2013, 61(15): 5743-5755.

27. Wang J, Zhang B, Yu Y, et al. Study of high temperature friction and wear performance of (CoCrFeMnNi) 85Ti15 high-entropy alloy coating prepared by plasma cladding[J]. Surface and Coatings Technology, 2020, 384: 125337.

28. Cheng J B, Liang X B, Xu B S. Effect of Nb addition on the structure and mechanical behaviors of CoCrCuFeNi high-entropy alloy coatings[J]. Surface and Coatings Technology, 2014, 240: 184-190.

29. Lin D, Zhang N, He B, et al. Influence of laser re-melting and vacuum heat treatment on plasma-sprayed FeCoCrNiAl alloy coatings[J]. Journal of Iron and

Steel Research International, 2017, 24(12): 1199-1205.

30. Shi Y Z, Yang B, Liaw P K. Corrosion-resistant high-entropy alloys: A review[J]. Metals, 2017, 7(2): 43.
31. Qin Q, Qu J, Hu Y, et al. Microstructural characterization and oxidation resistance of multicomponent equiatomic CoCrCuFeNi–TiO high-entropy alloy[J]. International Journal of Minerals, Metallurgy, and Materials, 2018, 25(11): 1286-1293.
32. Fan Z, Wang H, Wu Y, et al. Thermoelectric performance of PbSnTeSe high-entropy alloys[J]. Materials Research Letters, 2017, 5(3): 187-194.
33. Zhang Y, Zuo T T, Cheng Y Q, et al. High-entropy alloys with high saturation magnetization, electrical resistivity and malleability[J]. Scientific reports, 2013, 3(1): 1-7.
34. Liu C, Peng W, Jiang C S, et al. Composition and phase structure dependence of mechanical and magnetic properties for AlCoCuFeNix high entropy alloys[J]. Journal of Materials Science & Technology, 2019, 35(6): 1175-1183.
35. Li Xinling. Effects of Cr and Al on the structure and properties of FeCoCrNiAl high-entropy alloys[D]. Lanzhou University of Technology, 2020.
36. Wang F J, Zhang Y. Effect of Co addition on crystal structure and mechanical properties of Ti0. 5CrFeNiAlCo high entropy alloy[J]. Materials Science and Engineering: A, 2008, 496(1-2): 214-216.
37. CHEN Z H, CHEN D. Mechanical alloying and solid-liquid reaction ball milling[M]. Beijing: Chemical Industry Press, 2006.
38. Suryanarayana C. Mechanical alloying and milling[J]. Progress in materials science, 2001, 46(1-2): 1-184.
39. Varalakshmi S, Kamaraj M, Murty B S. Formation and stability of equiatomic and

nonequiatomic nanocrystalline CuNiCoZnAlTi high-entropy alloys by mechanical alloying[J]. Metallurgical and Materials Transactions A, 2010, 41(10): 2703-2709.

40. Moravcik I, Cizek J, Gavendova P, et al. Effect of heat treatment on microstructure and mechanical properties of spark plasma sintered AlCoCrFeNiTi0. 5 high entropy alloy[J]. Materials Letters, 2016, 174: 53-56.
41. Vaidya M, Karati A, Marshal A, et al. Phase evolution and stability of nanocrystalline CoCrFeNi and CoCrFeMnNi high entropy alloys[J]. Journal of Alloys and Compounds, 2019, 770: 1004-1015.
42. Atkinson H V, Davies S. Fundamental aspects of hot isostatic pressing: an overview[J]. Metallurgical and Materials Transactions A, 2000, 31(12): 2981-3000.
43. Tang Z, Senkov O N, Parish C M, et al. Tensile ductility of an AlCoCrFeNi multi-phase high-entropy alloy through hot isostatic pressing (HIP) and homogenization[J]. Materials Science and Engineering: A, 2015, 647: 229-240.
44. Liu X, Cheng H, Li Z, et al. Microstructure and mechanical properties of FeCoCrNiMnTi0. 1C0. 1 high-entropy alloy produced by mechanical alloying and vacuum hot pressing sintering[J]. Vacuum, 2019, 165: 297-304.
45. Alshataif Y A, Sivasankaran S, Al-Mufadi F A, et al. Manufacturing methods, microstructural and mechanical properties evolutions of high-entropy alloys: a review[J]. Metals and Materials International, 2019: 1-35.
46. Yim D, Sathiyamoorthi P, Hong S J, et al. Fabrication and mechanical properties of TiC reinforced CoCrFeMnNi high-entropy alloy composite by water atomization and spark plasma sintering[J]. Journal of Alloys and Compounds, 2019, 781: 389-396.
47. Qiu X W, Zhang Y P, Liu C G. Microstructure and properties of $Al_2CrFeCo_xCuNiTi$

high entropy alloy coating prepared by laser cladding[J]. Materials Science and Engineering of Powder Metallurgy, 2013, 18 (5): 735–740.

48. Mattox D M. Handbook of physical vapor deposition (PVD) processing[M]. William Andrew, 2010.
49. Cropper M D. Thin films of AlCrFeCoNiCu high-entropy alloy by pulsed laser deposition[J]. Applied Surface Science, 2018, 455: 153-159
50. Handbook of thermal spray technology[M]. ASM international, 2004.
51. Liang X B, Guo W, Chen Y X. Microstructure and mechanical properties of FeCrNiCoCu(B) high-entropy alloy coatings[J]. Materials Science Forum, 2011, 694 : 502–507.
52. Löbel M, Lindner T, Mehner T, et al. Microstructure and wear resistance of AlCoCrFeNiTi high-entropy alloy coatings produced by HVOF[J]. Coatings, 2017, 7(9): 144.
53. Yin S, Cavaliere P, Aldwell B, et al. Cold spray additive manufacturing and repair: Fundamentals and applications[J]. Additive Manufacturing, 2018, 21: 628-650.
54. Song Kaiqiang, Cong Dalong, He Qingbing, et al. Application and prospect of advanced cold spray technology[J]. Equipment Environmental Engineering, 2019, 16(8).
55. Zhu S, Du W B, Wang X M, et al. Research on surface protection technology for magnesium alloys based on high entropy alloy[J]. Journal of Academy of Armored Force Engineering, 2013, 27 (6): 79–84.
56. Yin S, Li W, Song B, et al. Deposition of FeCoNiCrMn high entropy alloy (HEA) coating via cold spraying[J]. Journal of Materials Science & Technology, 2019, 35(6): 1003-1007.

57. Xu Y, Li W, Qu L, et al. Solid-state cold spraying of FeCoCrNiMn high-entropy alloy: an insight into microstructure evolution and oxidation behavior at 700-900℃[J]. Journal of Materials Science & Technology, 2021, 68: 172-183.

58. Zhao Qin, Ma Guozheng, Wang Haidou, et al. Research progress in the preparation and application of high-entropy alloy coatings[J]. Materials Review, 2018, 31(7): 65-71.

59. Shen W J, Tsai M H, Yeh J W. Machining performance of sputter-deposited (Al0. 34Cr0. 22Nb0. 11Si0. 11Ti0. 22) 50N50 high-entropy nitride coatings[J]. Coatings, 2015, 5(3): 312-325.

60. Chang S Y, Huang Y C, Li C E, et al. Improved diffusion-resistant ability of multicomponent nitrides: from unitary TiN to senary high-entropy (TiTaCrZrAlRu) N[J]. Jom, 2013, 65(12): 1790-1796.

61. Castro D, Jaeger P, Baptista A C, et al. An overview of high-entropy alloys as biomaterials[J]. Metals, 2021, 11(4): 648.

62. Sharma A. High Entropy Alloy Coatings and Technology[J]. Coatings, 2021, 11(4): 372.

63. Vaidya M, Prasad A, Parakh A, et al. Influence of sequence of elemental addition on phase evolution in nanocrystalline AlCoCrFeNi: Novel approach to alloy synthesis using mechanical alloying[J]. Materials & Design, 2017, 126: 37-46.

64. Wang W R, Wang W L, Yeh J W. Phases, microstructure and mechanical properties of AlxCoCrFeNi high-entropy alloys at elevated temperatures[J]. Journal of Alloys and Compounds, 2014, 589: 143-152.

65. Manzoni A, Daoud H, Völkl R, et al. Phase separation in equiatomic AlCoCrFeNi high-entropy alloy[J]. Ultramicroscopy, 2013, 132: 212-215.

66. Wang Y P, Li B S, Ren M X, et al. Microstructure and compressive properties of AlCrFeCoNi high entropy alloy[J]. Materials Science and Engineering: A, 2008, 491(1-2): 154-158.

67. Chen W.P., Fu Z.Q., Fang S.C, et al. Alloying behavior, microstructure and mechanical properties in a $FeNiCrCo_{0.3}Al_{0.7}$ high entropy alloy[J]. Materials and Design, 2013, 51: 854-860

68. Chen Y.L., Hu Y.H., Hsieh C.A., et al. Competition between elements during mechanical alloying in an octonary multi-principal-element alloy system[J]. Journal of Alloys and Compounds, 2009, 481 (1-2): 768-775 .

69. Yin S, Li W, Song B, et al. Deposition of FeCoNiCrMn high entropy alloy (HEA) coating via cold spraying[J]. Journal of Materials Science & Technology, 2019, 35(6): 1003-1007.

70. Левченко О. Г. Охорона праці та цивільний захист: навч. посіб. для студ. спеціальностей 132 «Матеріалознавство» та 136 «Металургія». – Київ: КПІ ім. Ігоря Сікорського, 2019. – 337 с. – [Електронний ресурс] / Режим доступу: https://ela.kpi.ua/handle/123456789/31215.

71. ДСН 3.3.6.042-99. Державні санітарні норми мікроклімату виробничих приміщень.

72. ДСН 3.3.6.037-99. Санітарні норми виробничого шуму, ультразвуку та інфразвуку.

73. ДСН 3.3.6.039-99. Державні санітарні норми виробничої загальної та локальної вібрації.

74. ДНАОП 0.00-1.21-98. Правила безпечної експлуатації електроустановок споживачів.

75. НПАОП 28.0-1.37-14. Правила охорони праці при нанесенні металопокриттів.
76. ДБН В.2.5-67:2013. Опалення, вентиляція та кондиціонування.
77. НПАОП 0.00-1.07–94 («Правила устройства и безопасной эксплуатации сосудов, работающих под давлением»).
78. ДБН В.2.2-28:2010. Державні будівельні норми україни. Будинки адміністративного та побутового призначення.
79. ДБН В.2.5-28-2006. Природне і штучне освітлення.
80. ДСТУ ГОСТ 12.2.061:2009. ССБТ. Оборудование производственное. Общие требования безопасности к рабочим местам.
81. Местные вытяжные устройства к оборудованию для сварки и резки металлов: Методические указания по проектированию. – Л.: ВНИИОТ. – 1980. – 52 с.
82. ДСТУ 7239:2011. Національний стандарт України. Система стандартів безпеки праці. Засоби індивідуального захисту. Загальні вимоги та класифікація.
83. ДСТУ EN 133:2005. Засоби індивідуального захисту органів дихання. Класифікація.
84. ДСТУ EN 420-2017. Загальні вимоги до рукавиць.
85. ДСТУ EN 397:2001. Каски захисні промислові.
86. Положення щодо розробки планів локалізації та ліквідації аварійних ситуацій і аварій,№ 424/3717 від 30.06.1999 р.
87. ДСТУ 3273-95. Безпечність промислових підприємств. Загальні положення та вимоги.
88. НАПБ Б.03.002-2007. Визначення категорії приміщень, будинків там зовнішніх установок за вибухопожежною та пожежною небезпекою.